universität wien

DISSERTATION

Titel der Dissertation

The role of *Schizosaccharomyces pombe* cyclophilin Rct1 in RNA polymerase II transcription

angestrebter akademischer Grad

Doktorin der Naturwissenschaften (Dr. rer.nat.)

Verfasserin / Verfasser:	Mag. Tatsiana Skrahina
Matrikel-Nummer:	0600442
Dissertationsgebiet (lt. Studienblatt):	Molecular Biology
Betreuerin / Betreuer:	Dr. Zdravko Lorković

Wien, am 11. Dezember 2009

Маёй сям'і прысвячаецца: дзеду Мішу, маме, тату, дзядзьку, Олі, Авечцы і, канечне, Каці.

Acknowledgments

I would like to express my gratitude to everybody who was with me all these years.

My supervisors and colleagues - for your assistance and advice.

My friends - for your STRONG support and the GREAT times we had together.

My nearest and dearest - for ALWAYS being there.

I owe my deepest gratitude to you, as this marathon was a team effort and crossing the finish line would not have been possible without your contribution.

Abstract

The C-terminal domain (CTD) of the largest subunit of RNA polymerase II (RNAP II) consists of multiple tandem heptapeptide repeats (Tyr1-Ser2-Pro3-Thr4-Ser5-Pro6-Ser7). The CTD undergoes dynamic phosphorylation on Ser2 and Ser5 residues during transcription. Changes in the CTD phosphorylation pattern orchestrate recruitment of different transcription, mRNA-processing and histone-modifying factors.

Rct1, a nuclear multidomain cyclophilin from *Schizosaccharomyces pombe*, consists of a peptidyl-prolyl *cis-trans* isomerase (PPIase) domain, an RNA recognition motif (RRM) and a C-terminal domain enriched in arginine-serine/arginine-aspartic acid (RS/RD) repeats. Previous work has shown that Rct1 negatively regulates RNA polymerase II (RNAP II) C-terminal domain (CTD) phosphorylation and associates with transcriptionally active chromatin. However, the mechanism of this regulation remained elusive. Therefore, in this work Rct1 interactions with the RNAP II CTD and CTD kinases and phosphatases were checked. *In vitro* pull-downs indicate that the PPIase domain of Rct1 is responsible for binding to the RNAP II CTD as well as to CTD kinases Cdk9 and Lsk1. Cdk9 and Lsk1, which are known to regulate transcription by phosphorylating Ser2 of the CTD, bind Rct1 with the help of their non-kinase parts. The performed kinase assays have revealed that Rct1 negatively controls specific activity of Cdk9 towards the RNAP II CTD via its PPIase domain. Chromatin immunoprecipitation (ChIP) analysis of RNAP II occupancy along transcription units indicates that amount of RNAP II bound to chromatin during transcription elongation and termination steps is significantly increased in Rct1 overexpressing cells and decreased in Rct1 depleted cells. ChIP of histone H3 acetylated at lysines 9 and 12 (an active transcription mark) has revealed that the acetylation is reduced in both cases (Rct1 overexpression and depletion). However, the reduction is more pronounced when Rct1 is overexpressed. Moreover, the outcome of nuclear run-on experiment shows that under the conditions of either Rct1 over- or underexpression mRNA production is decreased. The evidence presented suggests that although over- and underexpression of Rct1 cause opposite effect on the amount of RNAP II bound to chromatin, both changes in Rct1 expression level negatively regulate transcription.

Zusammenfassung

Die größte Untereinheit der RNA Polymerase II (RNAP II) wird in ihrer C-terminalen Domäne (CTD) aus multiplen heptameren Peptidsequenzwiederholungen (Tyr1-Ser2-Pro3-Thr4-Ser5-Pro6-Ser7) aufgebaut. Die CTD wird während der Transkription an Ser2 und Ser5 phosphoryliert, Unterschiede in diesem Phosphorylierungsmuster bewirken differentielle Regulierungen von Transkription, mRNA-Prozessierung und Histonmodifizierung.

Rct1, ein nukleäres Cyclophilin der Spalthefe *Schizosaccharomyces pombe,* enthält eine Peptidyl-Prolyl *cis-trans* Isomerase (PPIase) Domäne, ein RNA Erkennungsmotif (RRM) und eine CTD mit Arg-Ser/Arg-Asp (RS/RD) Sequenzwiederholungen. Es wurde bereits nachgewiesen, dass Rct1 die Phosphorylierung der CTD von RNAP II negativ reguliert und mit transkriptionell aktivem Chromatin assoziiert ist. Die zugrunde liegenden Mechanismen wurden jedoch nicht erforscht. In dieser Arbeit wurden sowohl die Interaktionen zwischen Rct1 und der CTD von RNAP II als auch von Rct1 mit den beschriebenen RNAP II Kinasen und Phosphatasen durchgeführt. Mit *in vitro* Experimenten konnte nachgewiesen werden, dass die PPIase Domäne von Rct1 sowohl für die Interaktion mit der RNAP II CTD als auch für die Interaktionen mit den RNAP II CTD Kinasen Cdk9 und Lsk1 verantwortlich ist. Cdk9 und Lsk1, welche die Transkription durch Phosphorylierung des Ser2 der CTD regulieren, interagieren mit Rct1 über ihre nicht-katalytischen Domänen. Kinase-Aktivitätsmessungen ergaben, dass Rct1 über die PPIase Domäne die Aktivität von Cdk9 auf die RNAP II CTD negativ reguliert. Mit Hilfe von Chromatin-Immunopräzipitation (ChIP) konnte gezeigt werden, dass die Assoziation von RNAP II an Chromatin während Elongation und Termination der Transkription durch Rct1 beeinflusst wird. Eine ChIP-Analyse des Histons H3 konnte nachweisen, dass die Azetylierung der Lysinreste 9 und 12 sowohl bei Rct1-Überexpression als auch bei -Verminderung reduziert ist, wobei jedoch die Reduktion durch Rct1-Überexpression stärker betont ist. Nuclear run-on Experimente bestätigten weiters eine Reduktion der mRNA-Transkriptionsrate, welche sowohl unabhängig von Rct1-Überexpression als auch von Rct1-Reduktion war. Diese Ergebnisse zeigen, dass veränderte Rct1-Expression unterschiedliche Effekte auf die Bindung von RNAP II an Chromatin ausübt, die Transkription jedoch immer negativ reguliert wird.

Contents

Abbreviations

AcH3K9K12	acetylated histone H3 at lysines 9 and 12
Arg	arginine
BSA	bovine serum albumin
CaM	calmodulin
Cdk	cyclin dependent kinase
ChIP	chromatin immunoprecipitation
CN	calcineurin
CPF	cleavage-polyadenilation factor
CsA	cyclosporin A
CTD	RNA Polymearse II C-terminal domain
CUT	cryptic unstable transcript
CyPA	cyclophilin A
dH2O	distilled water
DMSO	dimethylsulphoxide
DRB	5,6-dichloro-1-*b*-D-ribofuranosylbenzimidazole
ELL	eleven-nineteen lysine-rich in leukemis
FKBP	FK506 binding proteins
GST	glutathione S-transferase
H	histone
H1	histone 1
H2Bub1	histone H2B monoubiquitylation
H3K36me2	histone H3 lysine 36 dimethylation
H3K36me3	histone H3 lysine 36 trimethylation
H3K4me	histone H3 lysine 4 monomethylation
H3K4me2	histone H3 lysine 4 dimethylation
H3K4me3	histone H3 lysine 4 trimethylation
H3K9	histone 3 lysine 9
H3K9K12	histone 3 lysines 9 and 12
HA	hemagglutinine
HCE	human capping enzymes
Hcm1	mammalian methyltransferase
HIV	human immunodeficiency virus
IF	immunofluorescence
IL-2	interleukin-2
IP3R	1,4,5-triphosphate receptor
K	lysine
Leu	leucine
Mce1	mammalian triphosphatase-guanylyltransferase
mRNA	mature messenger RNA
NaOAc	sodium acetate

NIMA	mitotic kinase, never in mitosis
NELF	negative elongation factor
NF-AT	nuclear factor of activated T-cells
NRO	nuclear run-on
OD	optical density
ORF	open reading frame
PAF	RNA Polymearse II associated factor
PEB	protoplast extraction buffer
PHD2	prolyl hydroxylase
PP2A	protein phosphatase 2A
PPIases	peptidyl-prolyl *cis-trans* isomerases
Pro	proline
pSer	phosphorylated serine
p-TEFb	positive transcription elongation factor b
PTPA	parvulins and protein phosphatase 2A phosphatase activator
qRT-PCR	real-time PCR
RNAP II	RNA Polymearse II
RRM	RNA recognition motif
RS/RD domain	domain, rich in arginine-serine/ arginine-aspartic acid repeats
RT	room temperature
RyRs	ryanodine receptors
Scp1	small phosphatases of the RNA Polymearse II C-terminal domain
Ser	serine
snoRNA	small nuclear RNA
snRNA	small nuclear RNA
SR	serine-arginine rich domains
TGF- β	transforming growth factor-β
Thr	threonine
TPR	tetratricopeptide repeat
uRNA	upstream regulatory RNA
Y2H	yeast-two hybrid
wt	wild type

1. Introduction

1.1. Peptidyl-prolyl *cis-trans* isomerases

The peptide bond has approximately 40% double-bond character, therefore it can exist in two forms: *cis* and *trans* (Fig. 1.1.). During translation most peptide bonds are connected in energetically favorable *trans* conformation and this form also dominates in native structures of peptides (Ramachandran & Sasisekharan, 1968). However, in case of peptide bond on the N-terminal side of proline residues (peptidyl-prolyl bond), both *cis* and *trans* forms exist, because the free energy difference between these two conformations is much smaller for proline than for any other amino acid. In fact, the frequency of the *cis* form occurrence in proteins is 5-6% (Stewart et al, 1990), (Pal & Chakrabarti, 1999). In addition to that, a great number of *cis* isoforms occur on the surface of proteins. The structural difference between these two distinct forms can be crucial in case of change between functional states of the protein or distinguishing between binding partners (Schiene & Fischer, 2000).

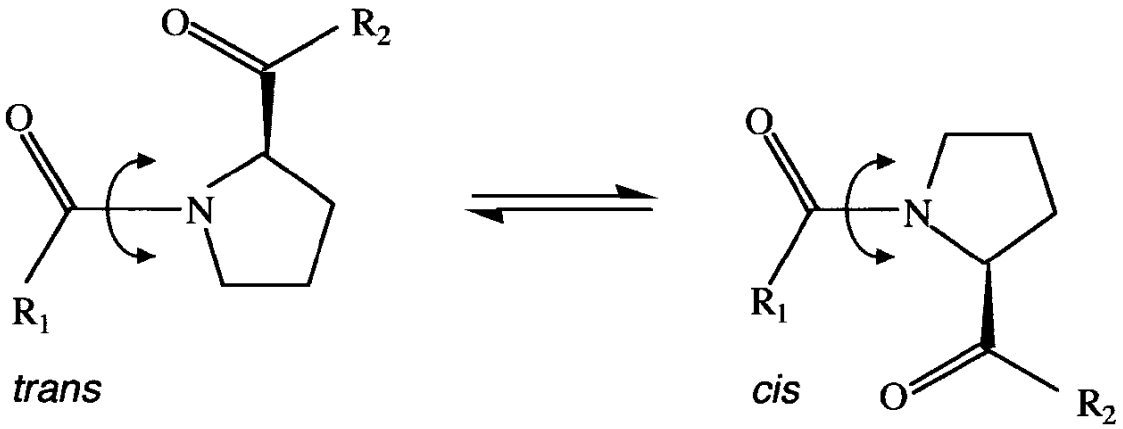

Fig. 1.1. A schematic illustration of the *cis* and *trans* isomers of the peptide bond on the N-terminal side of proline residues.

Spontaneous isomerization of the peptidyl-prolyl bond is a slow reaction that requires free energy. The process is rate limiting (Gothel & Marahiel, 1999) and can be accelerated by peptidyl-prolyl *cis-trans* isomerases (PPIases). PPIases, also called rotamases, can be classified into four structurally unrelated families: cyclophilins, FK506

binding proteins (FKBP), parvulins and protein phosphatase 2A phosphatase activator (PTPA). Cyclophilins and FKBP were first discovered PPIases (Handschumacher et al, 1984), (Fischer et al, 1984), (Fischer et al, 1989), (Harding et al, 1989), (Siekierka et al, 1989). They are also known as immunophilins for their ability to bind immunosuppressive drugs: cyclophilins form complexes with cyclosporin A (CsA) and FKBP bind FK506 and rapamycin (Schreiber, 1991), (Gothel & Marahiel, 1999) (Fig. 1.2.). Later, an irreversible inhibitor of several parvulins, juglone, was discovered as well (Hennig et al, 1998).

In addition to mentioned PPIases, dual-family PPIases in lower organisms have been lately described. The proteins possess both cyclophilin and FKBP-like domains (Adams et al, 2005).

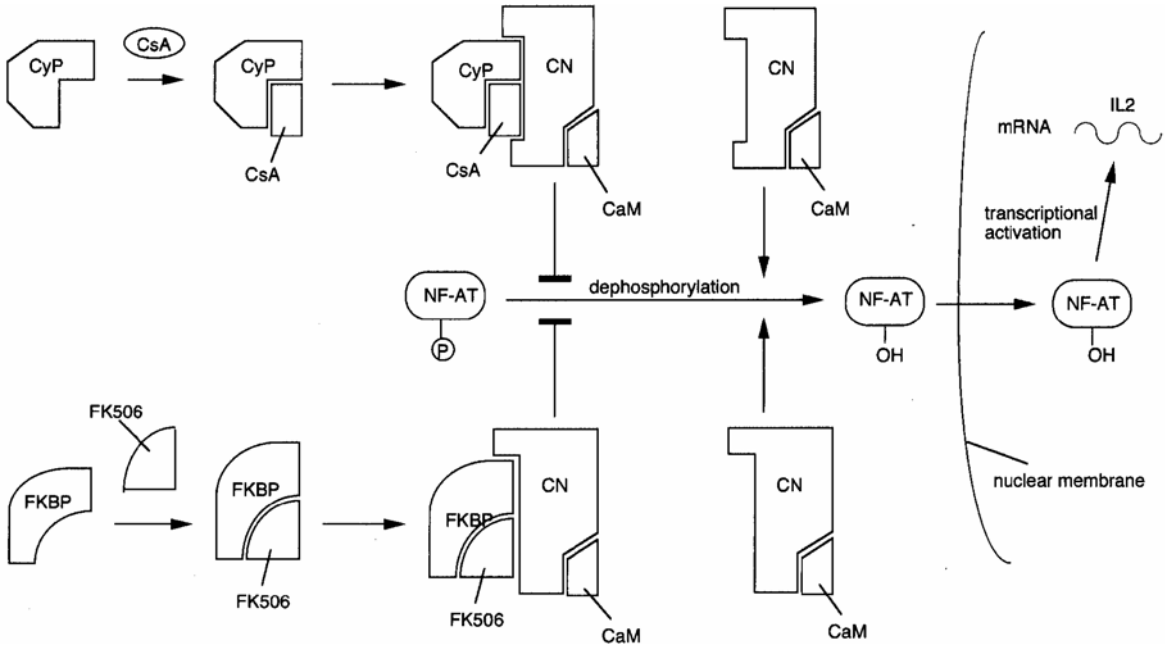

Fig. 1.2. Immunosuppressive actions performed by the CyPA (Cyclophilin A) – CsA and FKBP-FK506 complexes. Increase of the free intracellular calcium during T-cell activation causes interaction between calmodulin (CaM) and phosphatase calcineurin (CN). The complex dephosphorylates nuclear factor of activated T-cells (NF-AT), as a result NF-AT can cross the nuclear membrane and activate transcription of interleukin-2 (IL-2). The Cyp-CsA complex disables phosphatase activity of CN-CaM complex by interacting with CN. The FKBP-FK506 complex inhibits phosphatase activity of CN-CaM in the similar way. From: (Gothel & Marahiel, 1999). The FKBP-ramapycin complex binds to mammalian target of rapamycin (mTOR) instead of CaM (Sharma et al, 1994).

1.1.1. FKBPs

FKBPs were discovered in all organisms investigated. FKBP12, the prototype of the FKBP family, contains a single FKBP domain evolutionary conserved in most of FKBPs. The structure of the domain, responsible for both PPIase- and FK506/rapamycin-binding activities, corresponds to an amphipathic five-stranded β-sheet (Fig.1.3.), (Itoh & Navia, 1995). By contrast, FKBP51 and 52 consist of tandem FKBPs and multiple tetratricopeptide repeat (TPR). In both proteins only the N-terminal FKBP domains are able to perform PPIase- and FK506/rapamycin-binding activities, while C-terminal FKBP domains are responsible for interactions with different binding partners (Sinars et al, 2003), (Wu et al, 2004). Studies of a noncanonical FKBP, FKBP38, reveal that its structure is similar to FKBP12 and closely resembles C-terminal FKBP domains of FKBP51 and 52. Although FKBP38 FKBP domain lacks conserved amino acids required for FK506-binding and PPIase activities, it preserves rotamase activity in calmodulin (CaM) presence. Besides FKBP domain, FKBP38 has also TPR domain, prolyl hydroxylase (PHD2)-interacting region, putative calmoduline and transmembrane motifs (Maestre-Martinez et al, 2006), (Edlich et al, 2006), (Kang et al, 2005), (Kang et al, 2008).

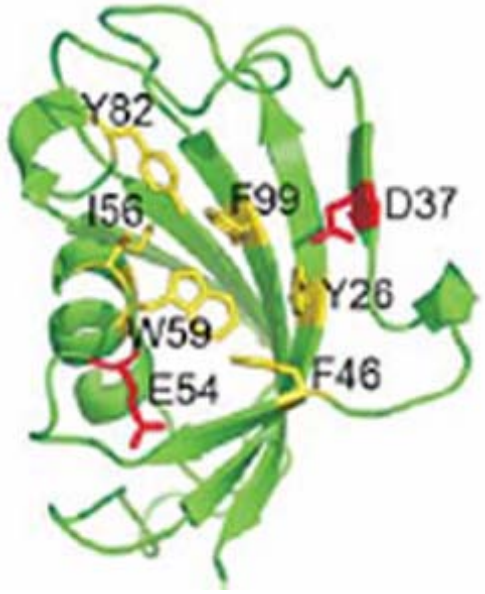

Fig. 1.3. Structure of FKBP12 bound to FK506. From: (Itoh & Navia, 1995).

FKBPs mediate various cellular processes. For example, FKBP12 is enrolled in protein-protein interactions and orchestrates its partners' activities. It functions as a

constituent component of the intracellular calcium release channel. It binds members of this calcium release family: the ryanodine receptors (RyRs), modulating RyR complexes, and the inositol 1,4,5-triphosphate receptor (IP_3R), enabling its binding to CN (Marks, 1996). FKBP12 is also known to interact with transforming growth factor-β (TGF-β), which is implicated in many cellular processes (Wang et al, 1994). Numerous FKBPs function as chaperons. For instance, FKBP51 and FKBP52 act as co-chaperons in steroid receptor signaling, their TPR domains serve as binding sites of the ubiquitous molecular chaperone Hsp90 (Sinars et al, 2003), (Davies & Sanchez, 2005). FKBP38 also interacts with Hsp90, but its main function is protection from apoptosis. FKPB38 performs targets anti-apoptotic proteins Bcl-X_L and Bcl-2 to the mitochondrial membrane (Kang et al, 2005), (Shirane & Nakayama, 2003), (Edlich et al, 2007). Besides, numerous FKBPs, including the mentioned ones, are highly expressed in neuronal tissues after nerve injury. They take part in synaptic vesicle assembly, axonal transport and maybe in neuroprotection against abnormal protein aggregation, suggesting potential treatment. Immunosuppressive ligands such as GPI-1046 and N-cycloheximide bind to FKBP12 and FKBP38, respectively, and show neuroprotective and neuroregenerative effects (Avramut & Achim, 2003), (Poulter et al, 2004).

1.1.2. Protein phosphatase 2A phosphatase activator

Protein phosphatase 2A (PP2A) is a major group of serine/threonine (Ser/Thr) phosphatases involved in the regulation of numerous cellular pathways; i.e. cell growth and signaling (Janssens & Goris, 2001). Protein phosphatase 2A phosphatase activator (PTPA) is an essential and evolutionary conserved protein. Its two homologues in S. *cerevisiae* have been described so far, Rdr1 and Rdr2 (Rempola et al, 2000). PTPA and its homologues activate the phosphoserine/threonine-specific activity of PP2A and PP2A-like phosphatases (Van Hoof et al, 1994), (Fellner et al, 2003), (Van Hoof et al, 2005), (Hombauer et al, 2007). It was also shown that PTPA and its *S. cerevisiae* homologues have PPIase activity, which is similar to the activity of cyclophilin A (CypA) and FKBP12. Therefore, it was suggested that PTPA could use PPIase mechanism in order to regulate PP2A phosphatase activity (Jordens et al, 2006).

1.1.3. Cyclophilins

Cyclophilins have been found in numerous organisms including vertebrates, plants, fungi and bacteria. They all have one structurally conserved domain, which possesses PPIase activity (Wang & Heitman, 2005). First discovered cyclophilin, CypA, has only one PPIase domain, which corresponds to an eight-stranded antiparallel β-barrel enclosed by two α helixes (Fig. 1.4.), (Ke et al, 1991), (Kallen et al, 1991). Unlike single domain CypA, other cyclophilins can be more complex and include amino-terminal signal peptides directing them to endoplasmitic reticulum (ER) or mitochondria, transmembrane domains, TPR repeats and serine/arginine (Ser/Arg) rich domains (SR) (Wang & Heitman, 2005). For example, human Cyp358 (Nup358), largest cyclophilins known so far, apart from the PPIase domain, has also a Leucine (Leu) rich domain, a Zinc-finger and Ran-binding domains. It is a Ran-binding component of nuclear pores (Wu et al, 1995). Human cyclophilin Cyp40 has PPIase domain at N-terminus and TPR repeats at C-terminus. As other cyclophilins it is evolutionally conserved and the structure is preserved in its *S. cerevisiae*, Cpr6 and Cpr7, and *S. pombe*, SpCyp5, homologues (Arevalo-Rodriguez et al, 2004),(Pemberton & Kay, 2005).

Cyclophilins are expressed in most tissues and fulfill various functions. CypA, apart from immunosuppressive actions performed by CypA – CsA complexes (Fig. 1.2.), also performs other functions via its PPIase activity. For example, it promotes formation of human immunodeficiency virus (HIV) virions (Bosco et al, 2002). CypA is also involved in maturation of oligometic receptors (Helekar et al, 1994) and in regulation of activity of essential Zn-finger proteins (Ansari et al, 2002). CypA was indentified recently as a mediator of endothelial activation and linked to rheumatoid arthritis (Kim et al, 2004), (Pap, 2005). Another cyclophilin family member, Cyp358, is a nucleoporin. It is required for nuclear import and plays important role in cell polarization (Hutten et al, 2009), (Murawala et al, 2009). Cyp40 is a well-studied cyclophilin and regulates the activity of transcriptional factor c-Myb (Leverson & Ness, 1998). Like FKBP51 and FKBP52 (Section 1.1.2.), Cyp40 has also been indentified in steroid receptor complexes as co-chaperon. It is also most abundant in progesterone receptor complexes (Freeman et al, 1996).

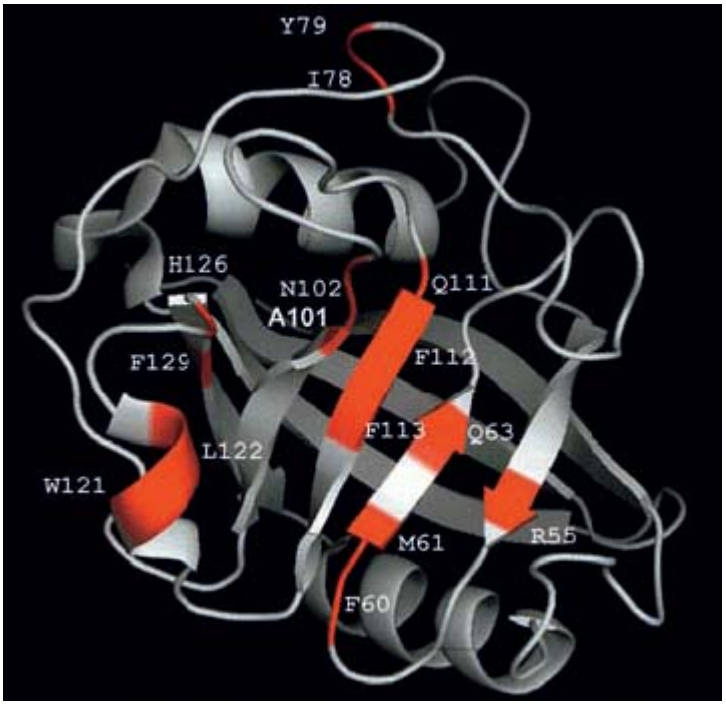

Fig. 1.4. Ribbon presentation of CypA structure. From: (Barik, 2006).

1.1.3.1. Cyclophilins with Ser/Arg rich domains.

An interesting member of cyclophilin family is human SRcyp – a Ser/Arg-rich nuclear matrix associated cyclophilin. The protein has an RS domain (serine/arginine rich domain) similar to the domain found in SR protein family of pre-mRNA splicing regulators. It has been shown to interact specifically with the phosphorylated C-terminal domain (CTD) of RNA Polymearse II (RNAP II) (Section 1.2.). Therefore, it was suggested that SRcyp links RNA transcription to pre-mRNA processing (Bourquin et al, 1997). Two similar SR cyclophilins were discovered in *A. thaliana*, CypRS64 and CypRS92. They consist of an N-terminal PPIase domain and a C-terminal RS domain, that has many Ser/Arg and serine/proline (Ser/Pro) repeats. They were shown to interact with *A. thaliana* SR proteins and U1 and U11 small nuclear ribonucleoprotein (snRNP)-associated proteins U1-70K and U11-95K, respectively. The fact that interaction between CypRS64 and SRp34/SR1 is phosphorylation dependent is noteworthy (Lorkovic et al, 2004). Studies of SR cyclophilins U4/U6 snRNP-associated cyclophilin USA-Cyp as well as several others cyclophilins associated with different spicosomal complexes indicate their involvement in the dynamic organization of splicing machinery (Horowitz et al, 1997), (Lorkovic et al, 2004), (Mesa et al, 2008).

One of the most complex cyclophilins is Kin241 from *Paramecium tetraurelia*. Similar to the above described SR cyclophilins, it has a PPIase domain at its N- terminus and an RS domain – at its C-terminus. These two domains are separated with an RNA recognition motif (RRM). Kin241 is a conserved protein involved in cell morphogenesis (Krzywicka et al, 2001). One of Kin241 homologues, AtCyp59 from *Arabidopsis thaliana*, was isolated in a yeast two hybrid (Y2H) screen with SR protein SCL33/SR33 as bait. It has same domain arrangement as Kin241. In addition, there is a zinc knuckle motif in front of the RS domain (Fig. 1.5.) and this feature seems to be specific for plant homologues only (Gullerova et al, 2006).

Fig. 1.5. AtCyp59 domain composition. PPIase – peptidyl-prolyl *cis/trans* isomerase domain; RRM – RNA recognition motif; Zn - Zinc knuckle; RS/RD – domain, rich in RS/RD (arginine, serine/arginine, aspartic acid) repeats.

Orthologues of AtCyp59 were found in the majority of eukaryotic genomes, such as *H. sapiens* (PPIL4), *M. musculus*, *D. melanogaster* and *S. pombe* (Rct1) (Zeng et al, 2001), (Carninci et al, 2000), (McKee et al, 2005), (Adams et al, 2000), (Mount & Salz, 2000), (Gullerova et al, 2007). Proteins from different organisms exhibit particularly high conservation in the RRM domains. As AtCyp59 was shown to bind RNA *in vitro*, this motif most probably mediates AtCyp59 interaction with RNA. RS domain is the least conserved one and is responsible for nuclear localization of the protein and its interaction with *Arabidopsis* SR proteins. The study also revealed that AtCyp59 not only interacts with the CTD of RNAP II, but also affects its phosphorylation (Gullerova et al, 2006), (Section 1.3.).

As there was no T-DNA insertion *Arabidopsis* mutant available, further investigation of AtCyp59 was continued on its *S. pombe* homologue Rct1, which is 49% identical and 66% similar to AtCyp59 (Gullerova et al, 2007). There is no homologue of AtCyp59 in *S. cerevisiae* and in general the similarity level of *S. pombe* cyclophilin repertoire is higher to metazoans than to that of *S. cerevisiae* (Pemberton & Kay, 2005). In addition to that, in *S. cerevisiae* all the cyclophilins have been individually and

collectively knocked out showing no effect on cell viability (Dolinski et al, 1997). Rct1, on the contrary, turned out to be an essential gene (Gullerova et al, 2007).

Rct1 is a nuclear protein and has same domain order as AtCyp59, but like Kin241 lacks Zinc knuckle. Knocking out one of *rct1* alleles caused pleiotropic phenotype resulting in growth, morphological and meiotic defects. Last ones are manifested by enhanced sporulation of $rct1^{+/-}$ cells in EMM-N. Observed phenotypes are clearly a consequence of the reduced Rct1 levels, as they can be rescued by Rct1 episomal expression. Moreover, Rct1 has been shown to affect CTD phosphorylation status and RNAP II transcription (Gullerova et al, 2007), (Section 1.3.).

1.1.4. Parvulins

Another group of proteins that has PPIase activity are pavulins. First parvulin Par10 was discovered in *E. coli* (Rahfeld et al, 1994). Later, parvulins were found in prokaryotic and eukaryotic organisms. Prokaryotic parvulins, apart from PPIase activity, demonstrate chaperon-like functions (Missiakas & Raina, 1997).

Human Pin1 is the most extensively studied parvulin so far. It was identified as an interaction partner of *A. nidulans* NIMA (never in mitosis), a mitotic kinase (Lu et al, 1996). Pin1 is evolutionary conserved and has homologues in many eukaryotes including Dodo in *D. melanogaster*, Pin1 in *A. nidulans*, Pin1 in *M. musculus*, Ess1 in *S. cerevisiae* and Pin1 in *S. pombe* (Maleszka et al, 1996), (Crenshaw et al, 1998), (Hanes et al, 1989), (Huang et al, 2001). Structural studies of Pin1 have shown that it is the only PPIase that specifically recognizes phosphorylated serine/threonine-proline (pSer/Thr-Pro) sequences. Pin1 WW domain binds to specific motifs and the PPIase domain accelerates isomerization of pSer/Thr-Pro sequences (Fig.1.6.), (Yaffe et al, 1997), (Ranganathan et al, 1997), (Lu & Zhou, 2007).

Ser/Thr-Pro is a main regulatory phosphorylation motif in cells and kinases, responsible for its phosphorylation, play crucial role in different cellular processes. That is why Pin1 discovery was a breakthrough in understanding the importance of the pSer/Thr-Pro isomerization. A new signaling mechanism was proposed, where Pin1 regulates isomerization of its substrates after phosphorylation in order to control their function (Zhou et al, 1999), (Wulf et al, 2005). Subsequent studies revealed an important impact of

Pin1-catalyzed conformation on numerous proteins involved in such processes as cell cycle, transcription, stress and immune responses, embryo development, neuronal function and aging (Xu & Manley, 2007a), (Xu & Manley, 2007c), (Yeh & Means, 2007), (Section 1.2.1.2.), (Xu & Manley, 2007b), (Shaw, 2007), (Xu & Manley, 2004), (Zheng et al, 2002), (Goutagny et al, 2006), (Atchison & Means, 2004), (Becker & Bonni, 2007), (Liou et al, 2003), (Lu et al, 2007), (Lu & Zhou, 2007),(Wulf et al, 2005). Moreover, Pin1 deregulation was shown to play a critical role in an increasing number of pathologies including cancer, Alzheimer's disease, asthma and infection (Lu, 2004), (Maudsley & Mattson, 2006), (Butterfield et al, 2006), (Yeh & Means, 2007), (Balastik et al, 2007), (Wang et al, 2007), (Takahashi et al, 2008), (Eckert et al, 2005), (Goutagny et al, 2006), (Lu et al, 2007), (Lu & Zhou, 2007),(Wulf et al, 2005).

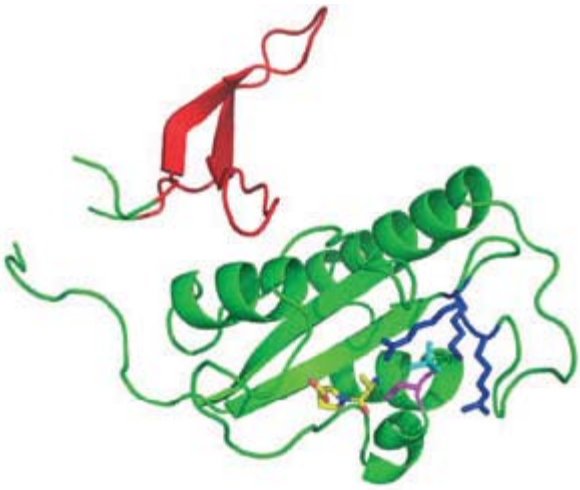

Fig. 1.6. Molecular structure of Pin1. PPIase domain is green, WW domain – red, linker region – yellow. From: (Lippens et al, 2007).

1.2. RNAP II transcription

RNAP II is responsible for transcription of protein-coding genes and small non-coding RNA in eukaryotes. The RNAP II transcription cycle include following steps: initiation, elongation and termination. During the initiation, RNAP II forms complex with general transcription factors and cofactors at promoter region, followed by the alignment of the DNA template to the active RNAP II site. Nucleotides are paired to the template and

form an RNA transcript during elongation. Final step is the termination, when the mature messenger RNA (mRNA) is released and transcription complex dissociates from the DNA. Formation of mature mRNA requires several processing events: capping, splicing and polyadenylation. They are tightly connected to transcription and often happen in parallel to it. Capping results in addition of a methylated guanosine to the 5' end of the transcript. Splicing removes introns from the transcript. During polyadenylation 3' end of the mRNA precursor is cleaved and supplied with poly(A) tail. Capping and polyadenilation stabilize transcript (Saunders et al, 2006), (Sims et al, 2004), (Hirose & Manley, 2000).

Histone modifications, so called histone code, are tightly associated with transcription (Jenuwein & Allis, 2001). Covalent histone changes can alter properties of chromatin and influence RNAP II progression along a transcription unit. The best studied modifications are acetylation and methylation. Besides, histone ubiquitination, phosphorylation and biotinylation play important roles in chromatin turnover (Kouzarides, 2007), (Berger, 2007). Histones are reversibly acetylated on lysine (K) residues by histone acetyltransferases, whereas histone deacetylases remove the acetyl groups. Acetylation of histones H3 and H4 typically correlates with active genes and dominates at the promoters and 5'-end regions, however it is also important at coding regions (Kurdistani & Grunstein, 2003), (Liu et al, 2005), (Pokholok et al, 2005), (Munshi et al, 2009). Histone acetylation is a dynamic process, whereas histone methylation is considered as a stable mark. Lysine and arginine residues are mono-, di- and tri-methylated by a large family of methyltransferases, which are specific for individual residues. Demethylation is performed by demethylases, which also reveal substrate specificity. Together, two groups of enzymes provide a transcription unit with a distinctive pattern of methylation, which can correlate with either activation, or repression of transcriptional activity. Thus, trimethylated H3 lysine 4 (H3K4me3) prevails at promoter-proximal regions and correlates strongly with active transcription, dimethylated H3 lysine 4 (H3K4me2) is associated with the 5'-end and middle of a gene and monomethylated H3 (H3K4me) lysine 4 peaks at the 3'-end, marking transcriptional inhibition. Histone H3 lysine 36 tri- and di-methylations (H3K36me3 and me2) are present throughout open reading frames (ORFs) of active genes (Schneider et al, 2004), (Liu et al, 2005), (Pokholok et al, 2005), (Rao et al, 2005), (Munshi et al, 2009). Another histone modification, ubiquitination, has been recently described. Monoubiquitylated H2B (H2Bub1) is localized at the promoter and the coding

region. This histone modification is associated with actively transcribed genes. H2A monoubiquitinitaion, however, is found at silenced promoters (Weake & Workman, 2008), (Suganuma & Workman, 2008).

1.2.1. The CTD

RNAP II consists of 12 subunits (Rpb1-Rbp12) that comprise together about 0.5 MDa. The largest subunit Rpb1 possesses a very unusual C-terminal domain (the CTD). It is a unique eesential structure consisting of heptapeptide repeats Tyr1-Ser2-Pro3-Thr4-Ser5-Pro6-Ser7. The motif is conserved among most eukaryotes, although number of repeats grows with the genome complexity: 26 in *S. cerevisiae*, 29 in *S. pombe*, 45 in *D. melanogaster* and 52 in *H. sapiens* (Egloff & Murphy, 2008). In many eukaryotes, for example in yeast, the sequence in the most repeats is strictly conserved, whereas in mammals proximal 26 repeats closely correspond the consensus and sequences of distal ones are more diverse. Previous studies have revealed that Tyr1, Ser2 and Ser5 are essential and deletion of more than two-thirds of the CTD heptads makes cells non-viable (Bartolomei et al, 1988), (Nonet et al, 1987), (Corden, 1990), (West & Corden, 1995). Moreover, it was shown that functional unit of the CTD lies within heptapeptide pairs (Stiller & Cook, 2004), (Chapman et al, 2008).

The CTD serves as a platform for a broad range of factors and plays a crucial role in transcription and its coupling to histone modifications and RNA processing. The CTD interacts dynamically with various factors at different time points of the RNAP II transcription cycle. Reversible CTD modifications, especially its phosphorylation, define efficient transcript synthesis and recruitment of transcription and processing factors. In other words there is a “CTD code” that determines RNAP II position in the transcription cycle (Buratowski, 2003), (Fig. 1.7.).

This code is defined by such modifications of the heptapeptade residues as phosphorylation of tyrosine, threonine and all three serines, glycosylation of serines and

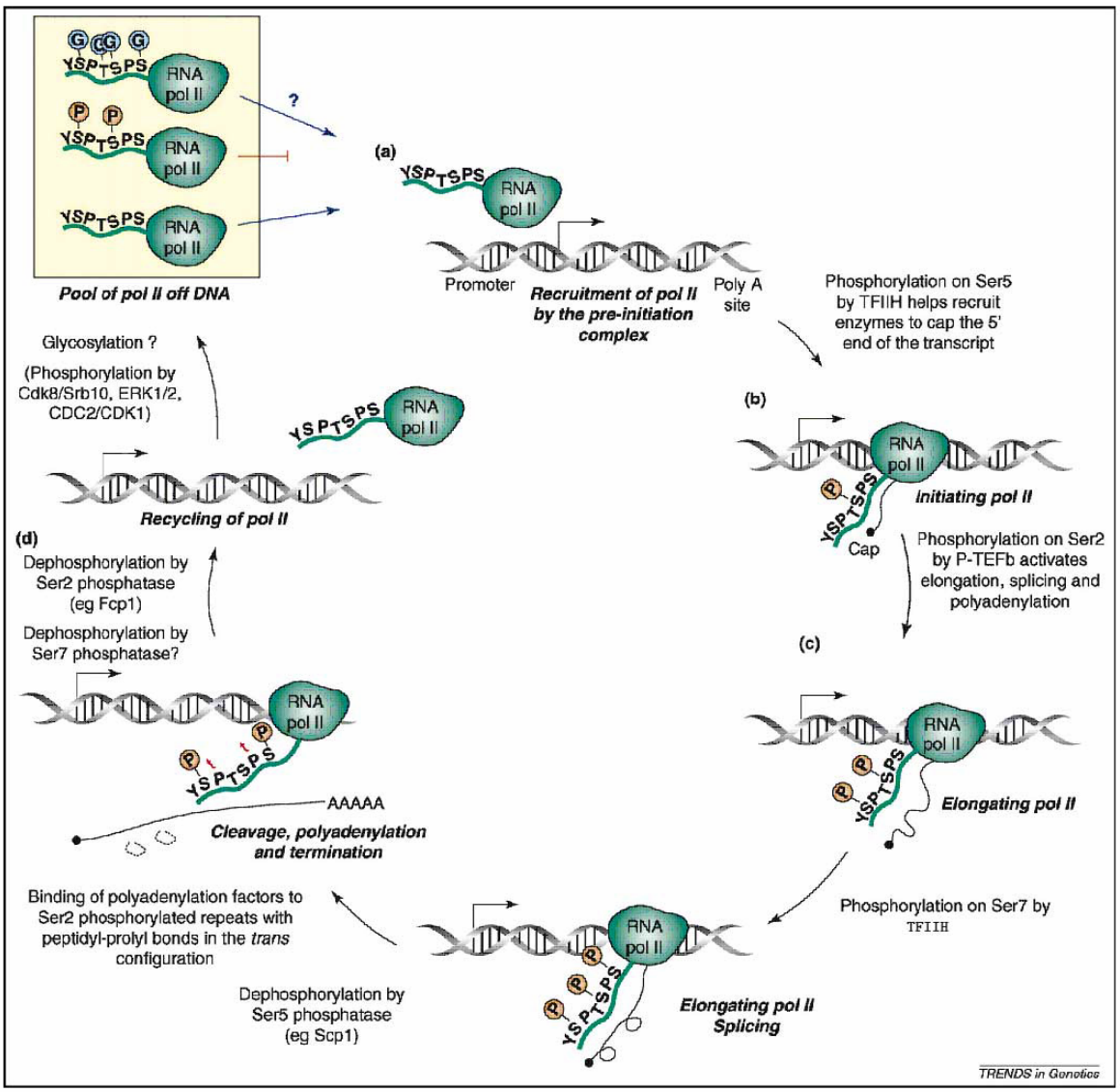

Fig. 1.7. The CTD modifications during the transcription cycle. (A) RNAP II recruitment at the promoter, the CTD is unphosphorylated, might be glycosilated. Phosphorylation of RNAP II prior to initiation is thought to block the recruitment. (B) Phosphorylation of Ser5 by Cdk7, component of TFIIH, helps to recruit capping enzymes. (C) Cdk9, component of p-TEFb, phosphorylates Ser2, that reaction activates RNA elongation and processing. Ser7 gets also phosphorylated by TFIIH (Kim et al, 2009), (Akhtar et al, 2009), (Glover-Cutter et al, 2009). Ser5 gets dephosphorylated during the elongation. (D) Once the cleavage and polyadenilation are over, CTD dephosphorylation prepares RNAP II for a new round of transcription. Adopted from: (Egloff & Murphy, 2008).

threonines and isomerization of prolines (Meinhart et al, 2005). Nonconsesus repeats of the CTD add complexity as well. They are preferred substrates for Cdc2 and cyclin-

dependent kinase 7 (Cdk7) kinases *in vitro* and their substitution to the consensus repeats does not affect cell viability (Rickert et al, 1999), (Chapman et al, 2005), (Chapman et al, 2007). Besides, a short motif at the very C-terminus of the CTD was found to play a role in the stability and functions (transcription, splicing, 3' end processing) of the RNAP II CTD (Fong et al, 2003), (Chapman et al, 2004).

1.2.1.1. CTD phosphorylation

Phosphorylation of CTD residues is the best studied modification so far (Phatnani & Greenleaf, 2006). First, two distinct fractions of RNAP II were identified: RNAP IIA – hypophosphorylated and RNAP IIO – hyperphosphorylated. Later it was shown that *in vivo* mainly Ser2 and Ser5 residues of the heptapeptide repeats get phosphorylated by cyclin-dependent proline-directed Ser/Thr kinases. Serine 5 phosphorylation correlates with transcription initiation and early elongation whereas Ser2 phosphorylation correlates with elongation and termination (Komarnitsky et al, 2000), (Palancade & Bensaude, 2003), (Phatnani & Greenleaf, 2006).

The transcription cycle starts with recruitment of hypophophosphorylated RNAP II to a promoter (Fig. 1.7.). Phosphorylation of Ser5 CTD residue by Cdk7 (Kin28 in *S. cerevisiae*, Mcs6 in *S. pombe*), a component of TFIIH transcription factor, is necessary for promoter escape and transcript capping (Komarnitsky et al, 2000), (Ho & Shuman, 1999). The initiating RNAP II complex is unstable and could abort transcription after few nucleotides. Once escaped from promoter, RNAP II progresses to pausing site where it is suppressed by negative factors. The pause release and subsequent productive elongation onset require phosphorylation of CTD Ser2 residue by Cdk9 (Ctk1/Bur1 in *S. cerevisiae*, Cdk9/Lsk1 in *S. pombe*), catalytic subunit of positive transcription elongation factor b (p-TEFb). TFIIH phosphorylation of the CTD and capping assists recruitment of p-TEFb (Lolli, 2009), (Guiguen et al, 2007), (Pei et al, 2003), (Viladevall et al, 2009), (Qiu et al, 2009). Besides, p-TEFb was reported to phosphorylate Ser5 as well (Jones et al, 2004), (Zhou et al, 2000a), (Pei et al, 2006), (Viladevall et al, 2009). Phosphorylation of Ser2 increases towards the 3' end of the gene and it seems to be involved in recruitment of splicing and polyadenylation factors to a nascent transcript (Proudfoot et al, 2002). For

example, elongation factor Spt6 binds specifically to Ser2-phosphorylated heptads in order to direct splicing (Yoh et al, 2007). During transcription the CTD was also found to be phosphorylated on both Ser2 and Ser5 residues by budding yeast Srb10, a subunit of the Mediator complex, and on Ser5 residues by its human homologue Cdk8 (Hengartner et al, 1998), (Rickert et al, 1999), (Sun et al, 1998).

Phosphorylation of Ser7 residues, identified in *S. cerevisiae* and *H. sapiens*, is less understood. Serine 7 phosphorylation is performed by Cdk7 (Kin28). It peaks at promoter and 3' end of the gene, suggesting its role in transcription and 3' end processing (Chapman et al, 2007), (Akhtar et al, 2009), (Glover-Cutter et al, 2009), (Kim et al, 2009). Additionally, it is essential for small nuclear RNA (snRNA) transcription (Egloff et al, 2007).

CTD phosphatases are required to perform RNAP II dephosphorylation, which is necessary to start a new cycle of transcription. Fcp1 is a conserved and essential protein, which dephosphorylates both the free and the DNA bound CTD. Fcp1 was reported to dephosphorylate Ser2 and Ser5 in humans (Lin et al, 2002). In fission and budding yeast, however, Fcp1 was shown to remove phosphates from Ser2 residues (Hausmann & Shuman, 2002), (Cho et al, 2001). It is recruited at early transcription stages and stimulates elongation (Cho et al, 2001), (Mandal et al, 2002). Small CTD phosphatases (Scp1), characterized recently in mammals, also belong to the Fcp1 family and preferentially dephosphorylate Ser5 of the CTD, suggesting their role in initiation-elongation transition phase (Yeo et al, 2003), (Zhang et al, 2006). Another new CTD phosphatase, Rtr1, from *S. cerevisiae* has similar function. It targets Ser5 as well and was reported to direct the RNAP II CTD transition from pSer5 (phosphorylated Ser5) form to pSer2 stage (Mosley et al, 2009). Ssu72 is also a conserved and essential phosphatase that is required for elongation and termination. In budding yeast it is a subunit of a cleavage-polyadenilation factor (CPF) and was shown to dephosphorylate Ser5 residue of the CTD (Steinmetz & Brow, 2003), (Krishnamurthy et al, 2004). Mammalian Ssu72 was reported to bind another subunit of yeast CPF, Pta1 (St-Pierre et al, 2005).

1.2.1.2. Proline izomerization

The CTD of RNAP II is rich in Ser/Thr-Pro motifs, that are specific targets of certain Cdks. Importantly, Pro-directed kinases and phosphatases were reported to functions only on the *trans* conformation of Ser/The relative to Pro (Weiwad et al, 2000), (Brown et al, 1999), (Zhou et al, 2000b). The proline residues of the RNAP II CTD perform the conformational change of the CTD and thereby assist binding of its partners. Recent structural studies support the idea of the CTD dynamic structure, as capping enzyme Cgt1, Pin1 and 3'-end processing factor Pcf11 bind the C-terminus only in *trans* proline conformation (Meinhart et al, 2005). As the prolyl peptide bond shows a slow rate of *cis/trans* isomerization, this step could be rate limiting in transcription and its coupling with RNA processing. Therefore, the CTD appears to be an optimal target for the PPIases due to the multiple binding motifs.

Human Pin1 and its homologue from budding yeast, Ess1, were shown to bind and isomerize specifically pSer/Thr-Pro motifs (Section 1.1.4.), (Yaffe et al, 1997), (Hani et al, 1999). Pin1 and Ess1 were reported to interact with the phosphorylated CTD (Verdecia et al, 2000), (Morris et al, 1999), (Wu et al, 2000), showing *in vitro* preference for Ser5 phosphorylated heptapeptides (Albert et al, 1999), (Gemmill et al, 2005). Pin1 overexpression causes CTD hyperphosphorylation, RNAP II release from active genes and, consequently, transcription and splicing inhibition (Xu & Manley, 2007b). *Ess1* mutants, however, are suppressed by Fcp1 phosphatase overexpression and accumulate Ser5 phosphorylated form of the CTD, whereas Ess1 overexpression leads to Ser5 dephosphorylation (Wu et al, 2000), (Krishnamurthy et al, 2009), (Singh et al, 2009). Pin1 affects transcription initiation stage, inhibiting transition to elongation. This data go in line with the facts that Pin1 inhibits Fcp1 dephosphorylation of the CTD and associates with Spt5 (Kops et al, 2002), (Xu et al, 2003), (Lavoie et al, 2001), (Shaw, 2007). Spt5 is an essential protein rich in Ser/Thr-Pro repeats. Together with Spt4, Spt5 comprises a 5,6-dichloro-1-*b*-D-ribofuranosylbenzimidazole (DRB) sensitivity factor (DSIF) and is required for the onset of productive elongation (Section 1.2.2.). Moreover, Fcp1, as mentioned above, might be responsible for transition from initiation to elongation. Unlike Pin1, Ess1 affects multiple transcription stages (Wu et al, 2000), (Wu et al, 2003), (Krishnamurthy et al, 2009). Genetic interactions of Ess1 with general transcription factor TFIIB, component of RNAP II preinitiation complex, and Ser5 kinase Kin28 suggest

involvement of this PPIase in transcription initiation. Ess1 is also engaged in elongation phase, as it has been reported to interact genetically with Ser2 CTD kinases, Ctk1 and Bur1, and Ser2 CTD phosphatase, Fcp1. Functional interactions of Ess1 with components of CPF, Ssu72 and Pta1, provide evidence for its role in termination of transcription (Wilcox et al, 2004), (Krishnamurthy et al, 2009). Ess1 function in pre-mRNA 3'-end processing was reported (Hani et al, 1999), (Morris et al, 1999), but the authors of the recent article claim that Ess1 is not required for 3'-end processing (Krishnamurthy et al, 2009). Recent studies demonstrate Ess1 function in Nrd1-dependant termination of small nuclear RNAs (snoRNA), cryptic unstable transcripts (CUTs) and upstream regulatory RNA (uRNA) (Singh et al, 2009).

Many experiments provided the evidence that interaction of different transcription and processing factors with the CTD is mediated by enzymatic proline isomerization. However, it has not been shown unequivocally yet.

1.2.2. The CTD code meets the histone code

Chromatin state of a transcribed gene is tightly connected to RNAP II CTD phosphorylation (Berger, 2007). Histone methylation is a good example for this link. In *S. cerevisiae* histone methyltransferase Set1, that catalyzes H3K4me3, interacts with the Ser5 phosphorylated CTD through the PAF (polymerase associated factor) complex. Methyltransferase Set2, which is responsible for H3K36 methylation, binds directly the Ser2/Ser5 phosphorylated CTD. Accordingly, H3K4me3 and the pSer5 CTD are associated with early transcribed regions of a gene, hence transcription initiation, whereas H3K36me and the Ser2/Ser5 phosphorylated CTD correlate with elongation and termination steps (Hampsey & Reinberg, 2003).

1.2.3. P-TEFb and its role in promoter-proximal stalling and mRNA capping

P-TEFb in humans is a heterodimer composed of one of four C-type cyclins (T1, T2a, T2b or K) and Cdk9 (represented by two isoforms – 42 kDa and 55 kDa). An inactive form of pTEFb in bound to 7SK snRNA, which in turn associates with specific 7SK

snRNA methylphosphate capping enzyme (MePCE) and La-related protein 7 (LARP7), that stabilizes 7SK snRNA. The 7SK snRNA is highly conserved in vertebrates and plays one of the key roles in RNAP II transcription by mediating the interaction between inactive p-TEFb and either HEXIM1 or HEXIM2 proteins (Marz et al, 2009), (Diribarne & Bensaude, 2009). Cooperative binding of Cdk9/cyclin/7SK snRNA/HEXIM1 or HEXIM2/MePCE/LARP7 has been identified as inactive p-TEFb form (Kohoutek, 2009). Three major cellular substrates of p-TEFb are the RNAP II CTD, DSIF and negative elongation factor (NELF) (Marshall et al, 1996), (Kim & Sharp, 2001), (Fujinaga et al, 2004), (Yamada et al, 2006), (Peterlin & Price, 2006).

In fission and budding yeast functions of p-TEFb are split between an essential kinase/cyclin dimmer, Cdk9/Pch1 in fission yeast and Bur1/Bur2 in budding yeast, and a nonessential trimer complex, kinase/cyclin/regulatory subunit, Lsk1/Lsc1/Lsg1 in fission yeast and Ctk1/Ctk2/Ctk3 in budding yeast. Lsk1/Lsc1/Lsg1 and Ctk1/Ctk2/Ctk3 appear to be primarily responsible for Ser2 phosphorylation (Pei & Shuman, 2003), (Wood & Shilatifard, 2006), (Karagiannis & Balasubramanian, 2007), (personal communication with Sukegawa). At the same time Cdk9/Pch1 and Bur1/Bur2 promote productive elongation providing high level of the Ser2 phosphorylated CTD (Viladevall et al, 2009), (Qiu et al, 2009). Cdk9/Pch1 in fission yeast and Bur1/Bur2 in budding yeast activate Spt5, a subunit of DSIF, which is critical for transcriptional elongation, mRNA processing and cotranscriptional histone modifications (Pei & Shuman, 2003), (Schwer et al, 2009), (Liu et al, 2009), (Chen et al, 2009), (Zhou et al, 2009), (Chen et al, 2009). Additionally to that, Cdk9/Pch1 complex is stably associated with Pcm1, guanine-N7 methyltransferase component of mRNA capping machinery in fission yeast in 1:1 stoichiometry. Besides, if during Cdk9 complex purification protein extracts are treated with RNase A, Cdk9/Pch1/Pcm1 complex shifts to a smaller size, suggesting a ribonucleoprotein constituent. However, the putative RNA does not seem to affect the kinase activity of the recovered fraction (Pei et al, 2006).

P-TEFb was also reported to regulate histone modifications such as H2Bub1, H3K4me3 and H3K36me3 through pSer2- and DSIF-dependent mechanisms (Pirngruber et al, 2009a), (Pirngruber et al, 2009b). In budding yeast these functions are split between Bur1 and Ctk1. Ctk1 launches H3K36me3 modification by catalyzing Ser2 phosphorylation of the CTD (Krogan et al, 2003), (Xiao et al, 2003). Ctk1 also specifically regulates H3K4 trimethylation localizing it to the 5' ends of genes (Xiao et al, 2007). Bur1

was shown to regulate H2Bub1 and H3K4me3 by phosphorylating Rad6 (E2 ubiquitin conjugase), Spt5 and the RNAP II CTD (Kao et al, 2004), (Liu et al, 2005), (Laribee et al, 2005), (Wood et al, 2005), (Zhou et al, 2009), (Chu et al, 2007).

Phosphorylation of cyclin and Cdk9 is crucial for p-TEFb activation. The most important step for full activation of Cdk9 is phosphorylation of its conserved Thr residue in the T-loop. In mammals it is autophosphorylated whereas PPM1A phosphatase regulates its dephosphorylation (Li et al, 2005), (Baumli et al, 2008), (Wang et al, 2008). In yeast, however, p-TEFb activation is regulated by upstream kinases, Cak1 (budding yeast) and Csk1 (fission yeast) (Yao & Prelich, 2002), (Ostapenko & Solomon, 2005), (Pei et al, 2006). Besides, human p-TEFb activity was reported to be controlled by ubiquitination and acetylation of Cdk9, cyclin T1 and HEXIM1 (Kiernan et al, 2001), (Barboric et al, 2005), (Fu et al, 2007), (Sabo et al, 2008), (Lau et al, 2009), (Cho et al, 2009), (Kohoutek, 2009).

Promoter-proximal stalling occurs when RNAP II pauses after transcribing 20 to 40 nucleotides and needs to be stimulated to continue into productive elongation phase (Fig. 1.8.). It was first found in heat-shock inducible *Drosophila* genes (Gilmour & Lis, 1986) and later confirmed in an abundant number of both inducible and housekeeping genes in eukaryotes and during viral transcription. Recent findings support the idea that promoter-proximal stalling might even be an obligatory step for RNAP II transcription (Core et al, 2008). It can provide a check point for correctly prepared elongation complex and rapid gene expression regulation (Lis, 1998), (Wu & Snyder, 2008), (Core & Lis, 2008), (Fuda et al, 2009).

Main pausing factors are DSIF, conserved from yeast to humans (Hartzog et al, 1998), (Wada et al, 1998), (Yamaguchi et al, 2002) and negative elongation factor (NELF), which consists of four subunits A, B, C/D and E. NELF is conserved between *D. melanogaster* and mammals. As it is not present in *S. cerevisiae* and *S. pombe*, it might be a less general elongation factor than DSIF (Yamaguchi et al, 1999), (Narita et al, 2003).

The first pre-mRNA processing event, the 5'-end capping of a nascent RNAP II transcript, occurs during promoter-proximal pausing, which might facilitate the process (Rasmussen & Lis, 1993), (Pei et al, 2003). The unique structural properties of the cap play important role in further gene expressing steps (Maniatis & Reed, 2002), (Orphanides & Reinberg, 2002). Three enzymatic activities are necessary for capping of the mRNA 5' end. RNA triphosphatase removes the first nucleotide γ-phosphate, RNA

guanylyltransferase transfers GMP to the remaining diphosphate and RNA methyltransferase adds a methyl group at the N7 position on the guanine. In metazoans there are a bifunctional triphosphatase-guanylyltransferase (Mce1 in mammals) and a methyltransferase (Hcm1 in mammals). Yeast has three separate enzymes: triphosphatase (Cet1 in *S. cerevisiae* and Pct1 in *S. pombe*), guanylyltransferase (Ceg1 in *S. cerevisiae* and Pce1 in *S. pombe*) and methyltransferase (Abd1 in *S. cerevisiae* and Pcm1 in *S. pombe*). Capping occurs cotranscriptionally and is facilitated by interactions of capping proteins with RNAP II and transcription factors. Capping enzymes including mammalian Mce1, Ceg1 and Abd1 from budding yeast and fission yeast Pct1 and Pce1 interact with the Ser5 phosphorylated CTD. Besides, the human and fission yeast capping enzymes (Mce1, Pct1 and Pce1, respectively) bind Spt5 (Moteki & Price, 2002), (Mandal et al, 2004), (Schroeder et al, 2000), (Rodriguez et al, 2000), (Pei & Shuman, 2002), (Pei et al, 2003), (Pei et al, 2006).

Ser5 phosphorylated RNAP II is responsible for initiation step of the transcription, but not for productive elongation. DSIF binds to RNAP II during or straight after initiation, followed by NELF interaction with DSIF to pause RNAP II. In the meanwhile Spt5 as well as TFIIH via the pSer5 CTD recruit the capping machinery (Egloff & Murphy, 2008), (Fuda et al, 2009). The pre-mRNA transcript is getting capped, followed by the cap methylation. Later, the negative effects of DSIF and NELF on RNAP II elongation are relieved by p-TEFb. Phosphorylation of NELF, Spt5 and Ser2 of the CTD by p-TEFb as well as capping enzyme activity facilitate the release of stalled RNAP II into productive elongation (Sims et al, 2004), (Saunders et al, 2006), (Peterlin & Price, 2006), (Fujita et al, 2009).

In human cells several specific regulators and a general chromatin remodeling bromodomain-containing protein Brd4 are known to be responsible for the p-TEFb recruitment to the transcription unit (Yaffe et al, 1997), (Garriga & Grana, 2004), (Jang et al, 2005). In fission yeast, however, Pcm1 fulfills this function (Guiguen et al, 2007). Additionally, fission yeast Cdk9 was shown to interact with Pct1 in Y2H screen (Pei et al, 2003). Another example of p-TEFb recruitment is its role in HIV-1 transcription. P-TEFb associates with an early RNAP II elongation complex via cyclin T binding to the HIV-1 encoded Tat protein, which in turn interacts with the transactivation response (TAR) element in the HIV-1 transcript (Price, 2000), (Barboric & Peterlin, 2005), (Kohoutek, 2009).

RNA chain cleavage factor TFIIS is also important for RNAP II escape from the pause. It stimulates the intrinsic RNA-cleavage activity of RNAP II, which is responsible for creating a new 3'-OH end at the active site of RNAP II after its backtracking (Adelman et al, 2005). Spt5 methylation and Fcp1 phosphatase activity were reported to mediate RNAP II release from the pause as well (Cho et al, 2001), (Kwak et al, 2003). As a result NELF dissociates from the transcription complex where as TSIIF, DSIF and p-TEFb stay within the complex along the gene. Moreover, in humans such factors as eleven-nineteen lysine-rich in leukemia (ELL), general transcription factor IIF (TFIIF) and elongin are also involved in RNAP II escape from the stalling phase (Sims et al, 2004), (Saunders et al, 2006), (Peterlin & Price, 2006), (Fujita et al, 2009).

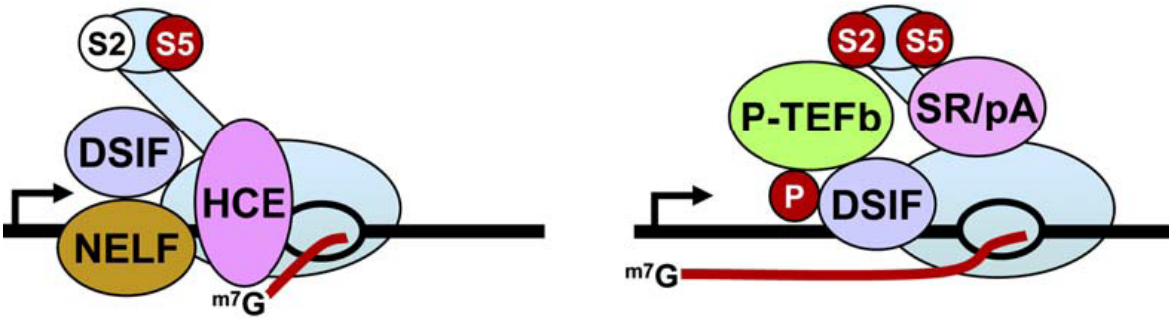

(a) Capping and pausing (b) Productive elongation

Fig. 1.8. RNAP II pausing. (a) Recruitment of human capping enzymes (HCE) (Mce1 and Hce1), capping of the 5'-end of the nascent transcript and RNAP II pausing. (b) Recruited p-TEFb phosphorylates DSIF and Ser2 of the CTD. Start of the productive elongation and processing by splicing (SR) and polyadenilation (pA) machineries. From: (Peterlin & Price, 2006).

1.3. Aims of the thesis

1. Main aim of the thesis was to **define the role of Rct1 in RNAP II transcription**

1.1. Specific aim 1: Interaction of Rct1 with the CTD, CTD kinases and phosphatases

Both *A. thaliana* AtCyp59 and its *S. pombe* homologue Rct1 were shown to interact with the RNAP II CTD. In addition, overexpression of both homologues resulted in the decrease of CTD phosphorylation whereas reduced levels of Rct1 in heterozygous cells *rct1*$^{+/-}$ lead to increased CTD phosphorylation and reduction of RNAP II transcriptional activity (Gullerova et al, 2006), (Gullerova et al, 2007), (Section 1.1.3.). These findings indicated that Rct1 regulates CTD phosphorylation status. However, the Rct1 target(s) were not identified. The abundance of proline residues in the CTD makes it a very good substrate for Rct1 PPIase activity. During transcription the RNAP II CTD undergoes phosphorylation and dephosphorylation of its 2nd and 5th serines, which define the functional state of the CTD. These modifications are performed in *S. pombe* by CDK kinases/cyclin pairs Msc6/Msc2, Lsk1/Lsc1, Cdk9/Pch1 and Srb10/Srb11, and by phosphatases Fcp1, Ssu72 and Scp1. CDK kinases phosphorylate specifically pSer/Thr-Pro sequences. Besides, Pro-directed kinases were reported to act only on *trans* conformation (Sections 1.2.1.1. and 1.2.1.2.). Thus, Rct1 could either inhibit or promote interaction of the CTD kinases and phosphatases with CTD by changing its conformation. The cyclophilin could also target the enzymes and/or their interaction partners (i.e. cyclins) directly and affect the activity of kinases/phosphatases towards the CTD.

I planned to study interactions between Rct1 and the CTD, CTD kinases, their cyclins and CTD phosphatases using Y2H and GST pull-downs of full-length and mutants proteins.

Kinase assays were planned for studying Rct1 effect on the activity of the CTD kinases/phosphatases.

1.2. Specific aim 1: Step(s) of an RNAP II transcription cycle affected by Rct1

CTD phosphorylation state correlates with RNAP II position along transcribing gene. RNAP II is recruited to a promoter in a hypophosphorylated state. Its escape from promoter requires Ser5 phosphorylation by TFIIH. Later, Ser2 phosphorylation enables the onset of productive elongation. The Ser2 phosphorylated CTD is also required for further stages of transcription cycle. Finally, RNAP II becomes dephosphorylated and able to re-enter next initiation step (Section 1.2.1.1.). Phosphorylation of the CTD is tightly interconnected with covalent histone modifications, which regulate transcriptional activity of genes. Rct1 was shown to regulate negatively CTD phosphorylation and activity of

RNAP II. Rct1 was reported to interact with the RNAP II CTD and be associated with transcriptionally active chromatin during the whole RNAP II transcription cycle (Gullerova et al, 2006), (Gullerova et al, 2007). However, the exact step(s) regulated by Rct1 remained unclear.

The step(s) of the transcription controlled by Rct1 were planned to be studied using chromatin immunoprecipitation (ChIP) method on a single gene under conditions of Rct1 over- and underexpression. ChIP with antibodies against the total RNAP II CTD (phospho- and nonphosphorylated) would show how Rct1 affects the RNAP II occupancy profile along a transcription unit. Performing ChIP with antibodies against phosphorylated forms of RNAP II would reveal phosphorylation changes of actively transcribing RNAP II. Transcriptional activity of the analyzed genes would be studied by doing ChIP with antibodies against total and covalently modified histones (acetylated or methylated), as such histone marks as acetylated H3K4 or H3K9 correlate strongly with active transcription. Complementary approach was planned - nuclear run on (NRO) on a single transcription unit. NRO would provide the information on the amount of RNA produced at a certain time in *wt* and under the conditions of Rct1 over- and underexpression.

2. I was also involved in **determination of functions of Rct1 domains**

Rct1 is an essential multidomain protein and consists of a PPIase domain, an RRM motif and a C-terminal domain enriched in RS/RD repeats. It has been previously shown that Rct1 expression depletion causes strong growth and morphological defects (Gullerova et al, 2007). It was important to find out functions of individual domains.

Deletion and mutational analysis of Rct1 was expected to reveal essential domain(s) and function(s) of each domain.

2. Materials and methods

2.1. *S. pombe* strains and handling of cells

Genotypes of *S. pombe* strains used are listed in Table 2.1.

General genetic methods, media and growth conditions were used as described previously (Moreno et al, 1991) and (Forsburg, http://www-rct.usc.edu~forsburg/). ClonNat (BioAgents) and Geneticin G418 (Gibco) were used at the final concentration of 100 μg/ml. Thiamine was added to repress *nmt1* promoter at the final concentration of 100 μg/ml.

Table 2.1. Genotypes of *S. pombe* strains.

Strain	Genotype	Reference
Diplods		
wt diploid	*h+/h- ade6/ade6-704 leu1/leu1-32 ura4/ura4-27*	
rct1+/-	*h+/h- rct1/rct1::ClonNat ade6/ade6-704 leu1/leu1-32 ura4/ura4-27*	(Gullerova et al, 2006)
rct1+/-^{pMG1}	*h+/h- rct1/rct1::ClonNat(pMG1 ade6/ade6-704 leu1/leu1-32 ura4/ura4-27*	(Gullerova et al, 2006)
rct1+/-^{pMG2}	*h+/h- rct1/rct1::ClonNat(pMG2) ade6/ade6-704 leu1/leu1-32 ura4/ura4-27*	(Lorkovic et al, 2009)
rct1+/-^{pMG3}	*h+/h- rct1/rct1::ClonNat(pMG3) ade6/ade6-704 leu1/leu1-32 ura4/ura4-27*	(Lorkovic et al, 2009)
rct1+/-^{pMG4}	*h+/h- rct1/rct1::ClonNat(pMG4) ade6/ade6-704 leu1/leu1-32 ura4/ura4-27*	(Lorkovic et al, 2009)
rct1+/-^{pMG5}	*h+/h- rct1/rct1::ClonNat(pMG5) ade6/ade6-704 leu1/leu1-32 ura4/ura4-27*	(Lorkovic et al, 2009)
rct1+/-^{pMG6}	*h+/h- rct1/rct1::ClonNat(pMG6) ade6/ade6-704 leu1/leu1-32 ura4/ura4-27*	(Lorkovic et al, 2009)
rct1+/-^{pMG4R3}	*h+/h- rct1/rct1::ClonNat(pMG4R3) ade6/ade6-704 leu1/leu1-32 ura4/ura4-27*	(Lorkovic et al, 2009)
rct1+/-^{pMG1F}	*h+/h- rct1/rct1::ClonNat(pMG1Flag) ade6/ade6-704 leu1/leu1-32 ura4/ura4-27*	this study
rct1+/-^{pMG4F}	*h+/h- rct1/rct1::ClonNat(pMG4Flag) ade6/ade6-704 leu1/leu1-32 ura4/ura4-27*	this study

Cdk9-HA, rct1Δ pMG1F	*h+ rct1::ClonNat(pMG1Flag) cdk9-3HA::KanR ade6-704*	this study
Cdk9-HA, rct1Δ pMG4F	*h+ rct1::ClonNat(pMG4Flag) cdk9-3HA::KanR ade6-M210*	this study
Haploids		
wt haploid	*h+ ade6-704*	
rct1Δ pMG1	*h- rct1::ClonNat(pMG1) ura4-27*	(Gullerova et al, 2006)
rct1Δ pMGR1	*h+ rct1::ClonNat(pMGR1) ade6-704 leu1 ura4*	(Lorkovic et al, 2009)
rct1Δ pMGR2	*h+ rct1::ClonNat(pMGR2) ade6-704 leu1 ura4*	(Lorkovic et al, 2009)
rct1Δ pMGR3	*h+ rct1::ClonNat(pMGR3) ade6-704 leu1 ura4*	(Lorkovic et al, 2009)
rct1Δ pMG2	*h+ rct1::ClonNat(pMG2) ade6-704 ura4-27*	(Lorkovic et al, 2009)
wt pMG4	*h+ (pMG4) ade6-704 leu1 ura4*	(Lorkovic et al, 2009)
rct1Δ pMG4	*h+ rct1::ClonNat(pMG4)*	(Lorkovic et al, 2009)
rct1Δ pMG4R3	*h+ rct1::ClonNat(pMG4R3) ade6-704*	(Lorkovic et al, 2009)
rct1Δ pMG1F	*h+ rct1::ClonNat(pMG1Flag) ade6-704*	this study
rct1Δ pMG4F	*h+ rct1::ClonNat(pMG4Flag) ade6-704*	this study
lsk1-HA	*h- lsk1-3HA::ura4 ura4-D18 leu1-32*	(Karagiannis & Balasubramanian, 2007)
cdk9-HA	*h- cdk9-3HA::KanR ura4-D18 ade6-M210 leu1-13*	(Guiguen et al, 2007)
mcs6-HA	*h+ mcs6-3HA::CloNat ura4-D18 ade6-216 leu1-32*	Kind gift of D. Hermand

2.2. Other strains

Genotypes of *E. coli* and *S. cerevisiae* strains used are listed in Table 2.2.

Table 2.2. Genotypes of *E. coli* and *S. cerevisiae* strains.

Strain	Genotype
E. coli	

XL1-Blue	endA1 gyrA96(nal^R)thi-1 recA1 lac glnV44 F'[::Tn10 proAB$^+$lacI^{q}Δ(lacZ)M15] hsdR17($r_k^-m_k^+$)
BL21 (DE3)	F-ompT hsdSB (rB-mB-) gal dcm
C41 (DE3)	Derived from BL21 (DE3), has at least one uncharacterized mutation allowing synthesis of some proteins at high levels
S. cerevisiae	
HF7c	*MATa, ura3-52, his3-200, ade2-101, lys2-801, trp1-901, leu2-3, 112, gal4-542, gal80-, 538, LYS2::GAL$_{uas}$-GAL1$_{tata}$-HIS3*
PJ69-4A	*MATa, trp1-901, leu2-3, 112, ura3-52, his3-200, gal4Δ, gal80Δ, LYS2::GAL$_{uas}$-GAL1$_{tata}$- HIS3, GAL2$_{uas}$-GAL2$_{tata}$-ADE2, MEL1*
AH109	*MATa, trp1-901, leu2-3, 112, ura3-52, his3-200, gal4Δ, gal80Δ, LYS2::GAL$_{uas}$-GAL1$_{tata}$-HIS3,MEL1, GAL2$_{uas}$-GAL2$_{tata}$-ADE2, URA3::MEL$_{uas}$-MEL1$_{tata}$-lacZ*

2.3. Plasmids construction

2.3.1. GST- tagged plasmids

Plasmids encoding GST-Cdk9, GST-Cdk9 kinase domain (residues 35-339) and GST-Cdk9 C-terminus (residues 340-591) were created by amplifying cDNA of *cdk9* and its corresponding parts with respective primers: Cdk9 Y2H fw, Cdk9 GST rev, Cdk9 kin fw, Cdk9 kin rev, Cdk9 C-t fw and Cdk9 C-t rev. The fragments were cut with BamHI and SalI and ligated into pGEX-5X-2 plasmid.

To obtain GST tagged Msc6, its cDNA was amplified with Mcs6 Y2H fw and Mcs6 Y2H rev oligonucleotides and inserted into XmaI/SalI lianerized pGEX-5X-2.

GST-Srb10, GST-Lsk1, GST-Lsk1 kinase domain and C-terminus (residues 276-594), GST-Lsk1 kinase domain (residues 276-560), GST- Lsk1 N-terminus (residues 1-275) and GST-Scp1encoding vectors were made by cloning corresponding cDNAs using following primers: Srb10 Y 2H fw, Srb10 Y2H rev, LskI Y2H fw, LskI Y2H rev, Lsk1 kin+C-t fw, Lsk1 kin+C-t rev, Lsk1 kin fw, Lsk1 kin rev, Lsk1 N-t fw, Lsk1 N-t rev, Scp1 Y2H fw and Scp1 Y2H rev, respectively. The PCR fragments were ligated into EcoRI and SalI sites of pGEX-4T-1.

To generate plasmids expressing Lsc1 and Pch1 fused to GST, products of the PCR reactions performed with Lsc1 GST fw, Lsc1 GST rev, Pch1 GST fw and Pch1 GST rev oligonucleotides were inserted into pGEX-5X-2 plasmid cut with BamHI/XhoI.

Plasmid expressing Fcp1-GST was Nakamura's kind gift.

2.3.2. Yeast-two hybrid plasmids

All genes of interest were cloned into vectors from Clontech pGAD424 and pGBT9.

Yeast-two hybrid (Y2H) plasmids encoding Msc6, Srb10, Scp1 and Lsk1 were created using same primers as for GST-tagged versions of the proteins (see Section 2.3.1. and Table 2.3.), resulting in pGAD424-Msc6, pGBT9-Msc6, pGAD424-Srb10, pGBT9-Srb10, pGAD424-Scp1, pGBT9- Scp1, pGAD424-Lsk1 and pGBT9-Lsk1.

In order to make pGAD424-Cdk9 and pGBT9-Cdk9 vectors, product of the PCR reaction performed with Cdk9 Y2H fw and Cdk9 Y2H rev primers was inserted into BamHI/Pst1 cut pGAD424 and pGBT9, respectively.

Fcp1 and Ssu72 were amplified with the corresponding oligonucleotides: Fcp1 Y2H fw, Fcp1 Y2H rev, Ssu72 Y2H fw and Ssu72 Y2H rev, and inserted into pGAD424 and pGBT9, opened with EcoRI and PstI. Created vectors were called pGAD424-Fcp1, pGBT9-Fcp1, pGAD424-Ssu72 and pGBT9-Ssu72.

Plasmids expressing Lsc1 and Pch1 (pGAD424- Lsc1, pGBT9- Lsc1, pGAD424-Pch1 and pGBT9- Pch1) were obtained by amplifying corresponding genes with following primers: Lsc1 Y2H fw, Lsc1Y2H rev, Pch1 Y2H fw and Pch1 Y2H rev, respectively. Products were ligated into pGAD424 and pGBT9 opened with EcoRI and BamHI.

pGAD424-Rct1 and pGBT9-Rct1 vectors were created by performing PCR reaction with following primers: Rct1 Y2H fw and Rct1 Y2H rev. Amplified DNA was inserted into pGAD424 and pGBT9 cut with XmaI and Pst1I.

Plasmids pA_2S_5-HA and pA_2S_2-HA have been described (Ursic et al, 2008).

Plasmids pGST-AtCyp59, pBD-AtCTD and pAD-AtCTD have been described (Gullerova et al, 2006).

Oligonucleotides used for cloning are listed in Table 2.3.

Table 2.3. Oligonucleotides for cloning.

Name	Restriction site	Sequence	In vector
CTD kinases			
Mcs6 Y2H fw	XmaI	gactagcccgggggatatcgaaaagtctgacaagtgg	pGAD424, pGBT9, pGEX-5X-2
Mcs6 Y2H rev	SalI	gactaggtcgacttaaacaaatttaatatttgcacgca	pGAD424, pGBT9, pGEX-5X-2
Mcs6 HA fw	XhoI	gactagctcgagatggatatcgaaaagtctgacaagt	pMG
Mcs6 HA rev	SalI	gactaggtcgacttatgcgtagtcaggcacatcatacggataaacaaatttaatatttgcacgcatt	pMG
Srb10 Y2H fw	EcoRI	gactaggaattcaaagacggttataaaattattgggttt	pGAD424, pGBT9, pGEX-4T-1
Srb10 Y2H rev	SalI	gactaggtcgacttaaaaatgggctaaaaagtgagttag	pGAD424, pGBT9, pGEX-4T-1
Srb10 HA fw	XhoI	gactagctcgagatgaaagacggttataaaattattggg	pMG
Srb10 HA rev	XmaI	gactagcccgggttatgcgtagtcaggcacatcatacggataaaaatgggctaaaaagtgagttagtaa	pMG
Cdk9 Y2H fw	BamHI	gactagggatccggaaacgctcaagcagcgtt	pGAD424, pGBT9, pGEX-5X-2
Cdk9 Y2H rev	PstI	gactagctgcagtcatttaggagtgtcatcaacgtt	pGAD424, pGBT9
Cdk9 GST rev	SalI	gactaggtcgactcatttaggagtgtcatcaacgtt	pGEX-5X-2
Cdk9 HA fw	SalI	gactaggtcgacatgaaacgctcaagcagcg	pMG
Cdk9 HA rev	XmaI	gactagcccgggttatgcgtagtcaggcacatcatacggatatttaggagtgtcatcaacgttgg	pMG
Cdk9 kin fw	BamHI	gactagggatccggtatcatttaatggaaaaattaggagaagg	pGEX-5X-2
Cdk9 kin rev	SalI	gactaggtcgactcaaaaatattcatgctctaaagcc	pGEX-5X-2
Cdk9 C-t fw	BamHI	gactagggatccggacaacaccaccatatccagcaaaccc	pGEX-5X-2
Cdk9 C-t	SalI	gactaggtcgactcatttaggagtgtcatcaacgt	pGEX-5X-2

rev			
LskI Y2H fw	EcoRI	gactaggaattctcatactcgaagagtacaatttatcgc	pGAD424, pGBT9, pGEX-4T-1
LskI Y2H rev	SalI	gactaggtcgacttatcttttagattttcgttttttactttc	pGAD424, pGBT9, pGEX-4T-1
LskI HA fw	SalI	gactaggtcgacatgtcatactcgaagagtacaatttatcg	pMG
LskI HA rev	XmaI	gactagcccgggttatgcgtagtcaggcacatcataccggatatcttttagattttcgttttttactttcccattcatgcc	pMG
Lsk1 kin+C-t fw	EcoRI	gactaggaattctatgagaaaatcgaccaaattggagaagg	pGEX-4T-1
Lsk1 kin+C-t rev	SalI	gactaggtcgacttatcttttagattttcgttttttactttc	pGEX-4T-1
Lsk1 kin fw	EcoRI	gactaggaattctatgagaaaatcgaccaaattggagaagg	pGEX-4T-1
Lsk1 kin rev	Sal1	gactaggtcgacttaatactcatgcatcaaggtctcatgagc	pGEX-4T-1
Lsk1 N-t fw	EcoRI	gactaggaattctatgagaaaatcgaccaaattggagaagg	pGEX-4T-1
Lsk1 N-t rev	Sal1	gactaggtcgacttaggcaggctttggatatgtatatgtataaattgg	pGEX-4T-1
CTD phosphatases			
Fcp1 Y2H fw	EcoRI	gactaggaattctcgaaacgattgacaccaatt	pGAD424, pGBT9
Fcp1 Y2H rev	PstI	gactagctgcagtcaagctgtatctttggacaattc	pGAD424, pGBT9
Ssu72 Y2H fw	EcoRI	gactaggaattcgctcccaaaaccaacctc	pGAD424, pGBT9
Ssu72 Y2H rev	PstI	gactagctgcagttaaaaaaaatgaatagtatacaatacaggaag	pGAD424, pGBT9
Ssu72 GST fw	EcoRI	gtcagtgaattcatggctcccaaaaccaacctccagatc	pGEX-4T-1
Ssu72 GST rev	SalI	gtcagtgtcgacttaaaaaaaatgaatagtatacaatac	pGEX-4T-1
Ssu72 HA fw	SalI	gactaggtcgacatggctcccaaaaccaacctc	pMG
Ssu72 HA rev	BamHI	gactagggatccttatgcgtagtcaggcacatcatacggataaaaaaaaatgaatagtatacaatacaggaag	pMG
Scp1 Y2H fw	EcoRI	gactaggaattcaaatcaacgaaaacccaaccctc	pGAD424, pGBT9,

			pGEX-4T-1
Scp1 Y2H rev	SalI	gactaggtcgacttataactgaagattaaggacagtactaacatc	pGAD424, pGBT9, pGEX-4T-1
Scp1 HA	XhoI	gactagctcgagatgaaatcaacgaaaacccaac	pMG1
Scp1 HA	XmaI	gactagcccgggttatgcgtagtcaggcacatcatacggatataactgaagattaaggacagtactaac	pMG1
Lsc1 and Cdk9 cyclins			
Lsc1 Y2H fw	EcoRI	gactaggaattcgcagaaaatgagaatcatg	pGAD424, pGBT9
Lsc1 Y2H rev	BamHI	gactagggatccttaaaccgtacctttatttctcc	pGAD424, pGBT9
Lsc1 GST fw	BamHI	gactagggatccgggcagaaaatgagaatc	pGEX-5X-2
Lsc1 GST rev	XhoI	gactagctcgagttaaaccgtacctttatttctcc	pGEX-5X-2
Pch1 Y2H fw	EcoRI	gactaggaattcagtgaagtaataaaatctgtacccc	pGAD424, pGBT9
Pch1 Y2H rev	BamHI	gactagggatccttatgaagcttccgtctcc	pGAD424, pGBT9
Pch1 GST fw	BamHI	gactagggatccggagtgaagtaataaaatctg	pGEX-5X-2
Pch1 GST rev	XhoI	gactagctcgagttatgaagcttccgtctcc	pGEX-5X-2
Rct1			
Rct1 GST fw	SalI	gactagggtcgactgtctgtactaattgaaactaca	pGEX-4T-1
Rct1 GST rev	XhoI	gactagctcgagtcatcgatatctatcatctctata	pGEX-4T-1
Rct1 ΔPPI GST fw	BamHI	gacaacggatccatggaggcagaagcagag	pGEX-4T-1
Rct1 ΔPPI GST rev	SalI	gacggcgtcgacttatcgatatctatcatctctataacg	pGEX-4T-1

2.3.3. pMG plasmids encoding Rct1 and its deletion and point mutants

All the plasmids were constructed by inserting *rct1* or its deletion or point mutants tagged with either hemagglutinine (HA) or FLAG (Fig. 2.2.) into multicloning site of pMG (Fig. 2.1.) and pMG1 (Gullerova et al, 2007).

Rct1 lacking RS/RD domain encoding vector was produced by amplifying respective part of pMG1 with following primers: Rct1 ΔRS fw, which introduced XhoI before the ATG codon, and Rct1 ΔRS rev, which encoded HA tag, stop codon and SalI site, in described order. The PCR product was cloned into XhoI and SalI opened pMG, resulting in pMG2.

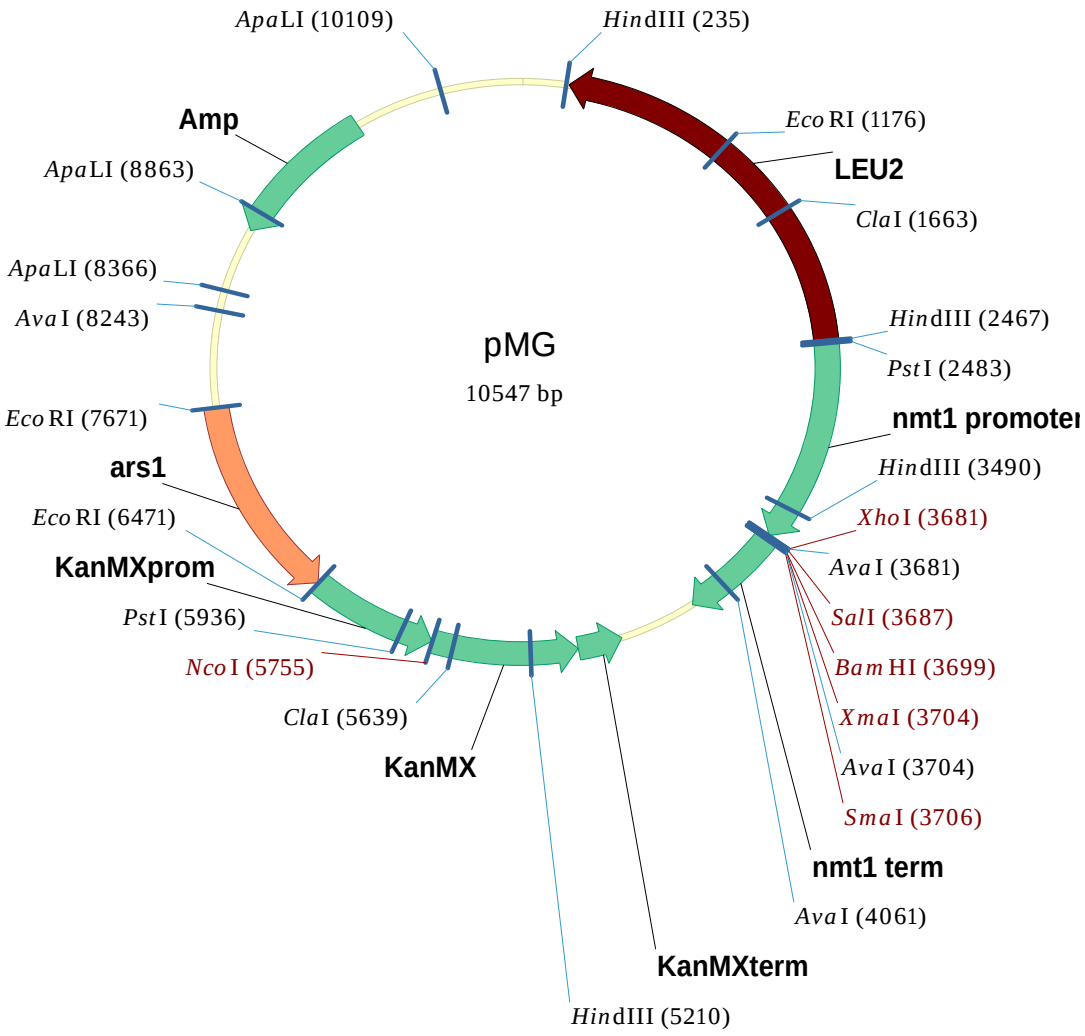

Fig. 2.1. Map of pMG vector.

To construct the plasmid containing HA tagged PPIase domain of Rct1, corresponding domain was amplified by PCR with forward oligonucleotide Rct1 PPI fw, which introduces XhoI site in front of ATG codon, and reverse - Rct1 PPI rev, which encodes HA, stop codon, and XmaI site. The PCR product was ligated into XhoI/SalI cut pMG, resulting in pMG3.

Overexpression plasmid encoding Rct1 without PPIase domain was created by amplifying respective *rct1* part using pMG1 as a template. The forward oligo used was Rct1 ΔPPI fw, which had XhoI site in front of ATG condon, and reverse oligo - Rct1 rev, which primes to pMG1 downstream of HA tag. Resulting PCR product was inserted into XhoI/XmaI linearized pMG, resulting in pMG4.

Plasmid pMG4R3, that expresses Rct1 without PPIase domain and has mutated RRM domain, was produced the same way as pMG4, but with pMG1R3 as a template. pMG1R3 was constructed by the site-directed mutagenesis of *rct1* within pMG1 plasmid. The following mutations were introduced into RRM domain of Rct1 Y287D, F289D, F292D (Lorkovic et al, 2009).

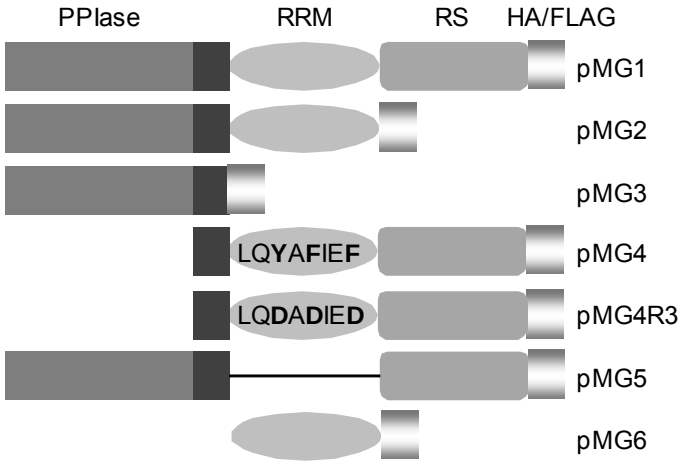

Fig. 2.2. Schematic representation of Rct1 deletion and point mutants. Names of the plasmids expressing the mutants are indicated on the right side.

Plasmid expressing Rct1 without RRM domain was created by fusing same PCR product used for pMG3 construction – PPIase domain of Rct1, which has also SpeI site in front of HA. The PCR product was cut with XmaI and SpeI, which cut off HA. RS domain of Rct1 was amplified using pMG1 as a template. Olidonucleotides used for RS domain amplification were: Rct1 RS fw, which introduces SpeI site, and Rct1 rev. Amplified RS domain was cut with SpeI and XhoI, ligated with PCR product mentioned above (PPIase domain) through SpeI site. The product of ligation was introduced into XmaI/XhoI opened pMG1 resulting in pMG5 plasmid.

To generate plasmid expressing RRM domain of Rct1 fused to HA, RRM encoding region was amplified with following oligonucleotides: Rct1 ΔPPI fw and Rct1 RRM rev,

which introduces HA, XmaI site and stop codon, sequentially. The PCR product was cloned into XmaI/XhoI digested pMG1, resulting in pMG6 plasmid.

Plasmid encoding FLAG-tagged Rct1 was constructed by amplifying Rct1 cDNA with following primers: Rct1 FLAG fw, which binds upstream ATG site and encodes XhoI site, and Rct1 FLAG rev, which introduces FLAG, XmaI site and stop codon, respectively. Amplified DNA was inserted into XmaI/XhoI cut pMG1. Resulting plasmid was named pMG1F.

To obtain pMG4F, plasmid expressing FLAG-tagged Rct1 without PPIase domain, corresponding sequence was amplified using pMG1F plasmid as a template and following primers: Rct1 ΔPPI fw and Rct1 rev. Product of the PCR reaction was ligated into XmaI/XhoI digested pMG1.

Oligonucleotides used for cloning are listed in Table 2.4.

Table 2.4. Oligonucleotides for cloning.

Name	**Restriction site**	**Sequence**	**in vector**	**new vector**
Rct1 FLAG fw	XhoI	gactagctcgagatgtctgtactaattgaaactacagttgg	pMG1	pMG1F
Rct1 FLAG rev	XmaI	gactagcccgggctatttatcatcgtcatctttataatctcgatatctatcatctctataacg	pMG1	pMG1F
Rct1 ΔRS fw	XhoI	gtcagtctcgagatgtctgtactaattgaa	pMG1	pMG2
Rct1 ΔRS rev	SalI	gtcagtgtcgactcatgcgtagtcaggcacatcatacggatacacgctttcccaaaaatctacgtg	pMG1	pMG2
Rct1 PPI fw	XhoI	gactagctcgagatgtctgtactaattgaaactacagttgg	pMG1	pMG3, pMG5
Rct1 PPI rev	SpeI XmaI	gactagcccgggtcatgcgtagtcaggcacatcatacggataactagtttccttctctctttgcaatttatcttccg	pMG1	pMG3
Rct1 ΔPPI fw	XhoI	gacgacctcgagatggaggcagaagca	pMG1	pMG4, pMG4R3, pMG4F, pMG6
Rct1 rev	XmaI	ctcatctaaaccactttctaa	pMG1	pMG4, pMG4R3, pMG4F, pMG5
Rct1 RS fw	SpeI	gactagactagtgctcgttacagacaatattacaact	pMG1	pMG5

		cc		
Rct1 RRM rev	XmaI	gactagcccgggtcatgcgtagtcaggcacatcat acggatacacgctttgggaaaaatctacg	pMG1	pMG6
Rct1 Y2H fw	XmaI	gactagcccgggatctgtactaattgaaactacagtt ggtg	pGAD 424, pGBT9	pGAD424 -Rct1, pGBT9-Rct1
Rct1 Y2H rev	PstI	gactagctgcagctatcgatatctatcatctctataac gtct	pGAD 424, pGBT9	

2.4. Generation of strains

2.4.1. *Rct1Δ^{pMG1F}*

Rct1$^{+/-}$ (Gullerova et al, 2007) cells were grown until mid-exponential phase in YES medium containing ClonNat at 32^{0}C. Two milliliters of culture were centrifuged at 13,000 rpm for 2 min at RT (room temperature). Pellet was washed with 1 ml of LiAc/TE and resuspended in 100 µl of LiAc/TE. One and a half micrograms of pMG1F plasmid and 2 µl of salmon sperm DNA (10 mg/ml) were added to the mixture and incubated for 10 min at RT. After addition of 360 µl of PEG/LiAc, solution was vortexed and incubated for 30 min at RT. Forty three microliters of DMSO (dimethylsulphoxide) were mixed into the reaction, which was then incubated for 5 min at 42^{0}C. Cells were spinned down, resuspended in 1 ml YES medium and incubated for 5 h at 30^{0}C. Afterwards cells were plated on selective YES Agar medium containing Geneticin and ClonNat. To confirm successful plasmid transformation few colonies were subjected to Western blot analysis. For this, cells were grown overnight in EMM2 medium with Geneticin and ClonNat, 1 ml of each culture was spinned down and 100 µl of 2 × LB were added to each sample. Rct1-FLAG expression was checked by Western blotting. Cells with pMG1F plasmid were streaked on EMM2-N (EMM2 media lacking nitrogen) plate and left for 3 days at 30^{0}C to sporulate. Strains with *rct1* knocked out allele were identified with the help of random spore analysis. For this, a three day old cross was checked for the presence of asci under the light microscope. A loopful of the cross was inoculated in 1 ml of sterile dH_2O and glusalase (Dupont/NEN) was added to a final concentration of 0.5%. The mixture was

incubated on rotary shaker overnight at RT. Spores were plated on YES agar medium containing Geneticin and ClonNat and in parallel on the same medium with addition of 5 mg/L phloxin B (Sigma). The plates were incubated at 32^0C for 3 days. Selected colonies, replicas of which turned light pink on phloxin B plates, were checked for Rct1-FLAG expression again and genotyped (see Table 2.5. for oligonucleotides) for *rct1* knock-out allele with forward primers: SpCypcon fw (*wt*) and SpCloncon fw (*rct1* knock out) and common reverse primer Spcheck3 rev, and for mating type with standard primers MM, MP and MT1 (Moreno et al, 1991).

Table 2.5. Oligonucleotides for genotyping.

Name	**Sequence**
MM	tacgttcagtagacgtagtg
MP	acggtagtcatcggtcttcc
MT1	agaagagagagtagttgaag
SpCypcon fw	gaggcagaagcagaggctgttacac
SpCloncon fw	gcgtggggacaattcaacgc
Spcheck3 rev	aacgtgccgcatttatggag

2.4.2. *Rct1Δ^{pMG4F}*

This haploid strain was created in the same way as *rct1Δ^{pMG1F}* (Section 2.4.1.), pMG4F plasmid was used instead of pMG1F.

Buffers (always prepared fresh ones from stock solutions)**:**

10 × TE

100 mM Tris–HCl

10 mM EDTA, pH 7.5

LiOAc/TE

100 mM LiOAc

1 × TE

PEG/LiAc

40 % PEG 3355

1 × TE

100 mM LiAc, pH 4.9

2 × LB buffer

4% SDS

20% glycerol

10% β-mercaptoethanol

0.004% bromphenol blue

0.125 M Tris – HCl, pH 6.8

2.4.3. *Cdk9-HA, rct1Δ^{pMG1F}, lsk1-HA, rct1Δ^{pMG1F}* and *cdk9-HA, rct1Δ^{pMG4F}*

Rct1Δ^{pMG1F} was crossed with either *cdk9-HA* or *Lsk1-HA* on EMM2-N plate for 3 days at 30^{0}C. In order to get desired strains, random spore analysis was performed as described previously (Section 2.4.1.). *Cdk9-HA rct1Δ^{pMG1F}* and *lsk1-HA rct1Δ^{pMG1F}* were identified with the help of genotyping (Section 2.4.1.) and Western blot analysis (Section 2.7.).

Cdk9-HA rct1Δ^{pMG4F} strain was obtained in the same way except that *rct1Δ^{pMG4F}* was used for crossing instead of *rct1Δ^{pMG1F}*.

2.5. Overexpression and purification of GST fusion proteins

The plasmids pGST-Rct1, pGST-Rct1ΔPPIase, pGST-CTD, pGST-Mcs6, pGST-Srb8, pGST-Cdk9, pGST-Cdk9 kin, pGST-Cdk9 C-t, pGST-Lsk1, pGST-Lsk1kin+C-t, pGST-Lsk1kin, pGST-Lsk1 N-t, pGST-Scp1, pGST-Ssu72, pGST-Fcp1, pGST-Lsc1 and pGST-Pch1 were transformed into *E.coli* strain BL21(DE3). Overnight cultures were grown at 37^{o}C in the presence of 100 μg/ml of ampicillin, diluted 100 times and grown further to 0.6 OD (optical density) at 600 nm. Protein synthesis was induced with 1 mM isopropyl-β-D-thiogalactopyranoside (IPTG) at 28^{o}C for 3 hours. Pellets from 200 ml of

cells were resuspended in 10 ml of lysis buffer and sonicated (Bandelin HD 200 Sonoplus) on ice 3 times for 10 sec, at power of 200 W, 50 cycles. Cell lysates were centrifuged at 14,000 rpm for 10 min at 4°C. The supernatant was mixed with 200 µl glutathione Sepharose beads (GE Healthcare) and mixed for 30 min at 4°C. The sepharose was washed three times with 15 ml of lysis buffer, buffer was exchanged to protoplast extraction buffer (PEB 200) and beads were stored at 4°C in 400 µl of PEB 200. Fifty microliters of beads were used for each pull-down. For kinase assays GST-Rct1, GST- Rct1ΔPPIase and GST-CTD were eluted with elution buffer. Elution buffer was exchanged to kinase buffer (Section 2.8.) by overnight dialysis 1:20,000. GST-Rct1 was concentrated using Amicon Ultra-4 cetrifugal filters. Twenty microliters of each sample was resuspended in 60 µl of 2 × LB, boiled for 5 min and 20 µl were loaded on 10% SDS-PAGE gel for analysis.

Buffers (always prepared fresh ones from stock solutions)**:**

Lysis buffer
20 mM Tris-HCl, pH 7.5
1 M NaCl
0.2 mM EDTA
1 mM DTT
1% Triton X-100
EDTA-free protease inhibitor cocktail (Roche)

PEB 200
50 mM HEPES-KOH, pH 7.9
200 mM KCl
1 mM DTT
0.1 % Triton X-100
2.5 mM $MgCl_2$
1 mM EDTA, pH 8.0
EDTA-free protease inhibitor cocktail (Roche)

Elution buffer

50 mM Tris-HCl, pH 8.0

10 mM reduced glutathione

2.6. Preparation of whole cell extracts from *S. pombe* cells, pull-down assay and immunoprecipitation

Four hundred ml of cells were collected at exponential phase by centrifugation (4,000 rpm, 5 min, RT), frozen in liquid nitrogen and stored at -80^{o}C until use. Cells were resuspended in 300 µl PEB 400 (the same as PEB 200, but with 400 mM KCl) and sonicated (Bandelin HD 200 Sonoplus) on ice six times for 5 sec, at power of 200 W, 50 cycles. Cell lysates were centrifuged at 14,000 rpm for 15 min at 4^{o}C. After that, supernatant was mixed with PEB without KCl to adjust KCl concentration to 200 mM.

For pull-down assays whole cell extracts were mixed with glutathione Sepharose beads coated with recombinant proteins or with beads only and incubated for 4 hours at 4^{o}C. After three washings with PEB200, beads were resuspended in 60 µl of 2 × LB, boiled for 5 min, 25 µl were loaded on SDS-PAGE gel and analyzed by Western blotting.

For immunoprecipitation with anti-HA (12CA5) antibody, 500 µl of the antibody (hybridoma supernatant) were incubated overnight pr at least 7 h during the day at 4^{o}C with 30 µl of 50 % slurry of protein A Sepharose CL-4B (GE Healthcare) in PEB 200. Protein A Sepharose was washed three times with PEB 200 buffer and added to the protein extract. Same amount of extract was supplied with protein A Sepharose only as a negative control. The mixture was incubated again at 4^{o}C, washed three times with PEB 200 and analyzed by Western blotting.

2.7. SDS-PAGE and Western blotting

Proteins were run on 10% SDS-PAGE and transfered onto PVDF membrane (Millipore) and Western blotting was performed according to standard procedure. See Table 2.6. the dilutions of the antibodies used.

All secondary antibodies for Western were conjugated with horseradish peroxidase. Blots were developed using a chemiluminescence kit (GE Healthcare) and exposed to Kodak Biomax MR film.

Table 2.6. Used antibodies for detection by Western blotting, IF and ChIP

Name	**Working dilution**
Primary	
Anti-HA, rat, monoclonal (Roche)	1:5,000 for Western 1:100 for IF
Anti-FLAG, mouse, monoclonal (Sigma)	1:10,000
Anti-CTD (H5), mouse, monoclonal (Covance)	1:500
Anti-Rct1, rabbit, polyclonal, 2 peptides (Gullerova et al, 2007)	1:1,000
Anti-PSTAIR, mouse, monoclonal (abcam)	1:1,000
Anti-phosphor-Cdc2 (Tyr 15), rabbit, polyclonal (Cell Signalling)	1:1,000
Anti-phospho RNAP II (S2), rabbit, polyclonal (Bethyl)	used for ChIP 0.4 µg, Section 2.11.
Anti-phospho RNAP II (S5), rabbit, polyclonal (Bethyl)	used for ChIP 0.4 µg, Section 2.11.
Anti-HA (12CA5) mouse, monoclonal	used for IP, Section 2.6.
Anti-RNAP II CTD repeat (4H8), mouse, monoclonal (Abcam)	used for ChIP 5 µg, Section 2.11.
Anti-histone 3 (anti-H3), rabbit, polyclonal (Abcam)	used for ChIP 4 µg, Section 2.11.
Anti- histone3 acetylated on lysine 9 (anti-AcH3K9K12), rabbit, polyclonal (Millipore)	used for ChIP 19 µg, Section 2.11.
Anti- tubulin (α-TAT1), mouse, monoclonal (kind gift of K. Gull)	1:10
Secondary	
Rabbit anti-rat ImmunoglobulinG (IgG) (Sigma)	1:10,000
Goat anti-mouse IgG (BioRad)	1:10,000

Goat anti-mouse IgM (Biosource)	1:10,000
Goar anti-rabbit IgG (BioRad)	1:10,000
Goat anti-mouse Alexa 568 (Molecular Probes)	1:100
Goat anti-rat Alexa 568 (Molecular Probes)	1:100

2.8. Kinase assay

Cdk9-HA, *rct1Δ^{pMG1F} cdk9-HA*, *cdk9-HA rct1Δ^{pMG4F}* and *msc6-HA* cells were grown at 32^{o}C in EMM2 media overnight, spinned down and diluted in YES media to OD_{600} 0.2. *cdk9-HA, msc6-HA* first batch of *cdk9-HA rct1Δ^{pMG1F}* and *cdk9-HA rct1Δ^{pMG4F}*were harvested at OD_{600} 0.5. Second batch of *rct1Δ^{pMG1F}* was supplied with thiamine (100 μg/μl) upon transfer into fresh YES media and grown for 24 h with occasional dilution, after last dilution it was collected at OD_{600} 0.5. Rct1 levels in samples were analyzed by Western blotting with anti-FLAG antibody.

Immunoprecipitations of *cdk9-HA* and *msc6-HA* with anti-HA antibody were performed as described in Section 2.6., samples were additionally washed once with kinase buffer before kinase reaction was performed.

For Rct1 depletion assay the protein A Sepharose with precipitated *cdk9-HA* was mixed with 10 μl kinase buffer, 0.2 μl 10 mM ATP, 1 μl [^{32}p]γ-ATP (10 μCi/μl) and 10 μl GST-CTD or GST (about 2 μg).

For kinase assays with increasing amounts of Rct1 or Rct1ΔPPIase 3 μl, 5 μl and10 μl of either Rct1 or Rct1ΔPPIase (10 ng/μl) were added additionally into reaction tubes and the volumes were adjusted with kinase buffer. Same assay was performed with 1 μl of histone 1 (H1) 1 mg/ml as a control.

Reactions were incubated for 30-40 min at 30^{o}C, stopped by addition of 20 μl of 2 × LB, boiled for 5 min at 95^{o}C and loaded in 2 replicas on SDS-PAGE gels. One was analyzed by Western blotting for Cdk9-HA and Msc6-HA immunoprecipitaiton. Another was stained with Coomassie and after destaining dried in vacuum gel-dryer for 1 h and to exposed to X-ray film and sussequently to PhosphoImager for quantification.

Kinase buffer

10 mM TRIS-HCL, pH 7.5

1 mM DTT

50 mM KCl

10 mM $MgCl_2$

2.9. Nuclear run-on (NRO)

S. pombe wt and *rct1Δ*^{pMG1F} cells were grown overnight in EMM2, spinned down, diluted in 60 ml of YES and harvested at OD_{600} 0.3. For Rct1 depleted sample another batch of *rct1Δ*^{pMG1F} cells after spinning down was again diluted in YES with addition of thiamine to final concentration of 100 μg/ml and further grown for 24 h (occasional dilution was performed) and also collected at OD_{600} 0.3. After harvesting samples were washed with 1 ml of ice-cold TNM buffer. Pellet was resuspended in 0.9 ml of ice-cold water, 50 μl 10 % *N*-lauryl sarcosine sulfate was added and the solution was incubated on ice for 20 min. Pelleted cells after gentle centrifugation at 3000 rpm for 1 min were resuspended in 60 μl of NRO buffer containing 100 μCi of αP^{32}-UTP. Cells were incubated 10 min at 30^{o}C, washed with TNM and total RNA was extracted (Section 2.10.). RNA samples were boiled for 5 min, added to the prehybridized membranes and incubated for 2 days at 42^{o}C. Membranes were washed twice with 2 × SSC 1% SDS mixture for 2 min at 42^{o}C, wrapped into plastic sheets and exposed to PhosphoImager for quantification.

DNA preparation for application onto membrane

Single gene NROs of *act1* and *cdc48* were performed. DsDNA was prepared by standard PCR (see Table 2.7. for oligonucleotides) and purified by phenol extraction. 10 M NaOH and 0.5 M EDTA (pH 8.0) were added to final concentration of 0.4 M and 10 mM, respectively, to 10 μg of prepared DNA. Mixture was boiled for 10 min and applied on membrane.

Membrane preparation

Nylon membrane (Hybond-N+, Amersham Biosciences) was soaked in distilled water for 10 min, placed on wet Whatmann paper and fixed in Bio-Dot Microfiltration

Apparatus (Bio-Rad). Each slot was washed with 500 µl of sterile water, prepared dsDNA was applied and slots were rinsed again with 0.4 M NaOH. Membrane was taken out of the apparatus, washed with 2 × SSC and dried.

Membrane was transferred to glass tube and prehybridized in hybridization buffer for 2 h at 42^{o}C.

Table 2.7. Oligonucleotides for ChIP and NRO

Name	Sequence	Product size (bp)
For *act1*		
Act1 1 fw	ggttgctcaatgttatccgtttc	83
Act1 1 rev	tgataaagccacacacagcgtta	
Act1 2 fw	ctcaaagcaagcgtggtattt	81
Act1 2 rev	tcttttccatatcatcccagttg	
Act1 3 fw	ccactatgtatcccggtattgc	81
Act1 3 rev	caatcttgaccttcatggagct	
Act1 4 fw	acaaggtggtaactgcgagatagtt	81
Act1 4 rev	actctacaggacgaaaagaaatggc	
Act1 5 fw	gcccgattagccagttgtatagt	82
Act1 5 rev	gtttatacagagaggcgtcgtca	
Act1 6 fw	cagctaatcattttcacggtaacac	82
Act1 6 rev	ccatgcattcaacatcccttt	
Act1 7 fw	agagggtgttaaatcagggacat	82
Act1 7 rev	accttcaagtcctacgctttctt	
For *TFIIB* (ChIP)		
TFIIB 1 fw	atcaatcctgcatctagcttgc	83
TFIIB 1 rev	tggacgtcttcccattctg	
TFIIB 2 fw	gttgcagatgtcttatctgcttt	84
TFIIB 2 rev	agacagtctctcccatctcattc	
TFIIB 3 fw	cgaaaaaatattggggaaaatc	80
TFIIB 3 rev	tgaaagaacttaagaaggagggc	
TFIIB 4 fw	gatttaatgcgtccgttattattc	79
TFIIB 4 rev	tcaatgcatggaaaagacca	
TFIIB 5 fw	catatcagattggttttgggtg	83
TFIIB 5 rev	ccactagcttcatcagagttgg	
TFIIB 6 fw	cacgagtacattcaaagcagttc	84
TFIIB 6 rev	caccgacataggaagcataagc	
TFIIB 7 fw	cgccttttacattgaggtcc	79
TFIIB 7 rev	gcgttcgataccagtgagg	
For *TFIIB* (NRO)		
TFIIB 1 fw	gtggtatagcgctttcaagc	219
TFIIB 1 rev	caaaaatttacaataaagtgctac	

TFIIB 2 fw	gtagcactttattgtaaatttttg	218
TFIIB 2 rev	cacaaacggtatcaccactc	
TFIIB 3 fw	gagtggtgataccgtttgtg	220
TFIIB 3 rev	acgccattcacttctcgtat	
TFIIB 4 fw	atacgagaagtgaatggcgt	220
TFIIB 4 rev	gcgcctatctccttatatgc	
TFIIB 5 fw	gcatataaggagataggcgc	210
TFIIB 5 rev	gacattggtcaaggtgcata	
TFIIB 6 fw	tatgcaccttgaccaatgtc	229
TFIIB 6 rev	agctctacgagccagttcag	
TFIIB 7 fw	ctgaactggctcgtagagct	209
TFIIB 7 rev	gcaatccatttaggatcaatc	
TFIIB 8 fw	gattgatcctaaatggattgc	220
TFIIB 8 rev	gatgatacaatcgcaaatatcatc	
TFIIB 9 fw	gatgatatttgcgattgtatcatc	212
TFIIB 9 rev	gtatttcctgtaaagttgca	
TFIIB 10 fw	tgcaactttacaggaaatac	182
TFIIB 10 rev	attgaaatctaccgaactcg	
For c*dc48*		
Cdc48 1 fw	aaagactcaactgcttacagatgttat	84
Cdc48 1 rev	ttgctcaaaaaggtaaattatttctaa	
Cdc48 2 fw	cgtcgagggtcttactggtt	82
Cdc48 2 rev	gcccttttcgaataggacgat	
Cdc48 3 fw	tgcagaagtccgtcgttatg	83
Cdc48 3 rev	cagccgaatcaaactggaat	
Cdc48 4 fw	tattttcaaggtgaactgctactatg	85
Cdc48 4 rev	gtagatttaacggggcgttg	
Cdc48 5 fw	tttgacggattcagaaagtttg	80
Cdc48 5 rev	aatcgtttttgaatgttttcactg	
Cdc48 6 fw	gtccttcacgtgccttgttt	80
Cdc48 6 rev	tcaagaggagaatcggaaatg	
Negative control (ChIP)		
18S fw	atggaagggtttgagtaagagca	83
18S rev	gtttcctctggcttcaccctatt	
For *rip1* (NRO)		
Rip1 1 fw	gttcttatacggaacctagt	229
Rip1 1 rev	catatccgaagttctccgaa	
Rip1 2 fw	ggagaacttcggatatgtag	224
Rip1 2 rev	cgaagatgctaacgacttag	
Rip1 3 fw	ctaagtcgttagcatcttcg	206
Rip1 3 rev	cattgtgcctaccatggcat	
Rip1 5 fw	ccaagaagccaattctgtag	222
Rip1 5 rev	aagttaagaggtgcaggacc	
Rip1 7 fw	tttgtcctagctgatttcct	227

Rip1 7 rev	gagaaggggtttgtatcag	
Rip1 9 fw	ccttgagtactcttcttgcc	215
Rip1 9 rev	taagccagcttcatgattcc	

Buffers (always prepared fresh ones from stock solutions)**:**

TNM

10 mM Tris-HCl, pH 7.4

5 mM MgCl

100 mM NaCl

20 × SSC

3 M NaCl

0.3 M sodium citrate

pH 7.0 with 1M HCl

Hybridization buffer

50% formamide

10 × Denhardt's

2 × SSPE

0.2% SDS

40 µg/ml tRNA

10 × Denhardts

1% Ficoll 400

1% polyvinylpyrrolidone (MW 40,000)

1% bovine serum albumin (BSA)

Filtered and stored at -20^{0}C in aliquots.

NRO buffer

20 mM Tris-HCl, pH 7.5

5 mM $MgCl_2$

100 mM KCl

2 mM DTT
2.5 mM ATP
2.5 mM GTP
2.5 mM CTP
Prepared fresh before use.

20 × SSPE
3 M NaCl
200 mM NaH2PO4 × H2O
200 mM EDTA
Adjusted the pH to 7.4 with 10N NaOH.
Sterilized by autoclaving.

2.10. RNA isolation

Pelleted cells were washed with sterile water and placed on ice. Cells were resuspended in 400 µl of AE buffer, 40 µl of 10 % SDS and 440 µl of AE phenol were added. Mixture was vortexed, incubated for 5 min at 65°C and left on dry ice until phenol crystallized. Cells were spinned down for 2 min at RT, liquid phase was transferred into a new tube and one volume of AE phenol/chlorophorm (1:1 freshly prepared mixture) was added. Samples were vortexed and centrifuged at 14,000 rpm for 5 min at RT. Liquid phase was transferred to new tube, 0.1 volume of 3M NaOAc, pH 5.3 and 2.5 volumes of 96% ethanol were added and samples were kept at -20°C for 10 min. RNA was spinned for 10 min at 14,000 rpm at 4°C, pellet was washed with 500 µl of ice cold 70 % ethanol and spinned again at the same conditions for 5 min. Pellet was air dried and dissolved in 30 µl of RNase-free water.

Buffers (always prepared fresh ones from stock solutions)**:**

AE buffer
50 mM NaOA
10 mM EDTA

pH 5.0 adjusted with acetic acid

AE Phenol (acidic phenol)
liquified phenol was equilibrated with an equal volume of AE buffer

2.11. Chromatin immunoprecipitation (ChIP)

ChIP was performed as described in (Takahashi et al, 2000). Fifty milliliters of cells were cultured to OD 0.5, cells grown with thiamine were treated as outlined in Sections 2.8. and 2.9. One tenth volume of 11% formaldehyde solution was added to the culture and it was incubated for 10 min at 26°C with occasional shaking. Cell culture was chilled on ice for 50 min, pelleted by centrifugation at 1,000 × *g* at 4°C for 5 min and washed three times with ice-cold ChIP buffer I. Whole cell extract was prepared as described in Section 2.6., but 0.5 ml of ice-cold ChIP buffer I was used instead of PEB and sonicated three times for 6 sec, at power of 200 W, 50 cycles. The extract was incubated with protein A Sepharose at 4°C for 1 h. Solution was spinned down, equal amounts of supernatant were taken for IP with antibodies and protein A Sepharose only. The input sample was one sixth of the amount used for one IP. For IP 5 µg of anti-RNAP II CTD repeat (4H8), 0.4 µg of anti-phospho RNAP II (S2), 0.4 µg anti-phospho RNAP II (S5), 4 µg anti-H3 or 19 µg anti-AcH3K9K12 (Table 2.6.) were mixed with 30 µl of protein A Sepharose and added to the whole cell extracts. Thirty microliters of protein A Sepharose only were mixed with the whole cell extracts as a negative control. Anti-HA antibody (12CA5) was prepared in advance by incubating 500 µl of hybridoma solution with 30 µl of protein A Sepharose o/n at 4°C. Bound antibody was washed with ChIP I buffer and then mixed with protein extracts. Samples were incubated with antibodies or protein A Sepharose only o/n at 4°C. Beads were pelleted and washed three times with ChIP buffer I, twice with ChIP buffer II and ChIP buffer III sequentially and once with TE. All buffers were ice-cold. One hundred microliters of TE containing 10 µg/ml RNase A was added to all samples including input and left at 37°C for 15 min. 2.5 µl of 10% SDS and 2.5 µl of 1 mg/ml Proteinase K solution were added to all samples, probes were incubated 8 h at 37°C and 6 h at 65°C. After that samples were supplemented with 10 µl of 3 M sodium acetate (pH 5.2) and 100 µl of phenol/chloroform/isoamyl alcohol, vortexed and centrifuged at

14,000 rpm for 5 min at RT. The upper aqueous phase was transferred to new tube, supplemented with 40 µg of glycogen and 250 µl of 100% ethanol and incubated o/n at -20°C. The DNA was precipitated by centrifuging for 15 min at 14,000 rpm at RT, washed with 1 ml of 70% ethanol, spinned down again and air-dried. The pellets were resuspended in TE buffer (50 µl if 50 ml of cells were taken) and stored at −20°C. The amount of precipitated DNA was quantified by real-time PCR (qRT-PCR). 18 µl of PCR reaction cocktail were added to 2 µl of DNA. PCR program: 1 cycle: 95°C - 2 min; 40 cycles: 95°C - 15 sec, annealing temperature depending on primers used - 15 sec, 68°C - 1 min; 1 cycle: 95°C - 15 sec, 60°C - 15 sec, 10 min, 95°C - 15 sec. Each reaction was run in triplicates. Results were calculated according to formula E (primer efficiency)^ (mean Ct(input)/6 - mean Ct(IP sample)). Primer efficiency was estimated by running real time PCR reactions with following dilutions of genomic *S. pombe* DNA: 1000 ng/µl, 200 ng/µl, 40 ng/µl, 8 ng/µl and 1.6 ng/µl. A logarithmic curve was built using mean Ct values and the trendline plotted. The gradient of the graph trendline was taken for further calculation. E = gradient/2 + 1. In ChIPs performed with anti-phospho RNAP II (S2) and anti-phospho RNAP II (S5) antibodies results for all primer pairs were normalized to the corresponding values obtained with anti-RNAP II CTD repeat (4H8) antibody. Same was done to calculate ChIP results with anti-AcH3K9K12 antibody. The values were normalized to corresponding values obtained with anti-H3 antibody.

Buffers (always prepared fresh ones from stock solutions)**:**

Formaldehyde Solution
11% Formaldehyde (v/v)
100 mM NaCl
1 mM EDTA-Na, pH 8
0.5 mM EGTA-Na
50 mM Tris-Cl, pH 8

ChIP Buffer I
50 mM HEPES-KOH, pH 7.5
140 mM NaCl
1 mM EDTA, pH 7.5

1% Triton X-100 (v/v)
0.1% Sodium deoxycholate (w/v)

ChIP Buffer II
50 mM HEPES-KOH, pH 7.5
500 mM NaCl
1 mM EDTA, pH 7.5
1% Triton X-100 (v/v)
0.1% Sodium deoxycholate (w/v)

ChIP Buffer III
10 mM Tris-HCl, pH 8.0
250 mM LiCl
1 mM EDTA, pH 7.5
0.5% Nonidet P-40 (v/v)
0.5% Sodium deoxycholate (w/v)

1 mg/ml Proteinase K Solution
1 mg/ml Proteinase K
50 mM Tris-HCl, pH 8.0
1 mM $CaCl_2$

10 mg/ml RNase A solution
10 mg/ml RNase A
15 mM sodium acetate, pH 5.0
1 mM Tris-HCl, pH 7.5

PCR Reaction Cocktail
10 µl 10 × PCR master mix (LightCycler 480 SYBR Green I Master, Roche)
2 µl 40 µM primers (see Table 2.7.)
6 µl distilled water

2.12. Immunofluorescence (IF)

Cells were grown o/n in EMM2 medium and corresponding antibiotics, 200 µl were diluted 10 times in YES and grown to mid-exponential phase for about 8 h. Two hundred microliters of freshly prepared formaldehyde were supplemented to 2 ml of cell culture, cells were incubated for 70 min at 32^0C and spinned down. Pellet was washed three times with PEM, resuspended in 1 ml PEMS with 0.5 mg Zymolase (Seikagaku corporation) and incubated at 37°C for 1 h. Afterwards cells were washed three times with PEMS, resuspended in 1ml of PEM containing 1% Triton X-100, left at RT for 2 min and washed three times with PEM. At this stage experiment was stopped, cell were kept in 100 µl of 0.1% NaN3 in PEM at 4^0C. For IF with α-TAT1 antibody (Table 2.6.) cells were spinned down and resuspended in 1ml of 1 mg/ml fresh sodium borohydride in PEM, incubated for 5 min and pelleted. The step was repeated two more times and after that cells were washed with PEM three times. Next, cells for IF with either anti-TAT1, or HA antibodies were resuspended in 100 µl of PEMBAL and incubated for 1 h at RT on a rotating wheel with tubes wrapped in aluminium foil. Pelleted samples were resuspended in 100 µl of PEMBAL with either α-TAT1, or anti-HA, rotated o/n at RT and washed three times with 100 µl of PEMBAL. Afterwards, cells were resuspended in 100 µL of PEMBAL with either anti-mouse Alexa 568 or anti-rat Alexa 568 secondary antibodies and incubated o/n at RT. Cells were washed four times with PEM and kept in 100 uL of 0,1% NaN3 in PEM at 4^0C. In addition, cells were stained with Hoechst (Molecular probes) to visualize DNA. Samples were analyzed by microscopy (Zeiss, Axioplan epifluorescence microscope), images were taken by a CCD camera and further processed in Adobe Photoshop.

Buffers (always prepared fresh ones from stock solutions)**:**

<u>38% formaldehyde</u>
Dissolved 380 mg paraformaldehyde in 700 uL PEM
Added 48 µl 5M NaOH

Incubated 30 min at 65^0C, vortexed every 10 min, centrifuged 5 min at 13,000 rpm and used supernatant.

PEM

100 mM Pipes

1 mM EGTA

1 mM $MgSO_4$

Adjusted 6.9 pH with 5 M NaOH

PEMS

PEM

1.2 M sorbitol

PEMBAL

PEM

1% BSA

100 mM lysine

0.1% NaN_3

2.13. Y2H

Y2H assay was performed according to manufacturer's instructions (Clontech).

3. Results

3.1. Rct1 interacts with the CTD of RNAP II and non-kinase parts of Cdk9 and Lsk1 *in vitro* via its PPIase domain

3.1.1. Rct1 binds CTD kinases Cdk9 and Lsk1 *in vitro*

It was previously shown that AtCyp59 from *A. thaliana* and its *S. pombe* homologue Rct1 interact with RNAP II and regulate phosphorylation status of the RNAP II CTD (Gullerova et al, 2006), (Gullerova et al, 2007). However, the mechanism of this regulation remained unclear. Rct1 could regulate the activities of CTD kinases and phosphatases. Therefore, I decided to check if Rct1 binds known CTD kinases and phosphatases by *in vitro* pull-down assays. GST fusions of CTD kinases Cdk7, Cdk9, Lsk1, Srb10 and phosphatases Fcp1, Scp1, Ssu72 were overexpressed in *E. coli* and purified on glutathione Sepharose beads (Fig. 3.1. A, lanes 1-8). Protein extracts from haploid *S. pombe* $rct1\Delta^{pMG1}$ cells, expressing HA tagged Rct1 from plasmid, were incubated with glutathione Sepharose beads coated with each of the GST tagged CTD kinases and phosphatases. Bound proteins were analyzed by SDS-PAGE and Western blotting with anti-HA antibody. Figures 3.1. B and C demonstrate that out of all tested proteins only Cdk9 and Lsk1 were able to bind Rct1 *in vitro* (Fig. 3.1. B, lanes 3 and 4). The interactions were specific as neither GST, nor glutathione beads alone were able to pull-down Rct1 (Fig. 3.1. B, lanes 5 and 6). As Rct1 has an RRM domain same experiment was repeated with an RNaseA treatment, but results did not change. This finding further supports the role of Rct1 in RNAP II transcription.

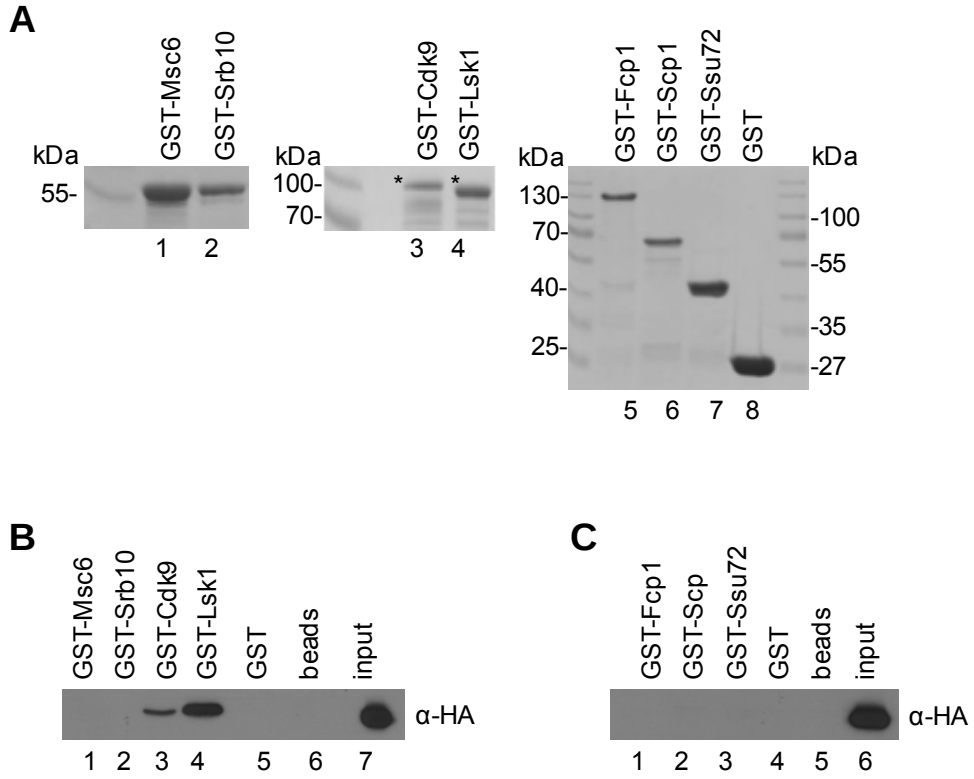

Fig. 3.1. Interaction of Rct1 with CTD kinases and phosphatases. (A) Coomassie blue-stained gel of purified recombinant GST tagged kinases Msc6, Srb10, Cdk9 and Lsk1 (full-length proteins are marked with an asterisk on the left side) (lanes 1-4, respectively) and phosphatases Fcp1, Scp1 and Ssu72 (lanes 5-7, respectively). Lane 8, purified GST. Molecular mass standards in kilodaltons are indicated on the sides. (B) Rct1 interacts with certain CTD kinases *in vitro.* Whole cell extracts from *S. pombe* cells expressing HA-tagged Rct1 were incubated with glutathione Sepharose beads coated with GST-tagged CTD kinases Msc6 (lane 1), Srb10 (lane 2), Cdk9 (lane 3) and Lsk1 (lane 4). Proteins left on the beads after washing were analyzed by Western blotting with rat anti-HA monoclonal antibody. Lane 7, 10% of the input extract used for pull-downs with beads coated with GST-Msc6, GST-Srb10, GST-Cdk9, GST-Lsk1 and GST alone (lane 5) or with beads alone (lane 6). (C) Same pull-down as in Fig. 3.1. B was performed with CTD phosphatases Fcp1, Scp1 and Ssu72. Lane 6, 10% of the input extract used for pull-downs with beads alone (lane 5) or beads coated with GST-Fcp1 (lane 1), GST-Scp10 (lane 2), GST-Ssu72 (lane 3) and GST alone (lane 4).

3.1.2. Rct1 interacts with non-kinase parts of Cdk9 and Lsk1 *in vitro*

Cdk9 and Lsk1 consist of a kinase domain and a distinct non-kinase extension. Therefore, I asked which of the part(s) is (are) responsible for Rct1 binding. GST fusion deletion mutants of Cdk9 and Lsk1: Cdk9 kinase, Cdk9 C-terminus, Lsk1 kinase, Lsk1 kinase together with C-terminus and Lsk1 N-terminus are schematically represented in Figure 3.2. A. The proteins were overexpressed in *E. coli* and purified (Fig. 3.2. B, lanes 1-5). Same *in vitro* pull-downs as in Section 3.1.1 with protein extracts from *rct1Δ*^{pMG1} cells were performed. Figure 3.3. (lanes 4 and 8) demonstrates interactions between non-kinase parts of Cdk9 as well as of Lsk1 and Rct1. Full-length Cdk9 and Lsk1 (Fig. 3.3., lanes 2 and 5) were used as positive controls. As kinase domains did not show any interactions in several repetitions, I conclude that Rct1 binds to Cdk9 and Lsk1 through their non-kinase extensions.

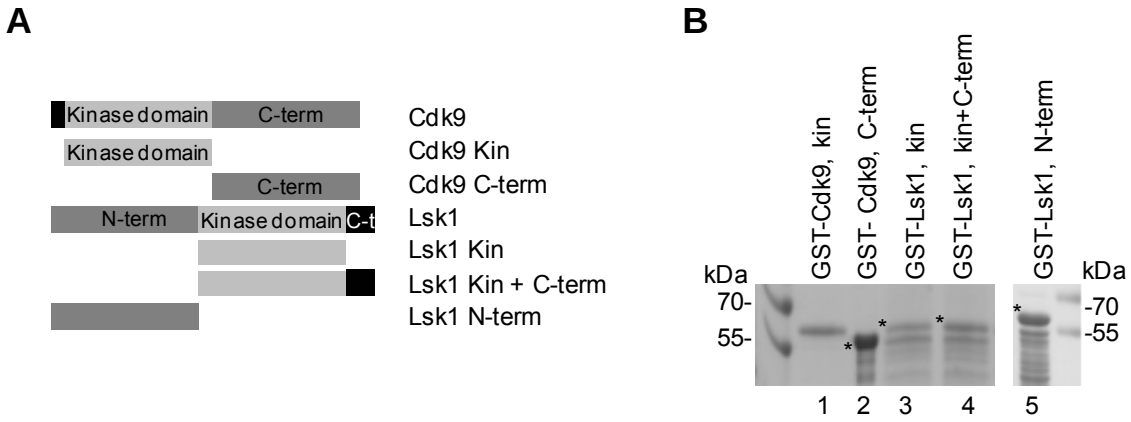

Fig. 3.2. CTD kinases Cdk9 and Lsk1 and their mutants. (A) Schematic presentation of Cdk9, Lsk1 and their deletion mutants tagged with GST. (B) Coomassie blue-stained gel of purified recombinant GST tagged Cdk9 and Lsk1 deletion mutants. Lane 1, GST-Cdk9 kinase domain; lane 2, GST-Cdk9 C-terminus; lane 3, GST-Lsk1 kinase domain; lane 4, GST-Lsk1 kinase domain with C-terminus; lane 5, and GST-Lsk1 N-terminus. Full-length proteins are marked with an asterisk on the left side. Molecular mass standards in kilodaltons are indicated on the right side.

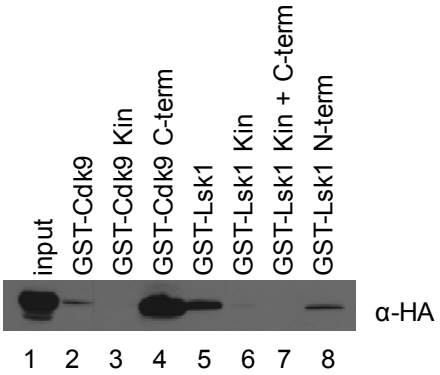

Fig. 3.3. Interaction of Rct1 with CTD kinases Cdk9 and Lsk1. Rct1 interacts with non-kinase parts of Cdk9 and Lsk1 *in vitro*. Pull-down experiment was performed with GST-tagged Cdk9 and Lsk1 deletion mutants as described in Fig. 3.1. C. Lane 1, 10% of the input extract used for pull-downs with beads coated with GST-Cdk9 (lane 2), GST-Cdk9 kinase domain (lane 3), GST-Cdk9 C-terminus (lane 4), GST-Lsk1 (lane 5), GST-Lsk1 kinase domain (lane 6), GST-Lsk1 kinase domain and C-terminus (lane 7) and GST-Lsk1 N-terminus (lane 8). Western blot was probed with anti-HA antibody.

3.1.3. PPIase domain of Rct1 is responsible for its interaction with the CTD and its kinases, Cdk9 and Lsk1

Rct1 is a multidomain protein, consisting of a PPIase domain, followed by an RRM domain and an RS domain at the C-terminus (Gullerova et al, 2007). Therefore, it was important to find out which of the domain(s) is(are) responsible for the Cdk9, Lsk1 and the CTD binding. To address the question, following *rct1* strains, expressing HA tagged deletion and point mutants of Rct1 from plasmids, were created: RS domain deleted - $rct1^{+/\text{-}pMG2}$, expressing PPIase domain only - $rct1^{+/\text{-}pMG3}$, PPIase domain deleted - $rct1^{+/pMG4}$, PPIase domain deleted and with point mutation of the 3 conserved amino acids in RRM domain - $rct1^{+/\text{-}pMG4R3}$, with no RRM - $rct1^{+/\text{-}pMG5}$ and expressing RRM domain only $rct1^{+/\text{-}pMG6}$ (Fig. 3.4. A). I used diploid cells for the subsequent experiments, because such haploid strains as $rct1\Delta^{pMG3}$ and $rct1\Delta^{pMG5}$ are barely viable (Lorkovic et al, 2009). The full-length GST tagged CTD was overexpressed in *E. coli* and purified (Fig. 3.4. B). The recombinant CTD, Cdk9 and Lsk1, bound to glutathione Sepharose beads, were

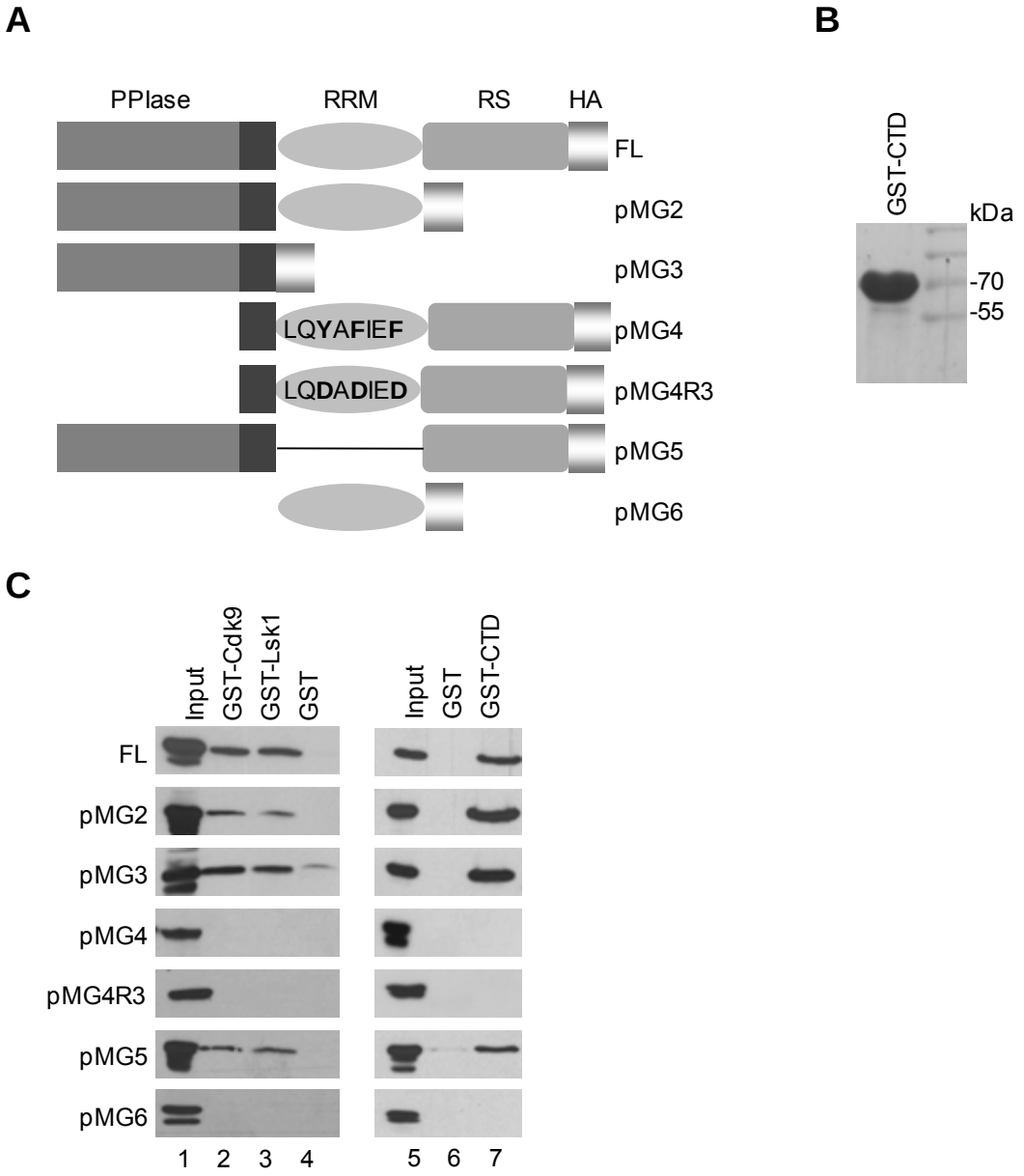

Fig. 3.4. Interaction of Rct1 deletion mutants with Cdk9, Lsk1 and the CTD. (A) Schematic representation of HA-tagged Rct1 deletion mutants. Names of the mutants correspond to the plasmid names, which are indicated on the right side. (B) Coomassie blue-stained gel of purified recombinant GST-CTD (full-length C-terminus of RNAP II Rpb1 subunit from *A.thaliana*). Molecular mass standards in kilodaltons are indicated on the left side. (C) Interaction of Rct1 deletion mutants with GST-Cdk9, GST-Lsk1 and GST-CTD. Pull-down experiments were performed as in Fig. 3.1. B with whole cell extracts from *S.pombe* cells expressing full-length or mutant Rct1. Rct1 versions used for each experiment are indicated on the left side. 10% of the input extract (lanes 1, 5) used for pull-downs with beads coated with GST-Cdk9 (lane 2), GST-Lsk1 (lane 3), GST (lanes 4 and 6) and GST-CTD (lane 7). Western blot analysis was performed with anti-HA antibody.

incubated with the protein extracts from strains expressing Rct1 deletion mutants. As shown in Figure 3.4. C only Rct1 mutants with PPIase domain present (pMG2, pMG3 and pMG5) could bind the CTD, Cdk9 and Lsk1 (Fig. 3.4. C, lanes 2, 3 and 7). There is a signal in lane 4 on the Figure 3.4. C (pMG3), which represents the pull-down with GST only. This could be due to the mutant extensive overexpression. As none of the other tested mutants bound GST (Fig. 3.4. C, lanes 4 and 7), I concluded that PPIase domain of Rct1 mediates its interaction with the CTD and its kinases, Cdk9 and Lsk1, *in vitro*.

3.1.4. Rct1 interacts with Lsk1 associated cyclin Lsc1

The interaction shown by *in vitro* pull-downs between Rct1 and CTD kinases, Cdk9 and Lsk1 (Figs. 3.1., 3.3. and 3.4.) are not necessarily direct *in vivo*. Cdk9 and Lsk1 are known to form complexes with cyclins Pch1 and Lsc1, respectively (Pei & Shuman, 2003), (Pei et al, 2003), (Karagiannis et al, 2005). I decided to check Rct1 binding to the kinases and the cyclins by using yeast two-hybrid assay (Y2H). The results were not reliable (data not shown), because only one of the positive controls worked (Cdk9 and Pch1), whereas interaction between Lsk1 and Lsc1 was not confirmed by Y2H. This outcome shows that Y2H method may not be applicable in this case. Next step was to check if Rct1 binds cyclins Pch1 and Lsc1 using *in vitro* pull-downs. Both cyclins were GST-tagged, overexpressed in *E. coli*, purified (Fig. 3.5. A) and incubated with protein extract derived from $rct1\Delta^{pMG1}$ strain using Sepharose beads coated with GST-Pch1 and GST-Lsc1. Lsc1 (cyclin of Lsk1) interacts only weakly, but reproducibly with Rct1 *in vitro* (Fig. 3.5. B, lane 2). The low strength of the Lsc1-Rct1 association could be explained that the GST tag of Lsc1 interferes with the interaction and/or the interaction is indirect; i.e. Lsc1 pulls down Rct1 together with Lsk1. It also could be that Lsg1, a newly characterized subunit of Lsk1/Lsc1/Lsg1 trimeric complex, might be involved in this interaction (Karagiannis & Balasubramanian, 2007), (personal communication with Sukegawa). Although Cdk9 binds Rct1 and forms complex with cyclin Pch1, Rct1 was not pulled down by Pch1 (Fig. 3.5. B, lane 3). This suggests that Rct1 binds directly Cdk9 and/or Pcm1 (cap-methyltransferase), a component of Cdk9/Pch1/Pcm1 complex (Pei et

al, 2003), (Pei et al, 2006). Thus, the mechanisms of Rct1 interactions with Cdk9/Pch1/Pcm1 and Lsk1/Lsc1/Lsg1 complexes are different.

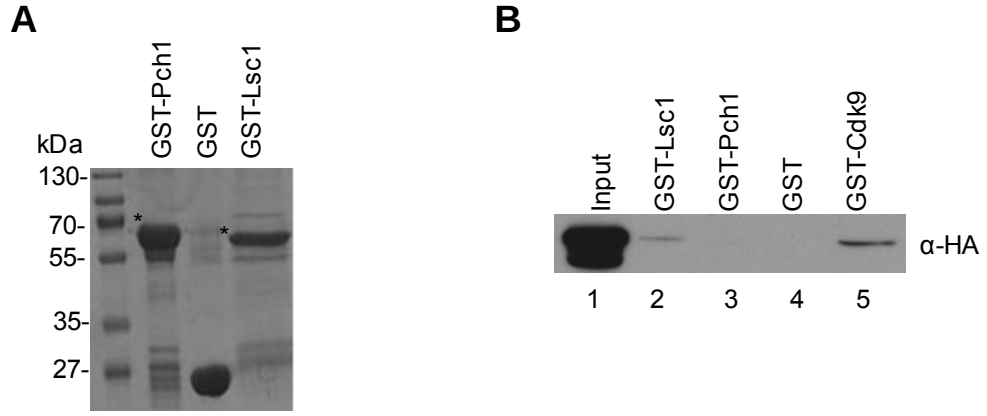

Fig. 3.5. Interaction of Rct1 with Cdk9 and Lsk1 associated cyclins Pch1 and Lsc1, respectively. (A) Coomassie blue-stained gel of purified recombinant GST-Pch1, GST and GST-Lsc1 (full-length proteins are marked with an asterisk on the left side). Molecular mass standards in kilodaltons are on the left side. (B) Rct1 interacts with Lsc1 *in vitro*, but not with Pch1. Pull-down experiment was performed with GST-Lsc1 (lane 2) and GST-Pch1 (lane 3) as described in Fig. 3.1. B. Lane 1, 10% of the input extract; lane 4, pull-down with GST only; lane 5, pull-down with GST-Cdk9. Western was performed with anti-HA antibody.

3.2. Rct1 negatively affects Cdk9 kinase activity towards the CTD

3.2.1. Cdk9 kinase activity towards the CTD is upregulated under the conditions of Rct1 depletion

As I have shown that Rct1 binds Cdk9, next question was if Rct1 affects the kinase activity of Cdk9 towards the CTD. To address this question, a strain *cdk9-HA rct1Δ*^{pMG1F} was generated, that has an HA-tagged Cdk9 on chromosome and is expressing Rct1 fused to FLAG under the control of thiamine repressible promoter. Rct1 level analysis in c*dk9-HA rct1Δ*^{pMG1F} cells before and after thiamine treatment demonstrated significant depletion

of the protein in the letter case (Fig. 3.6. A, middle panel, lanes 2 and 3). This result is supported by the equal amounts of Cdk9-HA and tubulin in both samples (Fig. 3.6. A,

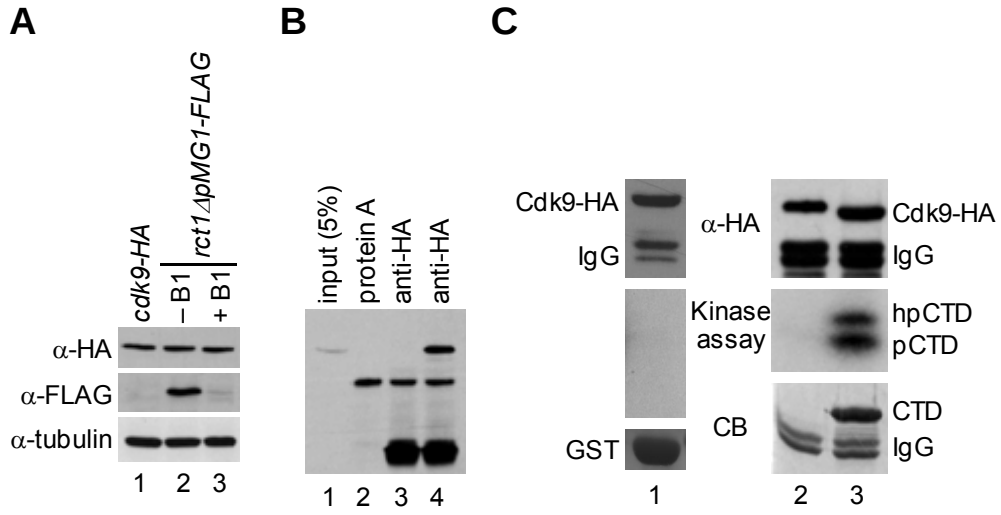

Fig. 3.6. Establishing system for Cdk9 kinase assay. (A) Western blots from *cdk9-HA* cells (lane 1) and *cdk9-HA rct1Δ*^{pMG1F} cells grown in the absence (lane 2) / the presence (lane 3) of thiamine (B1) were probed with the antibodies indicated on the left. (B) Immunoprecipitation of Cdk9. Lane 1, input protein extract from *cdk9-HA rct1Δ*^{pMG1F} cells. Lane 2, protein extract from *cdk9-HA rct1Δ*^{pMG1F} cells incubated with protein A Sepharose. Lane 3, protein extract from *wt* cells incubated with anti-HA antibody and protein A Sepharose. Lane 4, extract from *cdk9-HA rct1Δ*^{pMG1F} cells incubated with anti-HA antibody and protein A Sepharose. (C) Kinase assay with precipitated Cdk9-HA and recombinant GST or GST-CTD. Protein extracts were incubated with anti-HA beads and protein A Sepharose, supernatant was removed; proteins immobilized on protein A Sepharose were incubated with GST (lane 1), without GST-CTD or GST (lane 2) or with GST-CTD (lane 3) in the presence of γ-[^{32}P]-ATP. Upper panels, western blot analyses of kinase reactions performed with anti-HA antibody. Middle panels, autoradiographies of kinase assays. Note that kinase assays with only GST (lane 1) or without both GST and GST-CTD (lane 2) did not result in detectable amount of radioactive signal. Lower panels, Coomassie blue-stained gels of the same kinase reactions.

lanes 2 and 3 in upper and lower panels). HA antibody, bound to protein A Sepharose, was able to precipitate Cdk9-HA from *cdk9-HA rct1Δ*^{pMG1F} cells efficiently (Fig. 3.6. B, lane 4) and produced no background with *wt* cells (Fig. 3.6. B, lane 3). Additionally, there was no background after precipitating Cdk9-HA with protein A Sepharose only (Fig. 3.6. B, lane 2). Finally, kinase assay was successfully carried out with the precipitated Cdk9 and

the purified GST-CTD (Fig. 3.4. B) as a substrate (Fig. 3.6. C). As kinase assay performed without the CTD (Fig. 3.6. C, lane 2) did not show Cdk9 autophosphorylation, I conclude that both bands are indeed the phosphorylated CTD, which were defined as hypophosphorylated – pCTD (lower band) and hyperphosphorylated – hpCTD (upper band).

Having established successful system for Cdk9 immunoprecipitation and kinase activity measurement, I decided next to analyze the effect of the Rct1 depletion on the Cdk9 kinase activity towards the CTD. *Cdk9-HA rct1Δ*^{pMG1F} cells were grown in EMM overnight, diluted into YES and grown further till the mid-log phase. First batch was collected (-B) and the rest was diluted in YES+thiamine and grown 24 hours to deplete

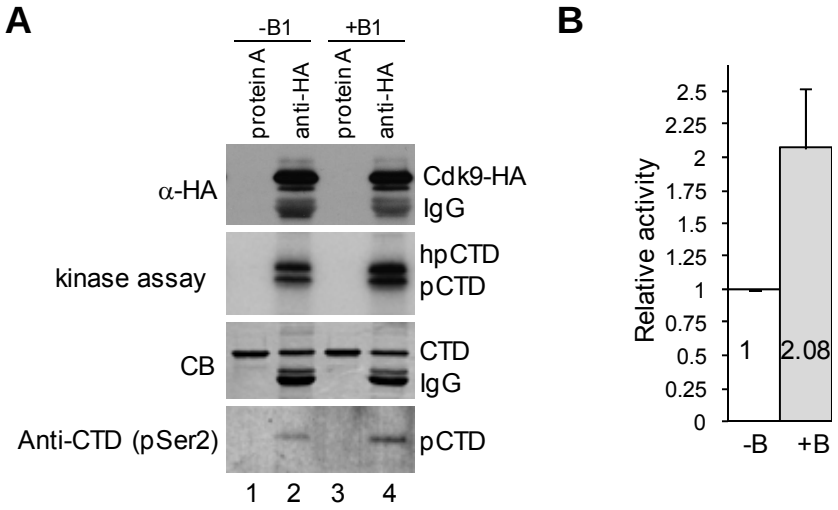

Fig. 3.7. Effect of Rct1 depletion on Cdk9 activity towards the CTD. (A) Cdk9 activity towards the CTD is increased in Rct1 depleted cells. Protein extracts from *cdk9-HA rct1Δ*^{pMG1F} cells grown in the absence (lanes 1 and 2) / the presence (lanes 3 and 4) of thiamine (B1) were incubated either with protein A Sepharose (lanes 1 and 3) only or with protein A Sepharose and anti-HA antibody (lanes 2 and 4). Immobilized proteins were incubated with γ-[^{32}P]-ATP and GST-CTD. Upper panel, Western blot analysis of kinase reactions performed with anti-HA antibody. No detectable amount of Cdk9-HA was immunoprecipitated with protein A Sepharose only. Second panel from above, autoradiogram of Cdk9 kinase assay. Note that both phosphorylated and hyperphosphorylated CTD signals are stronger with Cdk9 precipitated from Rct1 depleted cells. Third panel from above, Coomassie blue-stained gel of kinase reactions. Lowest panel, Western blot analysis of kinase reactions performed with H5 antibody (against Ser-2 phosphorylated RNAP II CTD (pSer2)). (B) Quantification of kinase assay shown in Fig. 3.7. A. Signals were quantified by Phosphoimaging and error bars indicate standard deviations from 5 independent repeats.

Rct1 (+B). Kinase assays were performed with Cdk9-HA precipitated from the *cdk9-HA rct1Δ^{pMG1F}* cells collected before and after thiamine treatment. Figure. 3.7. A (second panel from above, lanes 2 and 4) demonstrates the increase of the CTD phosphorylation in Rct1 depleted cells. Quantification of the phosphorylation signals (Fig. 3.7. B) reveals that kinase activity of Cdk9 increases two times in Rct1 depleted cells. Moreover, Western blot analysis of the same samples with the antibody against the Ser2 phosphorylated CTD (H5) (Fig. 3.7. A, lowest panel, lanes 2 and 4) was performed. The results demonstrate increased phosphorylation of Ser2 residue by Cdk9 immunoprecipitated from Rct1 depleted cells. As the same amount of Cdk9 was precipitated for each reaction (Fig. 3.7. A, upper panel, lanes 2 and 4) and the equal amount of the CTD was used (Fig. 3.7. A, third panel from above, lanes 1-4), I conclude that the decrease of Rct1 expression causes the increase of the Cdk9 kinase activity towards the CTD.

3.2.2. Increasing amounts of Rct1 cause the decrease of Cdk9 kinase activity towards the CTD

Having shown the increase of CTD phosphorylation by Cdk9 under the conditions of Rct1 depletion, I asked next whether a reverse effect would be observed in case of increasing Rct1 amount *in vitro*. GST tagged Rct1 was overexpressed in *E. coli* and purified (Fig. 3.8. A). Kinase assays were performed with Cdk9 immunoprecipitated from either *cdk9-HA rct1Δ^{pMG1F}* Rct1 depleted cells, or from *cdk9-HA* cells. Reactions were supplemented with increasing GST-Rct1 amounts. The results of both kinase assays (Fig. 3.8. B and C, second panels from above) revealed inhibition of Cdk9 activity as the amount of Rct1 increased. Quantification of the CTD phosphorylation signal revealed that pCTD signal decreases by more than 2.5 times, whereas hpCTD is more subjected to changes and its phosphorylation declines by more than 80% upon addition of 100 µg of GST-Rct1 (Fig. 3.8. B and C, lowest panels). The amounts of precipitated Cdk9 were equal in each reaction (Fig. 3.8. B and C, upper panels). Therefore, the obtained data provide further evidence that Rct1 negatively regulates kinase activity of Cdk9 towards the CTD.

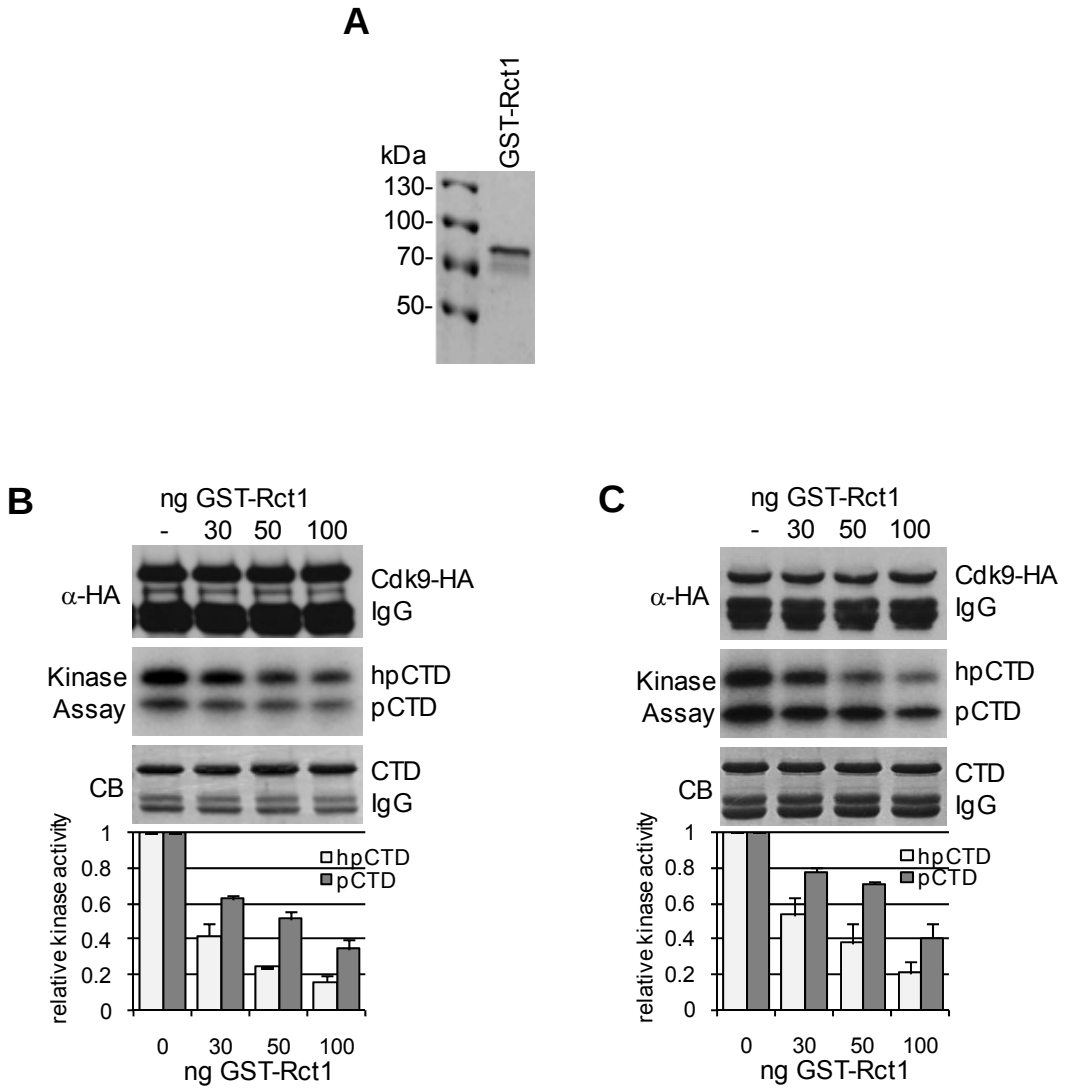

Fig. 3.8. The influence of increasing amounts of recombinant Rct1 on Cdk9 mediated CTD phosphorylation. (A) Coomassie blue-stained gel of purified recombinant GST-Rct1. Molecular mass standards in kilodaltons are indicated on the left side. (B-C) Increasing amounts of Rct1 cause decrease in the Cdk9 dependent CTD phosphorylation. Kinase reactions were carried out with Cdk9-HA precipitated from either (B) Rct1 depleted *cdk9-HA rct1Δ*^{pMG1F} or (C) *cdk9-HA* cells with addition of increasing amounts of GST-Rct1. Upper panel, Western blot analysis of kinase reactions performed with anti-HA antibody. Second panel from above, autoradiography of corresponding kinase assays. Note that both phosphorylated and hyperphosphorylated CTD signals decrease as the amount of Rct1 increases. Third panel from above, Coomassie blue-stained gel of kinase reactions (second panel). Lowest panel, quantification of kinase assay. Signals were measured by Phosphoimager, error bars indicate standard error of the mean.

Next step was to find out if Rct1 affects directly Cdk9. The kinase forms soluble complex with its cyclin Pch1 and methyltransferase Pcm1 (Pei et al, 2006), (Guiguen et al, 2007). Binding of Pch1 by Rct1 was ruled out by the pull-down performed (Fig. 3.5. B, lane 3). Interaction of Rct1 with Pcm1, however, was not checked. Kinase assays with non-specific substrate, histone 1 (H1), instead of the CTD were performed. Figure. 3.9. A (middle panel) does not show any considerable change in histone H1 phosphorylation signal upon Rct1 addition. As usual, reactions were supplemented with the same amount of immunoprecipitated Cdk9 and same amount of substrate, H1 (Fig. 3.9. A, upper and lower panels, respectively). The data show that Rct1 might not act solely on Cdk9 complex *in vitro*.

The pull-down experiment (Fig. 3.1. B, lane 1) has shown that CTD kinase Mcs6 does not bind Rct1. Thus, Rct1 should not affect the CTD phosphorylation via Msc6. Therefore, this kinase was a good candidate for the next kinase assay, designed to check if

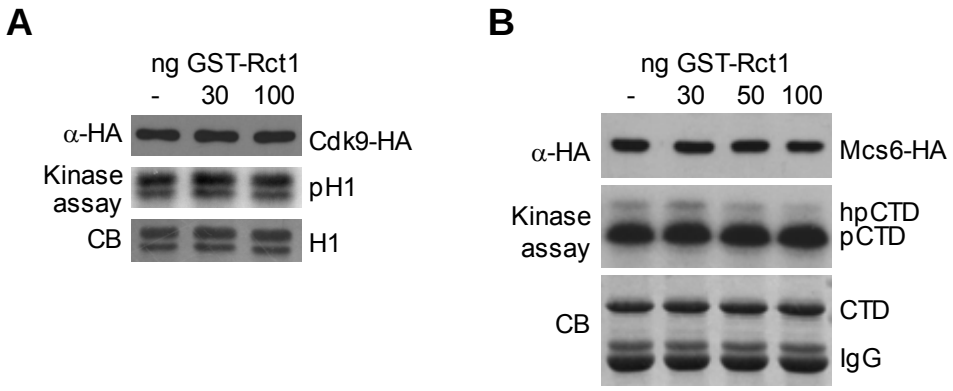

Fig. 3.9. The specificity of Rct1 regulation of Cdk9 activity towards the CTD. (A) Activity of Cdk9 towards histone H1 does not change under conditions of increasing Rct1 amounts. Kinase reactions were performed similarly to Fig. 3.8. B but instead of the CTD, H1 was used as a substrate. Upper panel, Western blot analysis of kinase reactions performed with anti-HA antibody. Middle panel, autoradiography of kinase assays. Note that no considerable changes in signal were observed. Lower panel, Coomassie blue-stained gel of kinase reactions. (B) Activity of Msc6 towards the CTD is not affected by the increasing amounts of Rct1. Kinase reactions were done by analogy to Fig. 3.8. B with precipitated Mcs6-HA instead of Cdk9-HA. Upper panel, Western blot analysis of kinase reactions performed with anti-HA antibody. Middle panel, autoradiography of kinase assay. Note that kinase assay with precipitated Msc6-HA and increasing amounts of recombinant GST-Rct1 did not result in CTD phosphorylation signal change. Lower panel, Coomassie blue-stained gel of kinase reactions.

Rct1 directly regulates CTD phosphorylation. The kinase assay was done with Msc6, immunoprecipitated from *msc6-HA* cells (Fig. 3.9. B). Again no significant changes in CTD phosphorylation were observed as Rct1 amount increased. The experiment suggests that Rct1 does not affect purely the CTD.

Together, performed kinase assays (Figs. 3.8. and 3.9.) suggest that Rct1 specifically mediates Cdk9 kinase activity towards the CTD. My hypothesis is that Rct1 inhibits Cdk9 phosphorylation of the CTD by interacting with Cdk9 and the CTD simultaneously. Thus, formation a trimeric complex between Rct1, Cdk9 and the CTD suppresses RNAP II phosphorylation.

3.2.3. PPIase domain is responsible for regulating Cdk9 kinase activity towards the CTD

I showed that PPIase domain of Rct1 mediates interaction between the cyclophilin and its binding partners, Cdk9 and the CTD (Section 3.1.3.). I could also demonstrate that Rct1 affects the CTD phosphorylation by Cdk9 (Sections 3.2.1 and 3.2.2.). Therefore, I asked whether PPIase domain was responsible for the phosphorylation regulation as well. GST-Rct1ΔPPIase mutant was overexpressed in *E. coli* and purified (Fig. 3.10. A). Kinase assays with immunoprecipitated Cdk9-HA from either *cdk9-HA rct1Δ*^{pMG1F} Rct1 depleted (Fig. 3.10. B) or *cdk9-HA* (Fig. 3.10. C) cells were performed. Increasing amounts of the GST-Rct1ΔPPIase protein were added to the reactions. Figures 3.10. B and C (middle panels) demonstrate that GST-Rct1ΔPPIase addition did not cause any significant change in the CTD phosphorylation status. Same amounts of precipitated Cdk9 and the CTD used in all reactions prove reliability of the results (Fig. 3.10. B and C, upper and lower panels, respectively). Next, kinase assay with H1 as a substrate was done by analogy with the assay described in Figure 3.9. A. Reactions were supplemented with the same amounts of Cdk9-HA immunoprecipitated from *cdk9-HA rct1Δ*^{pMG1F} Rct1 depleted cells, equal amounts of H1 (Fig. 3.10. D, upper and lower panels, respectively) and increasing amounts of GST-Rct1ΔPPIase. However, no considerable change in H1 phosphorylation level was observed (Fig. 3.10. D, middle panel). Thus, the results of these kinase assays clearly show that PPIase domain is crucial for Rct1 regulation of Cdk9 kinase activity towards the CTD.

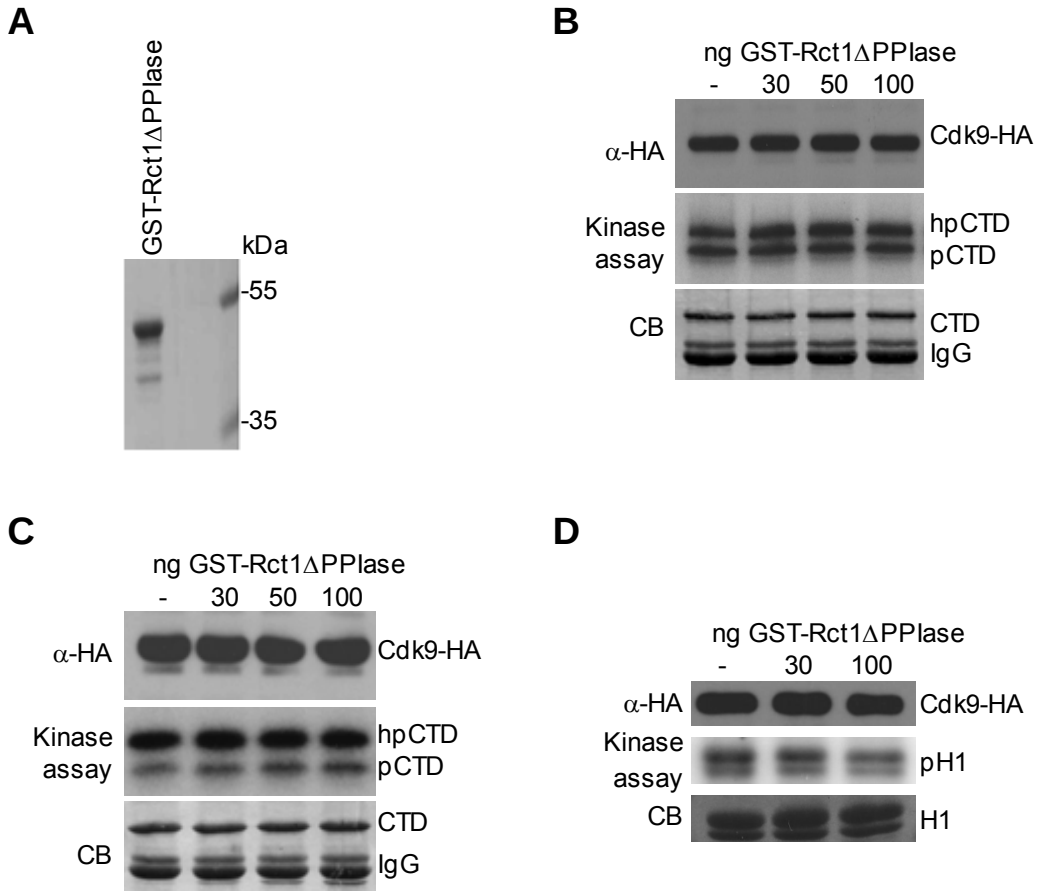

Fig. 3.10. Rct1 PPIase domain is responsible for Cdk9 kinase activity towards the CTD. (A) Coomassie blue-stained gel of purified recombinant GST-Rct1ΔPPIase. Molecular mass standards in kilodaltons are indicated on the right side. (B-C) Increasing amounts of Rct1ΔPPIase do not affect Cdk9 dependent CTD phosphorylation. Kinase reactions were performed similarly to Fig. 3.8. B and C. Cdk9 was precipitated from either (B) Rct1 depleted *cdk9-HA rct1Δ*^{pMG1F} or (C) *cdk9-HA* cells, but instead of GST-Rct1 increasing amounts of GST-Rct1ΔPPIase were added. Upper panels, Western blots of kinase reactions performed with anti-HA antibody. Middle panels, autoradiographies of corresponding kinase assays. Note phosphorylated CTD signals do not change as the amount of Rct1ΔPPIase increases. Lower panels, Coomassie blue-stained gels of kinase reactions. (D) Activity of Cdk9 towards H1 does not change in the conditions of increasing Rct1ΔPPIase amounts. Kinase reactions were carried out as described in Fig. 3.9. A. Rct1 depleted *cdk9-HA rct1Δ*^{pMG1F} cells were used and reactions were supplemented with increasing amounts of GST-Rct1ΔPPIase. Upper panel, Western blot analysis of kinase reactions performed with anti-HA antibody. Middle panel, autoradiography of kinase assays. Note that no considerable change in signal is observed. Lower panel, Coomassie blue-stained gel of kinase reactions.

3.3. Rct1 regulates RNAP II recruitment to chromatin and genes' activity

3.3.1. Rct1 overexpression promotes RNAP II recruitment to chromatin

It has been shown previously that ongoing RNAP II transcription is reduced in *rct1*$^{+/-}$ cells (Gullerova et al, 2007). Moreover, I could show here that Rct1 is required for regulation of Cdk9 kinase activity (Section 3.2.). Therefore, I decided to find out which stage(s) (initiation, elongation, termination) of RNAP II transcription is (are) affected by Rct1.

To this end, chromatin immunoprecipitation (ChIP) with antibody against the RNAP II CTD was performed with the aim to determine RNAP II occupancy on transcriptionally active protein coding genes. I used the antibody which recognizes both phospho- and nonphosphorylated CTD (4H8) in order to determine total RNAP II engaged into active transcription. Regions including *act1*, *cdc48* and *TFIIB* genes (Fig. 3.11. B-D) were chosen for ChIP analysis due to their constitutive transcription and location on chromosome with respect to neighbouring genes. As Rct1 could affect initiation and/or termination phases of transcription, the analyzed loci included intergenic regions between convergently (*act1* and *mei4*) and divergently (*cdc48* and *rst2*; *tif45* and *TFIIB*) transcribed genes. Three sets of primers were designed, which covered sequences from *act1* promoter to the 3' end of *mei4*, from *cdc48* promoter to the promoter of divergently expressed *rst2* and from open reading frame (ORF) of *tif45* to terminating regions of divergently expressed *TFIIB* (Fig. 3.11. B-D). ChIP analysis of RNAP II was performed with *wt* and *rct1Δ*^{pMG1} cells, collected before and after thiamine treatment.

Western blot analysis (Fig. 3.11. A) reveal that in the thiamine treated cells there was no or very little Rct1-HA detected with anti-HA antibody. However, the level of Rct1, measured with anti-Rct1 antibody, was almost the same as in *wt*. Although some genes were found to generate null phenotype under repressed nmt1 promoter (http://www-rcf.usc.edu/~forsburg/plasmids.html#promoter), leaky expression is common due to not complete nmt1 repression (Forsburg, 1993).

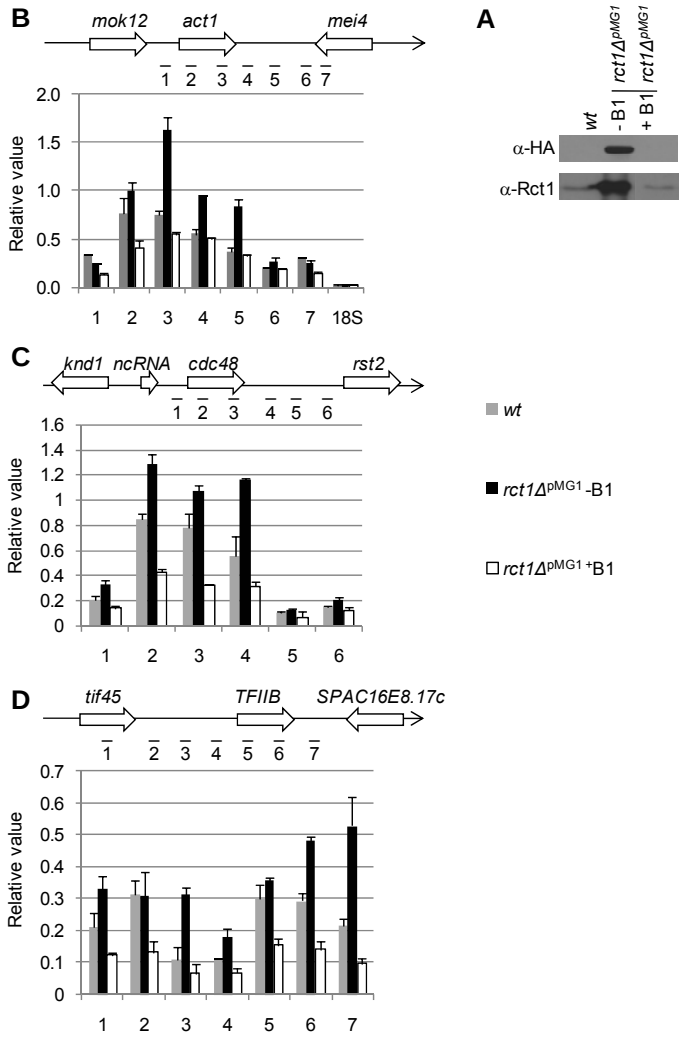

Fig. 3.11. Rct1 affects RNAP II occupancy profile along transcription units. (A) Repression of Rct-HA expression under thiamine addition. Western blot from *wt* (lane 1) and *rct1Δ*^{pMG1} cells gown without (lane 2) and with (lane 3) thiamine were analyzed with anti-HA and anti-Rct1 antibody. (B-D) ChIPs of chromosome regions that include *act1* (B), c*dc48* (C), *TFIIB* (D) and 18S rRNA as negative control (B) were performed with 4H8 antibody (against phospho- and nonphosphorylated RNAP II) and protein extracts from *wt* cells (grey bars), *rct1Δ*^{pMG1} cells grown without (black bars; Rct1 overexpression) and with thiamine (white bars; Rct1 depletion). In the diagrams above, open reading frames (ORFs) are shown by arrows that define transcription direction and numbered bars below the genes represent the approximate positions of the real-time PCR (qRT-PCR) products. The numbers of the bars correspond to the numbers on the x-axes. The y-axes represents the ratio of immunoprecipitated DNA versus input (see Section 2.11. for calculation). Coimmunoprecipitated DNA was analyzed by qRT-PCR. Error bars indicate standard deviations from 3 biological repeats (9 PCR reactions). Values of the negative controls, run with protein A Sepharose beads only, did not exceed one tenth for all samples (data not shown).

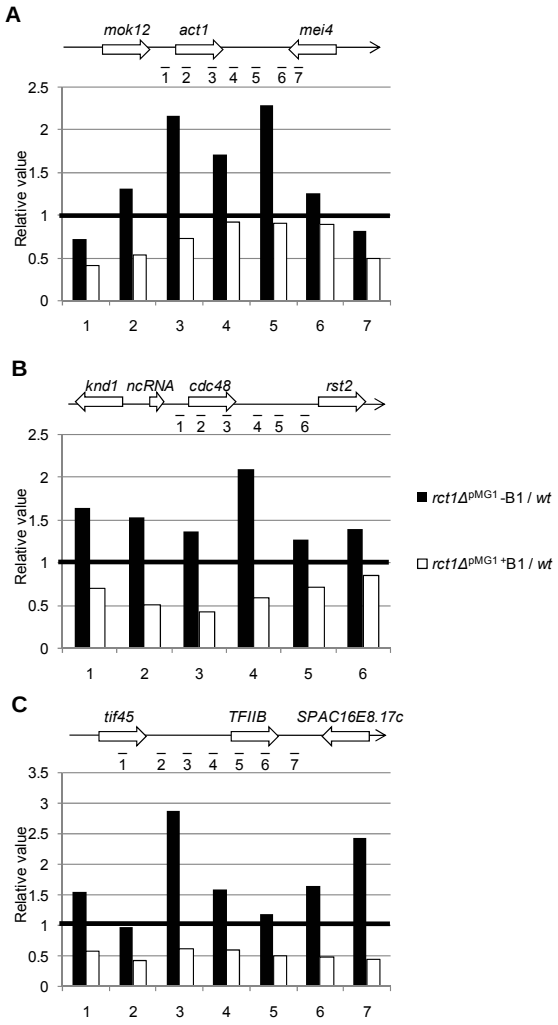

Fig. 3.12. Stages of transcription affected by Rct1. Analysis of RNAP II occupancy along transcription units shown in Fig. 3.11. The calculated ChIP signals in either Rct1 overexpressing (black bars) or underexpressing (grey bars) cells were normalized to the ChIP signals in *wt* cells for each point respectively.

Precipitated DNA was analyzed with real-time PCR (qRT-PCR) and quantified by normalizing to the input. The trendlines of the RNAP II occupancy profiles in *wt*, *rct1Δ*^{pMG1} cells before and after thiamine treatment are similar in all examined regions (Fig. 3.11.) and RNAP II profile in *wt* for *act1* 1-4 points corresponds to the previous studies (Guiguen et al, 2007). However, in most of the checked loci amount of cross-linked RNAP II is higher in cells with Rct1 overexpression than in *wt.* This ratio increases up to two-three times in the last ORF and/or terminating points (Fig. 3.12. B-D; see *act* – 3-5; *cdc48* - 4; *TFIIB* - 3,7 (also possible terminating region of *SPAC15E8.17c,* Section 3.3.3.)). Although signals for Rct1 in *wt* and Rct1 depleted cells seem to be almost same

on Western blots, the amount of RNAP II recruited to chromatin is overall lower in thiamine treated than in *wt* cells. This might be explained by changes in cell metabolism due to significant Rct1 level decrease in comparison to its initial overexpression (Fig. 3.11. A). The observed results show that (*i*) Rct1 affects the RNAP II occupancy along a whole transcription unit, (*ii*) the cyclophilin overexpression leads to increased binding of RNAP II to chromatin, especially towards the end of transcription and (*iii*) Rct1 depletion causes lower RNAP II binding to chromatin.

3.3.2. Rct1 affects the amount of the Ser2 and the Ser5 phosphorylated RNAP II CTD recruited to chromatin during active transcription

Phosphorylation state of RNAP II defines the stage of transcription (Palancade & Bensaude, 2003), (Egloff & Murphy, 2008). In previous study it was shown that Rct1 negatively regulates the RNAP II CTD phosphorylation (Gullerova et al, 2007). Moreover, I demonstrated that connection of CTD kinases to Rct1; i.e. it mediates Cdk9 kinase activity and interacts with Lsk1. Therefore, I decided to check how Rct1 influences CTD phosphorylation during ongoing transcription. To answer this question, ChIP analysis was performed on the regions including highly-transcribed *act1* and *TFIIB* genes (Fig. 3.13. A and D) with antibodies against the total RNAP II CTD (4H8) and the CTD phosphorylated on either Ser2 or Ser5 residues (pSer2 and pSer5, respectively) (Fig. 3.13. B, C, E and F). ChIP analysis of RNAP II was performed with *wt* and *rct1Δ*^{pMG1} cells, collected before and after thiamine treatment. Each experiment was done once with consequent qRT-PCR analysis run in triplicates. Real-time PCR was performed with the same sets of primers as in Section 3.3.1., as they cover ORFs and neighbouring regions. Precipitated DNA was quantified by normalizing to the input. The graphs represent pSer2 and pSer5 values normalized to total CTD values.

The distribution of the Ser2 and Ser5 phosphorylated RNAP II CTD in *wt* cells in *act1* (Fig. 3.13. B and C) is consistent with data shown by other groups (Mosley et al, 2009), (Kim et al, 2009), i.e. Ser2 phosphorylation is low at initiation stage and increases towards the end, whereas Ser5 phosphorylation is high at promoters and decreases as RNAP II moves along a transcription unit. The occupancy profile of phosphorylated RNAP II in *TFIIB* is less conventional (Fig. 3.13. E and F). The increasing

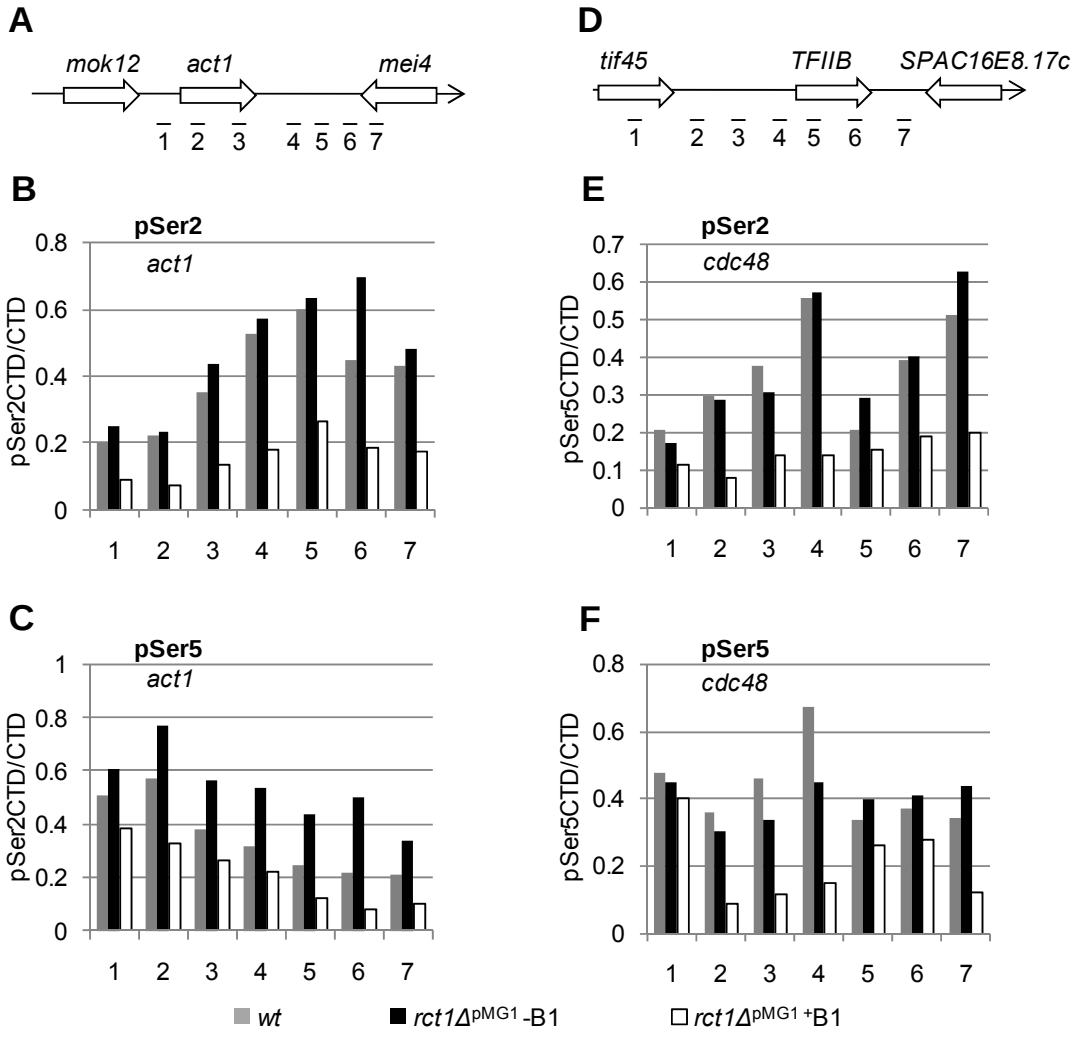

Fig. 3.13. Rct1 affects recruitment of the pSer2 and pSer5 RNAP II CTD to chromatin during transcription. (A and D) Diagrams of the regions analyzed by ChIP (A – *act1*; D – *cdc48*). ORFs are depicted by arrows that define transcription direction. Numbered bars represent the approximate positions of the qRT-PCR products used. (B, C, E and F) ChIPs of the regions indicated on diagrams above (B and C – *act1*; E and F - *TFIIB*) were done with protein extracts from *wt* cells (grey bars), *rct1Δ*^{pMG1} cells gown without (black bars; Rct1 overexpression) and with thiamine (white bars; Rct1 depletion). Following antibodies were used: 4H8 antibody, the pSer2 and the pSer5 RNAP II CTD (against the Ser2 and the Ser5 phosphorylated CTD, respectively). The y-axes show the relative phosphorylation of either Ser2 (B and E), or Ser5 (C and F) residues normalized to the total RNAP II CTD (see Section 2.11. for calculation). The numbers on x-axes correspond to the bars on the diagrams above (A and D). Coimmunoprecipitated DNA was analyzed in triplicates by qRT-PCR. Values of the negative controls, run with protein A Sepharose beads only, did not exceed one tenth for all samples (data not shown).

amount of the pSer2 CTD towards *TFIIB* promoter might be explained by expression of an unknown non-coding RNA.

Interestingly, the amount of cross-linked pSer2 RNAP II is very similar to *wt* in Rct1 overexpressing cells and significantly decreased in Rct1 depleted cells (Fig. 3.13. B and E).

The profile of the cross-linked Ser5 phosphorylated CTD in Rct1 overexpressing cells is again similar to *wt* (Fig. 3.13. C and F). However, in *act1* more RNAP II is bound to chromatin in case of Rct1 overexpression (Fig. 3.13. C). The amount of pSer5 RNAP II is decreased in Rct1 depleted cells in all analyzed loci (Fig. 3.13. C and F). Additionally to that, the profile of pSer5 RNAP II occupancy in these cells differs from *wt* in *TFIIB* (Fig. 3.13. F).

As a result, I came to conclusion that Rct1 depletion negatively affects recruitment of phosphorylated RNAP II to chromatin. Although expression levels of Rct1 in *wt* and Rct1 depleted cells are similar, the effect could be caused by the considerable change in the cyclophilin level from initial overexpression state (Fig. 3.11. A). These data does not support previous work where Rct1 depletion was shown to cause increase of CTD phosphorylation (Gullerova et al, 2007). However, different antibodies and methods were used. As the experiment was done once, it has to be repeated for more reliable conclusions.

3.3.3. RNAP II transcription is reduced under the conditions of Rct1 over- and underexpression

To find out if the observed differences in RNAP II occupancy along transcription units result in enhanced or reduced transcription rates, I performed nuclear run-on (NRO) analysis to measure ongoing transcription on *act1*, *TFIIB* and *rip1* genes (Fig. 3.14) in *wt*, Rct1 over- and underexpressing cells. For this, selected DNA probes (Fig. 3.14. A) were spotted on membrane and hybridized with α-[^{32}p]-UTP-labelled RNA isolated from *wt* and *rct1ΔpMG1* cells before (-B) and after (+B) Rct1 depletion. Surprisingly, I observed that both overexpresison (-B) and depletion (+B) of Rct1 results in strongly reduced transcription rates as compared to *wt* cells (Fig. 3.14. B). The synthesis of *TFIIB* and *rip1* is decreased up to 60%. For *act1* gene effect was less prominent in Rct1 overexpressing

cells (being 80% of that in *wt* cells), but it was comparable to that of *TFIIB* and *rip1* in Rct1 depleted cells (Fig. 3.14. B). These data go in line with previous work, where RNAP II transcription was shown to be lower in *rct1*+/- than in *wt* cells (Gullerova et al, 2007).

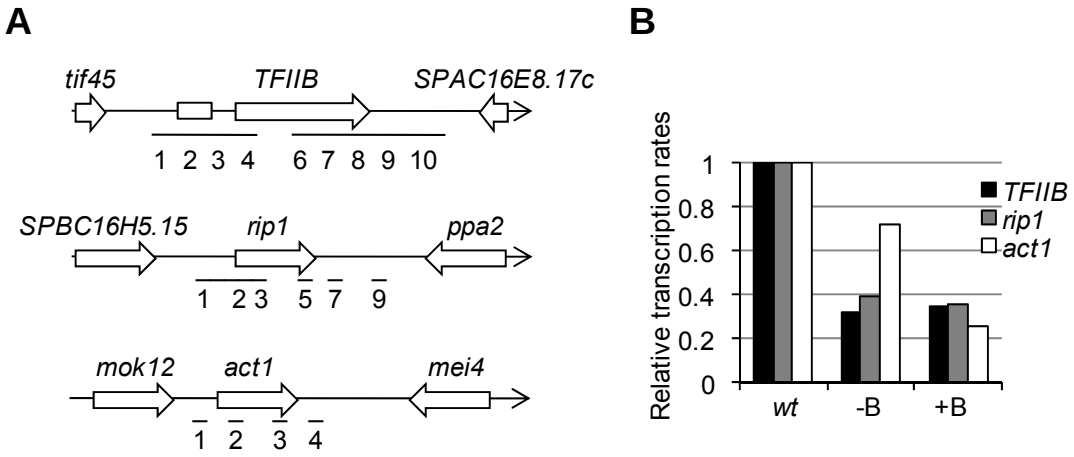

Fig. 3.14. Nuclear run-on (NRO) analysis of *act1*, *TFIIB* and *rip1* genes. (A) Diagrams of the regions analyzed by NRO. ORFs are depicted by arrows that define transcription direction. Numbered bars represent the approximate positions of the DNA probes used. (B) DNA probes, corresponding to the selected regions of the indicated genes (A), were spotted on membrane and hybridized with α-[^{32}p]-UTP-labelled RNA. Signals were measured by Phosphoimager. The signals for each analyzed region (*TFIIB*, black bars; *rip1*, grey bars; *act1*, white bars) were summed up and normalized to background. Transcription rates in *wt* cells were set to one and those in *rct1ΔpMG1* cells before (-B) and after (+B) Rct1 depletion are ratios to *wt* (y-axis). Presented data are mean values of two independent experiments.

Figure 3.15. shows NRO analysis of the transcription rate along the whole *TFIIB* gene. Reduced NRO signal in the point 3 might be explained by decrease of transcription speed due to splicing, as this region contains an intron (Fig. 3.15.). Again there was a significant reduction of transcription in both Rct1 over- and underexpressing cells (Fig. 3.15. A, lower panel, and B). Distribution profiles of the produced mRNA in *wt* cells correlate with the ones in *rct1ΔpMG1* cells before and after thiamine treatment everywhere along the analyzed region (Fig. 3.15. C). Exceptions are points at the end of *TFIIB* ORF and putative *SPAC16E8.17c* terminating region (Fig. 3.15. C, points 8 and 10; point 9 seems to localize between poly(A) sites of both genes *TFIIB* and *SPAC16E8.17c*). NRO signals in points 8 and 10 are higher in Rct1 overexpressing cells comparing to *wt*

and Rct1 depleted cells. This increase in the amount of produced mRNA in Rct1 overexpressing cells is more likely to be the result of numerous RNAP II molecules bound to chromatin (Fig. 3.11. D, *TFIIB* – 6 and 7); i.e. the rate of transcription as well as the amount of RNAP II decreases towards the end of the gene in *wt* and Rct1 underexpressing cells whereas the number of RNAP II molecules in Rct1 overexpressing cells grows

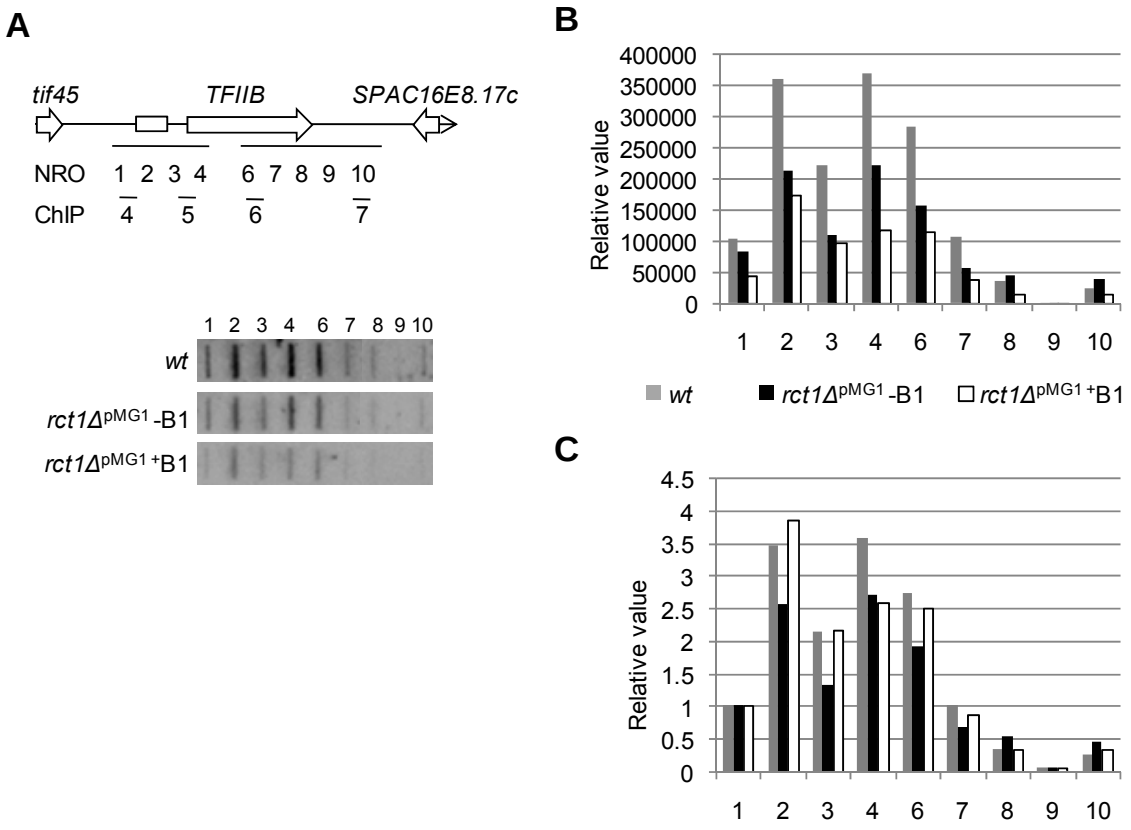

Fig. 3.15. NRO along the whole *TFIIB* gene. (A) DNA probes corresponding to different regions of *TFIIB* gene (exon-intron-exon) as indicated on the scheme (upper panel, NRO) were spotted on membrane and hybridized with α-[^{32}p]-UTP-labelled RNA (lower panel). Primers that were used for ChIP with 4H8 antibody for this gene (Fig. 3.11. D) are shown at the bottom of the upper panel. Lower panel represents result of hybridization after four days exposure. (B and C) Quantification of the data presented in part A. (B) Radioactivity was quantified and normalized to background. Numbers on x-axis correspond to DNA probes as depicted in part A (upper panel). Numbers on y-axis in represent absolute signal intensities (normalized to background). (C) The same as in B, but values in each sample at the first position are set to one and others are expressed relative to position one. Numbers on x-axis correspond to DNA probes as depicted in part A (upper panel). Numbers on y-axis in B represent absolute signal intensities normalized to background intensities relative to position one.

significantly thereby producing more mRNA. Altogether NRO and ChIP analyses indicate that higher levels of RNAP II on chromatin in Rct1 overexpressing cells most likely correspond to its less processive form.

3.3.3. Rct1 regulates histone acetylation during RNAP II transcription

Results of total RNAP II ChIPs (Section 3.3.1.) showed that the amount of RNAP II bound to chromatin is increased under Rct1 overexpression and decreased in case of Rct1 underexpression. However, it was not clear how it affects the ongoing transcription. In order to answer this question, I decided to study transcriptional activity by monitoring histone H3 acetylated on lysines 9 and 12 (K9 and K12), as this histone mark strongly correlates with 5' ends of actively transcribing genes (Liu et al, 2005). Thus, ChIP experiments were performed with antibodies against K9 and K12 acetylated H3 (AcH3K9K12) and total H3 and with the aim to determine chromatin state in protein coding genes.

Loci containing highly-transcribed *cdc48* and *TFIIB* genes (Fig. 3.16. A and B, diagrams above; Section 3.3.1.) were chosen for the ChIP analysis. Same sets of primers described in Section 3.3.1. were used as they cover ORFs and neighbouring regions of the analyzed genes. The experiment was done in *wt* and *rct1Δ*^{pMG1} cells, collected before and after thiamine treatment. Each experiment was done once and followed by qRT-PCR analysis run in triplicates. Precipitated DNA was quantified by normalizing to the input. Resulting graphs represent AcH3K9K12 values normalized to total H3.

Both graphs (Fig. 3.16. A and B) depict considerable reduction of H3 acetylation during transcription under the conditions of Rct1 overexpression; e.g. acetylation of H3K9K12 at promoter region is more than three times reduced in *cdc48* (Fig. 3.16. A, point 1). Acetylation of H3K9K12 is also lower in Rct1 depleted cells than in *wt*, but in a lesser extent. The distribution pattern of H3K9K12 acetylation is very similar in Rct1 depleted and *wt* cells. Besides, it also correlates with H3K9K12 acetylation distribution in Rct1 overexpressing cells.

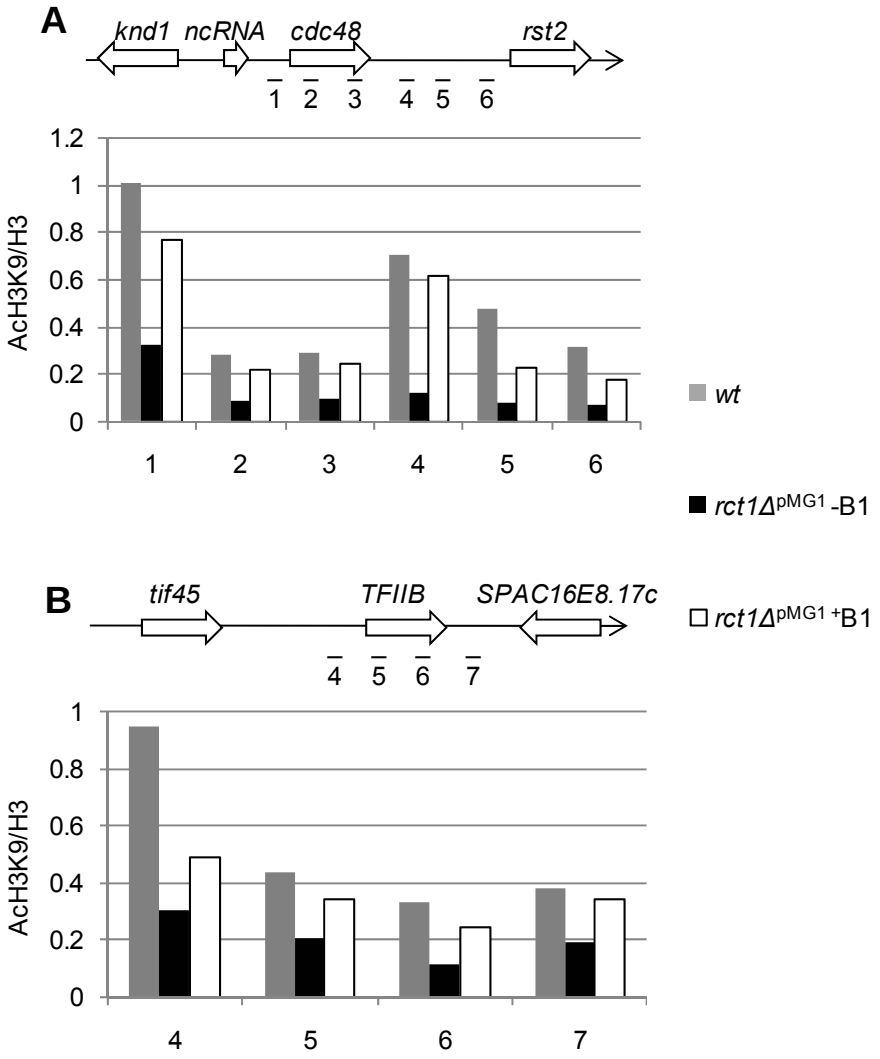

Fig. 3.16. Rct1 affects acetylation of histone H3 at Lys 9 and 12 (K9 and K12). ChIPs of loci that include *cdc28* (A) and *TFIIB* (B) were performed with anti-H3 antibody (against total H3), anti-AcH3K9K12 antibody (against acetylated Lys 9 and 12 of H3) and protein extracts from *wt* cells (grey bars), *rct1Δ*^{pMG1} cells gown without (black bars; Rct1 overexpression) and with thiamine (white bars; Rct1 depletion). In the diagrams above, ORFs are shown by arrows that define transcription direction and numbered bars below the genes represent the approximate positions of the qRT-PCR products. The numbers of the bars correspond to the numbers on the x-axes. The y-axes show the relative H3K9K12 acetylation normalized to the total H3 (see Section 2.11. for calculation). The experiment was done once. Coimmunoprecipitated DNA was analyzed in triplicates by qRT-PCR. Values of the negative controls, run with protein A Sepharose beads only, did not exceed one tenth for all samples (not shown).

The obtained results suggest that although upon Rct1 overexpression amount of RNAP II recruited to chromatin significantly increases, transcriptional activity is repressed and chromatin is deacetylated, hence, less active. Rct1 depletion seems to reduce both the amount of RNAP II cross-linked to DNA and gene activity. However, the influence of Rct1 underexpression on RNAP II cross-linking to chromatin and H3K9K12 acetylation is less significant compared to Rct1 overexpression most probably due to the insufficient depletion of Rct1.

4. Discussion

Eukaryotic RNAP II is responsible for transcription of mRNAs and small non-coding RNAs. The RNAP II CTD has a unique and evolutionary conserved sequence, which comprises multiple tandem heptapeptide repeats (Tyr1-Ser2-Pro3-Thr4-Ser5-Pro6-Ser7). Dynamic and reversible CTD phosphorylation turns it into a scaffold for the interaction of various transcription, mRNA-processing and histone-modifying factors. Ser2 and Ser5 residues were identified as main phosphorylation sites (Buratowski, 2009). Interestingly, PPIase Pin1/Ess1, which belongs to parvulin group, was found to recognize phosphorylated Ser-Pro pair of the CTD and it was suggested to change the conformation of the peptide bond (Xu & Manley, 2004), (Singh et al, 2009).

Rct1, a nuclear multidomain cyclophilin from *S. pombe*, was reported to be involved in RNAP II transcription; i.e. Rct1 interacts with the CTD, negatively regulates CTD phosphorylation and RNAP II transcriptional activity (Gullerova et al, 2007). However, the mechanism of this regulation remained largely unknown. Therefore, I analyzed interaction of Rct1 with *S. pombe* CTD kinases and phosphatases. I could show that out of all known CTD kinases and phosphatases Rct1 interacts *in vitro* with Cdk9 and Lsk1, which represent p-TEFb in *S. pombe* (Fig. 3.1. B). Although Rct1 has an RRM motif, results of the same pull-downs, repeated with RNase A, indicated that the binding is not RNA mediated. Moreover, deletion analysis of Rct1 has revealed that only PPIase domain plays crucial role in interactions with the both kinases (Fig. 3.4. C). I also report that Rct1 binds non-kinase parts of Cdk9 and Lsk1 kinases (Fig. 3.3.). These domains have prolines, which can adopt either *cis* or *trans* conformations. Moreover, these prolines, which are potential targets of Rct1 PPIase activity, may be constituents of certain undefined motifs within Cdk9 and Lsk1. The PPIase activity is impossible to prove *in vivo* so far, however, it would be interesting to perform a bioinformatic analysis of Cdk9 and Lsk1 protein sequences/structures for the presence of putative Rct1 binding motifs. Thus, Rct1 might allosterically regulate Cdk9 and Lsk1, affecting their activity and ability to bind their interaction partners. These data suggest involvement of Rct1 in the processes regulated by these two kinases. P-TEFb is a major switch that facilitates RNAP II transition into productive elongation phase. Lsk1 is a main Ser2 kinase, whereas Cdk9 seems to be responsible for multiple Ser2 phosphorylation. Besides, it phosphorylates Ser5

of the CTD as well as Spt5, transcription factor necessary for capping and escape from promoter-proximal pause into productive elongation (Pei & Shuman, 2003), (Wood & Shilatifard, 2006), (Karagiannis & Balasubramanian, 2007), (Viladevall et al, 2009), (Qiu et al, 2009), (Zhou et al, 2009), (Ni et al, 2008).

In previous study Rct1 was reported to coprecipitate RNAP II (Gullerova et al, 2007). Here I show that PPIase domain is crucial for the interaction between Rct1 and the RNAP II CTD (Fig. 3.4. C). Thus, PPIase domain of Rct1 might accelerate *cis/trans* isomerization of the proline residues in the CTD repeats. Recent structural studies support the importance of the CTD conformation; e.g. Pin1, capping enzyme Cgt1 and 3'-end processing factor Pcf1 bind the CTD only in *trans* proline conformation (Meinhart et al, 2005). Moreover, the CTD is phosphorylated by Ser/Thr-Pro directed kinases, which might also be conformation specific. This assumption is supported by the fact that some of the known Ser/Thr-Pro directed kinases and phosphatases were shown to act only on the *trans* conformation (Weiwad et al, 2000), (Brown et al, 1999), (Zhou et al, 2000b). As PPIase domain is responsible for Rct1 binding to the CTD, Cdk9 and Lsk1, it might also mediate interactions between the RNAP II CTD and its kinases Cdk9 and Lsk1.

The interactions between Rct1 and CTD kinases Cdk9 and Lsk1, indentified through pull-downs, are not necessarily direct. Cdk9 is known to form stable complex with its cyclin Pch1 and methyltransferase Pcm1, whereas Lsk1 is a subunit of a trimeric complex, which also includes cyclin Lsc1 and newly found Lsg1 protein (Pei et al, 2003), (Pei et al, 2006), (Karagiannis & Balasubramanian, 2007), (personal communication with Sukegawa). The pull-downs of Rct1 with cyclins Pch1 and Lsc1 have shown that Rct1 binds Lsc1, but not Pch1 (Fig. 3.5. B). I did not check if Pcm1 or Lsg1 interact with Rct1. Other possible Rct1 binding partner could be triphosphatase Pct1, a Cdk9 interaction partner detected in Y2H (Pei et al, 2003). Spt5 can also be an Rct1 target, because it is phosphorylated by Cdk9 and has similar to RNAP II C-terminal repeats (they also contain numerous Ser-Pro and Ser-Thr residues). Besides, phosphorylated Spt5 in humans was shown to bind Pin1 (Lavoie et al, 2001), (Kim & Sharp, 2001), (Pei & Shuman, 2003), (Yamada et al, 2006).

Cdk9 facilitates transition of RNAP II into productive elongation phase by phosphorylating Ser2 residue of the RNAP II CTD and phosphorylating Spt5, hence, turning it into positive elongation factor (Pei et al, 2003), (Pei & Shuman, 2003), (Peterlin & Price, 2006), (Viladevall et al, 2009). Performed kinase assays revealed that Rct1

negatively regulates Cdk9 kinase activity towards the CTD. Addition of Rct1 to reaction mixture with Cdk9 and the RNAP II CTD caused reduction of CTD phosphorylation (Fig. 3.8. B and C). The effect is most likely specific, as substitution of Cdk9 for Msc6 (Fig. 3.9. B) or the CTD for H1 (Fig. 3.9. A) did not bring to any phosphorylation change of the substrates under the increasing amount of Rct1. The usage of Msc6 as a control might be questionable. Msc6 phosphorylates Ser5 of the CTD, whereas Cdk9 was shown to phosphorylate both Ser2 and Ser5 (Komarnitsky et al, 2000), (Lee et al, 2005), (Marshall et al, 1996), (Pei et al, 2003), (Zhou et al, 2000a), (Pei et al, 2006), (Viladevall et al, 2009). One can argue that Rct1 does act directly on the CTD, but changes specifically conformation of the peptide bond between Ser2 and Pro3. This could explain the fact that Rct1 effect on the CTD is not detectable with Msc6 phosphorylation. However, previous study has shown an increase in Ser5 as well as Ser2 phosphorylation under the conditions of Rct1 decrease, providing the evidence for the fact that Rct1 influences phosphorylation of both serine residues (Gullerova et al, 2007). It is also important to note the questionable specificity of the antibodies used in the above-mentioned study: H14 and H5, against pSer5 and pSer2, respectively (Chapman et al, 2007), (Kim et al, 2009). Another performed kinase assay has shown that addition of Rct1ΔPPIase instead of full-length Rct1 did not cause any change in Cdk9 dependent CTD phosphorylation (Fig. 3.10. B and C). Together, the data suggest that Rct1 PPIase domain negatively mediates phosphorylation of the CTD by Cdk9.

It also turned out that Cdk9 precipitated from Rct1 depleted cells showed increased kinase activity towards the RNAP II CTD (Fig. 3.7.). Rct1 does not seem to coprecipitate with Cdk9, as published data reveal that only Pch1 and Pcm1 form complex and coprecipitate with the kinase (Pei et al, 2006), (Guiguen et al, 2007). This suggests that Rct1 negatively affects Cdk9 kinase activity *in vivo* towards the CTD and probably Spt5, as a domain at Spt5 C-terminus is similar to the RNAP II CTD. It would be of high interest in future to test if Rct1 regulates phosphorylation of Spt5 by Cdk9.

Based on the obtained data I suggest a model where PPIase domain of Rct1 binds Cdk9 and the RNAP II CTD simultaneously. These interactions and/or Rct1 PPIase activity restrain Cdk9 phosphorylation of the CTD. Cdk9 might also be specific to *trans* conformation of Ser2-Pro3 and Ser5-Pro6 peptide bonds in the CTD repeats and Rct1 could inhibit its activity catalyzing isomerization of the bonds into *cis* conformation. Additionally, negative influence of Rct1 on Cdk9 activity *in vivo* under the conditions of

Rct1 overexpression could be explained by inaccessibility of Cdk9 to its activating kinase Csk1 (Pei et al, 2006).

I could not perform same experiments described for Cdk9 with Lsk1 as there was a problem with Lsk1 expression in *lsk-HA* strain. Rct1 was shown to interact with this kinase; i.e. Rct1 binds non-kinase extension of Lsk1 with its PPIase domain (Fig. 3.2. B). Besides, Rct1 also interacts with cyclin of Lsk1, Lsc1 (Fig. 3.5. B). Therefore, I think it is important to pursue the study of Rct1 interaction with Lsk1/Lsc1. It would give more information on Rct1 regulation of RNAP II transcription.

Previous data have shown that Rct1 negatively affects the CTD phosphorylation status and RNAP II transcription is reduced in *rct1*$^{+/-}$ cells (Gullerova et al, 2007). In this study the question of the exact transcription stage(s) (initiation, elongation or termination) affected by Rct1 was addressed. ChIP experiments performed with anti-RNAP II antibody on three genes revealed increased amount of RNAP II cross-linked to chromatin in cells overexpressing Rct1 and terminating regions turned out to be the most affected ones (Figs. 3.11. and 3.12, B - 3-5; C - 4; C - 7). In contrast, in Rct1 depleted cells amount of RNAP II is decreased at all checked loci (Figs. 3.11. and 3.12). Thus, the data suggest that Rct1 regulates transcription throughout whole gene. Rct1 overexpression, however, makes stronger impact on elongation and termination. This is in line with the results on Rct1 interaction with Cdk9 and Lsk1, as they are also involved in these stages of transcription. The conclusion is also supported by the fact that RNAP II occupancy at initiation stage and behind predicted termination regions is similar in *wt* and Rct1 overexpressing cells (Figs. 3.11. and 3.12, A – 2 and 6; B – 5 and 6; C – 2 and 5), hence, initiation stage and RNAP II dissociating mechanism are less affected. Note that, although, Rct1 levels according to Western blot analysis with anti-Rct1 antibody (Fig. 3.11. A) are quite similar in *wt* and Rct1 depleted cells, RNAP II cross-linking is different especially in *cdc48* and *TFIIB* (Fig. 3.11. C and B). This might be a result of metabolic changes caused by significant decrease of Rct1 level in cells initially overexpressing this protein.

Performing ChIP analysis of Cdk9 recruitment under the conditions of Rct1 over- and underexpression in future would be a significant input into further studies of Rct1 role in RNAP II transcription.

Surprisingly, ChIP analysis revealed that level and occupancy profile of pSer2 RNAP II in Rct1 overexpressing cells is very similar to *wt* cells across the analyzed transcription units (Fig. 3.13. B and E). The trendlines of cross-linked pSer5 RNAP II in

mentioned samples are also in close agreement. Interestingly, the ratios of pSer5 RNAP II amounts between Rct1 overexpressing and *wt* cells are different in *act1* and *cdc48* genes. These results suggest that in cells with high Rct1 level Ser5 phosphorylation is more affected than that of Ser2. Occupancy of Ser2 phosphorylated RNAP II in Rct1 depleted cells undergoes significant alterations, i.e. in comparison to *wt* the amount is two to five times reduced. The cross-linking of Ser5 phosphorylated RNAP II in Rct1 underexpressing cells is less affected in *act1* than in *cdc48*, but the amount of the RNAP II is also lower than in *wt* cells. These data suggest that Rct1 overexpression does not cause significant changes in pSer2 RNAP II occupancy on a transcription unit. Under conditions of Rct1 depletion, however, the amount of the cross-linked pSer2 and pSer5 RNAP II reduces. Previous studies have shown that CTD phosphorylation increases under the conditions of Rct1 depletion (Gullerova et al, 2007). My data do not support the preceding article, but do not disprove it either. First, different antibodies were used in the studies. Second, in previous work total amount of phosphorylated RNAP II was measured, whereas I estimated phosphorylation of RNAP II bound to chromatin. The ChIP data do not contradict Rct1 ability to inhibit Cdk9 activity either, as Cdk9 is not the main RNAP II kinase. Rct1 binds both Lsk1, a major Ser2 kinase, and its cyclin Lsc1, therefore, it might positively regulate Lsk1 activity. The metabolic changes caused by Rct1 depletion could also affect CTD phosphatases. However, it would be necessary to repeat these experiments with different antibodies available for Ser2 and Ser5 phosphorylated RNAP II.

Previous study has revealed reduction of RNAP II transcription in *rct1*$^{+/-}$ cells (Gullerova et al, 2007). RNAP II ChIP provides the information on RNAP II occupancy along transcription units, but not directly on the transcriptional activity of the analyzed genes. NRO analysis, that measures the ongoing transcription rate, has shown reduced transcription in both Rct1 over- and underexpressing cells (Figs. 3.14. and 3.15.). ChIP analysis of H3K9K12 acetylation (Fig. 3.16.), which is a mark for active transcription (Kurdistani & Grunstein, 2003), (Berger, 2007), reveals moderate decrease in histone acetylation in Rct1 depleted cells whereas in Rct1 overexpressing cells it decreases three to six times. Note that this ChIP experiment has been done once, but both genes show similar results. Together, the data suggest that in Rct1 overexpressing cells RNAP II loses its processivity and abundantly occupies inactive chromatin. In spite of the multiple RNAP II cross-linking across all analyzed genes the transcription is repressed, as RNAP II might have problems with forcing its way through transcription unit and might move very

slowly. The increased amount of RNAP II could be explained by two non-mutually exclusive mechanisms. On the one hand, positive feedback loop causes increased recruitment of the RNAP II to promoter due to the reduction of mRNA produced. On the other hand, as RNAP II occupancy at the initiation step seems to be the least affected by Rct1, new rounds of transcription proceed to start at a normal rate (note, analyzed genes are constitutively and highly transcribed), whereas at elongation and termination steps RNAP II confronts difficulties and loses its speed, hence, processivity. The absence of increased amounts of stalled RNAP II in the intergenic regions behind 3' untranslated regions (Figs. 3.11. B and C and 3.12. A and B) supports the hypothesis that RNAP II has problems with moving along transcription unit, but not with dissociating from it. Note that data on H3 acetylation show that initiation phase is also affected by Rct1. More experiments will be performed to study the effect of Rct1 on the chromatin state by analyzing methylation marks.

Cdk9 homologue in *S. cerevisiae* Bur1 was shown to regulate H2 monoubiquitylation and H3K4 trimethylation (active transcription marks) via phosphorylation of its substrates Rad6 (E2 ubiquitin conjugase that modifies histone H2B), Spt5 and the RNAP II CTD (Kao et al, 2004), (Liu et al, 2005), (Laribee et al, 2005), (Wood et al, 2005), (Zhou et al, 2009), (Chu et al, 2007). Thus, Rct1 inhibition of Cdk9 activity towards its specific substrates could affect transcription not only by direct influence on RNAP II or Spt5 phosphorylation, but also by causing histone modifications, which in turn could inhibit transcription. In addition, Rct1 could affect chromatin structure during transcription via its interaction with Lsk1. Its *S. cerevisiae* homologue Ctk1 is essential for trimethylation of H3K36, which is present throughout the coding regions of active genes (Krogan et al, 2003), (Xiao et al, 2003). Ctk1 also regulates H3K4 trimethylation localizing it specifically to the 5' ends of genes (Xiao et al, 2007). Thus, further studies on the Rct1 influence on Cdk9 activity towards the RNAP II CTD, Spt5 and Rad6 as well as Rct1 interaction with Lsk1/Lsc1 should shed more light on the role of the cyclophilin in RNAP II transcription and histone modifications occurring in parallel.

5. References

Adams B, Musiyenko A, Kumar R, Barik S (2005) A novel class of dual-family immunophilins. *J Biol Chem* **280**(26)**:** 24308-24314

Adams MD, Celniker SE, Holt RA, Evans CA, Gocayne JD, Amanatides PG, Scherer SE, Li PW, Hoskins RA, Galle RF, George RA, Lewis SE, Richards S, Ashburner M, Henderson SN, Sutton GG, Wortman JR, Yandell MD, Zhang Q, Chen LX, Brandon RC, Rogers YH, Blazej RG, Champe M, Pfeiffer BD, Wan KH, Doyle C, Baxter EG, Helt G, Nelson CR, Gabor GL, Abril JF, Agbayani A, An HJ, Andrews-Pfannkoch C, Baldwin D, Ballew RM, Basu A, Baxendale J, Bayraktaroglu L, Beasley EM, Beeson KY, Benos PV, Berman BP, Bhandari D, Bolshakov S, Borkova D, Botchan MR, Bouck J, Brokstein P, Brottier P, Burtis KC, Busam DA, Butler H, Cadieu E, Center A, Chandra I, Cherry JM, Cawley S, Dahlke C, Davenport LB, Davies P, de Pablos B, Delcher A, Deng Z, Mays AD, Dew I, Dietz SM, Dodson K, Doup LE, Downes M, Dugan-Rocha S, Dunkov BC, Dunn P, Durbin KJ, Evangelista CC, Ferraz C, Ferriera S, Fleischmann W, Fosler C, Gabrielian AE, Garg NS, Gelbart WM, Glasser K, Glodek A, Gong F, Gorrell JH, Gu Z, Guan P, Harris M, Harris NL, Harvey D, Heiman TJ, Hernandez JR, Houck J, Hostin D, Houston KA, Howland TJ, Wei MH, Ibegwam C, Jalali M, Kalush F, Karpen GH, Ke Z, Kennison JA, Ketchum KA, Kimmel BE, Kodira CD, Kraft C, Kravitz S, Kulp D, Lai Z, Lasko P, Lei Y, Levitsky AA, Li J, Li Z, Liang Y, Lin X, Liu X, Mattei B, McIntosh TC, McLeod MP, McPherson D, Merkulov G, Milshina NV, Mobarry C, Morris J, Moshrefi A, Mount SM, Moy M, Murphy B, Murphy L, Muzny DM, Nelson DL, Nelson DR, Nelson KA, Nixon K, Nusskern DR, Pacleb JM, Palazzolo M, Pittman GS, Pan S, Pollard J, Puri V, Reese MG, Reinert K, Remington K, Saunders RD, Scheeler F, Shen H, Shue BC, Siden-Kiamos I, Simpson M, Skupski MP, Smith T, Spier E, Spradling AC, Stapleton M, Strong R, Sun E, Svirskas R, Tector C, Turner R, Venter E, Wang AH, Wang X, Wang ZY, Wassarman DA, Weinstock GM, Weissenbach J, Williams SM, WoodageT, Worley KC, Wu D, Yang S, Yao QA, Ye J, Yeh RF, Zaveri JS, Zhan M, Zhang G, Zhao Q, Zheng L, Zheng XH, Zhong FN, Zhong W, Zhou X, Zhu S, Zhu X, Smith HO, Gibbs RA, Myers EW, Rubin GM, Venter JC (2000) The genome sequence of Drosophila melanogaster. *Science* **287**(5461)**:** 2185-2195

Adelman K, Marr MT, Werner J, Saunders A, Ni Z, Andrulis ED, Lis JT (2005) Efficient release from promoter-proximal stall sites requires transcript cleavage factor TFIIS. *Mol Cell* **17**(1)**:** 103-112

Akhtar MS, Heidemann M, Tietjen JR, Zhang DW, Chapman RD, Eick D, Ansari AZ (2009) TFIIH kinase places bivalent marks on the carboxy-terminal domain of RNA polymerase II. *Mol Cell* **34**(3)**:** 387-393

Albert A, Lavoie S, Vincent M (1999) A hyperphosphorylated form of RNA polymerase II is the major interphase antigen of the phosphoprotein antibody MPM-2 and interacts with the peptidyl-prolyl isomerase Pin1. *J Cell Sci* **112 (Pt 15):** 2493-2500

Ansari H, Greco G, Luban J (2002) Cyclophilin A peptidyl-prolyl isomerase activity promotes ZPR1 nuclear export. *Mol Cell Biol* **22**(20)**:** 6993-7003

Arevalo-Rodriguez M, Wu X, Hanes SD, Heitman J (2004) Prolyl isomerases in yeast. *Front Biosci* **9:** 2420-2446

Atchison FW, Means AR (2004) A role for Pin1 in mammalian germ cell development and spermatogenesis. *Front Biosci* **9:** 3248-3256

Avramut M, Achim CL (2003) Immunophilins in nervous system degeneration and regeneration. *Curr Top Med Chem* **3**(12)**:** 1376-1382

Balastik M, Lim J, Pastorino L, Lu KP (2007) Pin1 in Alzheimer's disease: multiple substrates, one regulatory mechanism? *Biochim Biophys Acta* **1772**(4)**:** 422-429

Barboric M, Peterlin BM (2005) A new paradigm in eukaryotic biology: HIV Tat and the control of transcriptional elongation. *PLoS Biol* **3**(2)**:** e76

Barboric M, Zhang F, Besenicar M, Plemenitas A, Peterlin BM (2005) Ubiquitylation of Cdk9 by Skp2 facilitates optimal Tat transactivation. *J Virol* **79**(17)**:** 11135-11141

Barik S (2006) Immunophilins: for the love of proteins. *Cell Mol Life Sci* **63**(24)**:** 2889-2900

Bartolomei MS, Halden NF, Cullen CR, Corden JL (1988) Genetic analysis of the repetitive carboxyl-terminal domain of the largest subunit of mouse RNA polymerase II. *Mol Cell Biol* **8**(1)**:** 330-339

Baumli S, Lolli G, Lowe ED, Troiani S, Rusconi L, Bullock AN, Debreczeni JE, Knapp S, Johnson LN (2008) The structure of P-TEFb (CDK9/cyclin T1), its complex with flavopiridol and regulation by phosphorylation. *EMBO J* **27**(13)**:** 1907-1918

Becker EB, Bonni A (2007) Pin1 in neuronal apoptosis. *Cell Cycle* **6**(11)**:** 1332-1335

Berger SL (2007) The complex language of chromatin regulation during transcription. *Nature* **447**(7143)**:** 407-412

Bosco DA, Eisenmesser EZ, Pochapsky S, Sundquist WI, Kern D (2002) Catalysis of cis/trans isomerization in native HIV-1 capsid by human cyclophilin A. *Proc Natl Acad Sci U S A* **99**(8)**:** 5247-5252

Bourquin JP, Stagljar I, Meier P, Moosmann P, Silke J, Baechi T, Georgiev O, Schaffner W (1997) A serine/arginine-rich nuclear matrix cyclophilin interacts with the C-terminal domain of RNA polymerase II. *Nucleic Acids Res* **25**(11)**:** 2055-2061

Brown NR, Noble ME, Endicott JA, Johnson LN (1999) The structural basis for specificity of substrate and recruitment peptides for cyclin-dependent kinases. *Nat Cell Biol* **1**(7)**:** 438-443

Buratowski S (2003) The CTD code. *Nat Struct Biol* **10**(9)**:** 679-680

Buratowski S (2009) Progression through the RNA Polymerase II CTD Cycle. *Mol Cell* **36**(4)**:** 541-546

Butterfield DA, Abdul HM, Opii W, Newman SF, Joshi G, Ansari MA, Sultana R (2006) Pin1 in Alzheimer's disease. *J Neurochem* **98**(6)**:** 1697-1706

Carninci P, Shibata Y, Hayatsu N, Sugahara Y, Shibata K, Itoh M, Konno H, Okazaki Y, Muramatsu M, Hayashizaki Y (2000) Normalization and subtraction of cap-trapper-selected cDNAs to prepare full-length cDNA libraries for rapid discovery of new genes. *Genome Res* **10**(10)**:** 1617-1630

Chapman RD, Conrad M, Eick D (2005) Role of the mammalian RNA polymerase II C-terminal domain (CTD) nonconsensus repeats in CTD stability and cell proliferation. *Mol Cell Biol* **25**(17)**:** 7665-7674

Chapman RD, Heidemann M, Albert TK, Mailhammer R, Flatley A, Meisterernst M, Kremmer E, Eick D (2007) Transcribing RNA polymerase II is phosphorylated at CTD residue serine-7. *Science* **318**(5857)**:** 1780-1782

Chapman RD, Heidemann M, Hintermair C, Eick D (2008) Molecular evolution of the RNA polymerase II CTD. *Trends Genet* **24**(6)**:** 289-296

Chapman RD, Palancade B, Lang A, Bensaude O, Eick D (2004) The last CTD repeat of the mammalian RNA polymerase II large subunit is important for its stability. *Nucleic Acids Res* **32**(1)**:** 35-44

Chen H, Contreras X, Yamaguchi Y, Handa H, Peterlin BM, Guo S (2009) Repression of RNA polymerase II elongation in vivo is critically dependent on the C-terminus of Spt5. *PLoS One* **4**(9)**:** e6918

Cho EJ, Kobor MS, Kim M, Greenblatt J, Buratowski S (2001) Opposing effects of Ctk1 kinase and Fcp1 phosphatase at Ser 2 of the RNA polymerase II C-terminal domain. *Genes Dev* **15**(24)**:** 3319-3329

Cho S, Schroeder S, Kaehlcke K, Kwon HS, Pedal A, Herker E, Schnoelzer M, Ott M (2009) Acetylation of cyclin T1 regulates the equilibrium between active and inactive P-TEFb in cells. *EMBO J* **28**(10)**:** 1407-1417

Chu Y, Simic R, Warner MH, Arndt KM, Prelich G (2007) Regulation of histone modification and cryptic transcription by the Bur1 and Paf1 complexes. *EMBO J* **26**(22)**:** 4646-4656

Corden JL (1990) Tails of RNA polymerase II. *Trends Biochem Sci* **15**(10)**:** 383-387

Core LJ, Lis JT (2008) Transcription regulation through promoter-proximal pausing of RNA polymerase II. *Science* **319**(5871)**:** 1791-1792

Core LJ, Waterfall JJ, Lis JT (2008) Nascent RNA sequencing reveals widespread pausing and divergent initiation at human promoters. *Science* **322**(5909)**:** 1845-1848

Crenshaw DG, Yang J, Means AR, Kornbluth S (1998) The mitotic peptidyl-prolyl isomerase, Pin1, interacts with Cdc25 and Plx1. *EMBO J* **17**(5)**:** 1315-1327

Davies TH, Sanchez ER (2005) Fkbp52. *Int J Biochem Cell Biol* **37**(1)**:** 42-47

Diribarne G, Bensaude O (2009) 7SK RNA, a non-coding RNA regulating P-TEFb, a general transcription factor. *RNA Biol* **6**(2)

Dolinski K, Muir S, Cardenas M, Heitman J (1997) All cyclophilins and FK506 binding proteins are, individually and collectively, dispensable for viability in Saccharomyces cerevisiae. *Proc Natl Acad Sci U S A* **94**(24)**:** 13093-13098

Eckert B, Martin A, Balbach J, Schmid FX (2005) Prolyl isomerization as a molecular timer in phage infection. *Nat Struct Mol Biol* **12**(7)**:** 619-623

Edlich F, Erdmann F, Jarczowski F, Moutty MC, Weiwad M, Fischer G (2007) The Bcl-2 regulator FKBP38-calmodulin-Ca2+ is inhibited by Hsp90. *J Biol Chem* **282**(21)**:** 15341-15348

Edlich F, Weiwad M, Wildemann D, Jarczowski F, Kilka S, Moutty MC, Jahreis G, Lucke C, Schmidt W, Striggow F, Fischer G (2006) The specific FKBP38 inhibitor N-(N',N'-dimethylcarboxamidomethyl)cycloheximide has potent neuroprotective and neurotrophic properties in brain ischemia. *J Biol Chem* **281**(21)**:** 14961-14970

Egloff S, Murphy S (2008) Cracking the RNA polymerase II CTD code. *Trends Genet* **24**(6)**:** 280-288

Egloff S, O'Reilly D, Chapman RD, Taylor A, Tanzhaus K, Pitts L, Eick D, Murphy S (2007) Serine-7 of the RNA polymerase II CTD is specifically required for snRNA gene expression. *Science* **318**(5857)**:** 1777-1779

Fellner T, Lackner DH, Hombauer H, Piribauer P, Mudrak I, Zaragoza K, Juno C, Ogris E (2003) A novel and essential mechanism determining specificity and activity of protein phosphatase 2A (PP2A) in vivo. *Genes Dev* **17**(17)**:** 2138-2150

Fischer G, Bang H, Mech C (1984) [Determination of enzymatic catalysis for the cis-trans-isomerization of peptide binding in proline-containing peptides]. *Biomed Biochim Acta* **43**(10)**:** 1101-1111

Fong N, Bird G, Vigneron M, Bentley DL (2003) A 10 residue motif at the C-terminus of the RNA pol II CTD is required for transcription, splicing and 3' end processing. *EMBO J* **22**(16)**:** 4274-4282

Forsburg SL (1993) Comparison of Schizosaccharomyces pombe expression systems. *Nucleic Acids Res* **21**(12)**:** 2955-2956

Freeman BC, Toft DO, Morimoto RI (1996) Molecular chaperone machines: chaperone activities of the cyclophilin Cyp-40 and the steroid aporeceptor-associated protein p23. *Science* **274**(5293)**:** 1718-1720

Fu J, Yoon HG, Qin J, Wong J (2007) Regulation of P-TEFb elongation complex activity by CDK9 acetylation. *Mol Cell Biol* **27**(13)**:** 4641-4651

Fuda NJ, Ardehali MB, Lis JT (2009) Defining mechanisms that regulate RNA polymerase II transcription in vivo. *Nature* **461**(7261)**:** 186-192

Fujinaga K, Irwin D, Huang Y, Taube R, Kurosu T, Peterlin BM (2004) Dynamics of human immunodeficiency virus transcription: P-TEFb phosphorylates RD and dissociates negative effectors from the transactivation response element. *Mol Cell Biol* **24**(2)**:** 787-795

Fujita T, Piuz I, Schlegel W (2009) The transcription elongation factors NELF, DSIF and P-TEFb control constitutive transcription in a gene-specific manner. *FEBS Lett* **583**(17)**:** 2893-2898

Garriga J, Grana X (2004) Cellular control of gene expression by T-type cyclin/CDK9 complexes. *Gene* **337:** 15-23

Gemmill TR, Wu X, Hanes SD (2005) Vanishingly low levels of Ess1 prolyl-isomerase activity are sufficient for growth in Saccharomyces cerevisiae. *J Biol Chem* **280**(16)**:** 15510-15517

Gilmour DS, Lis JT (1986) RNA polymerase II interacts with the promoter region of the noninduced hsp70 gene in Drosophila melanogaster cells. *Mol Cell Biol* **6**(11)**:** 3984-3989

Glover-Cutter K, Larochelle S, Erickson B, Zhang C, Shokat K, Fisher RP, Bentley DL (2009) TFIIH-associated Cdk7 kinase functions in phosphorylation of C-terminal domain Ser7 residues, promoter-proximal pausing, and termination by RNA polymerase II. *Mol Cell Biol* **29**(20)**:** 5455-5464

Gothel SF, Marahiel MA (1999) Peptidyl-prolyl cis-trans isomerases, a superfamily of ubiquitous folding catalysts. *Cell Mol Life Sci* **55**(3)**:** 423-436

Goutagny N, Severa M, Fitzgerald KA (2006) Pin-ning down immune responses to RNA viruses. *Nat Immunol* **7**(6)**:** 555-557

Guiguen A, Soutourina J, Dewez M, Tafforeau L, Dieu M, Raes M, Vandenhaute J, Werner M, Hermand D (2007) Recruitment of P-TEFb (Cdk9-Pch1) to chromatin by the cap-methyl transferase Pcm1 in fission yeast. *EMBO J* **26**(6)**:** 1552-1559

Gullerova M, Barta A, Lorkovic ZJ (2006) AtCyp59 is a multidomain cyclophilin from Arabidopsis thaliana that interacts with SR proteins and the C-terminal domain of the RNA polymerase II. *RNA* **12**(4)**:** 631-643

Gullerova M, Barta A, Lorkovic ZJ (2007) Rct1, a nuclear RNA recognition motif-containing cyclophilin, regulates phosphorylation of the RNA polymerase II C-terminal domain. *Mol Cell Biol* **27**(10)**:** 3601-3611

Hampsey M, Reinberg D (2003) Tails of intrigue: phosphorylation of RNA polymerase II mediates histone methylation. *Cell* **113**(4)**:** 429-432

Handschumacher RE, Harding MW, Rice J, Drugge RJ, Speicher DW (1984) Cyclophilin: a specific cytosolic binding protein for cyclosporin A. *Science* **226**(4674)**:** 544-547

Hanes SD, Shank PR, Bostian KA (1989) Sequence and mutational analysis of ESS1, a gene essential for growth in Saccharomyces cerevisiae. *Yeast* **5**(1)**:** 55-72

Hani J, Schelbert B, Bernhardt A, Domdey H, Fischer G, Wiebauer K, Rahfeld JU (1999) Mutations in a peptidylprolyl-cis/trans-isomerase gene lead to a defect in 3'-end formation of a pre-mRNA in Saccharomyces cerevisiae. *J Biol Chem* **274**(1)**:** 108-116

Harding MW, Galat A, Uehling DE, Schreiber SL (1989) A receptor for the immunosuppressant FK506 is a cis-trans peptidyl-prolyl isomerase. *Nature* **341**(6244)**:** 758-760

Hartzog GA, Wada T, Handa H, Winston F (1998) Evidence that Spt4, Spt5, and Spt6 control transcription elongation by RNA polymerase II in Saccharomyces cerevisiae. *Genes Dev* **12**(3)**:** 357-369

Hausmann S, Shuman S (2002) Characterization of the CTD phosphatase Fcp1 from fission yeast. Preferential dephosphorylation of serine 2 versus serine 5. *J Biol Chem* **277**(24)**:** 21213-21220

Helekar SA, Char D, Neff S, Patrick J (1994) Prolyl isomerase requirement for the expression of functional homo-oligomeric ligand-gated ion channels. *Neuron* **12**(1)**:** 179-189

Hengartner CJ, Myer VE, Liao SM, Wilson CJ, Koh SS, Young RA (1998) Temporal regulation of RNA polymerase II by Srb10 and Kin28 cyclin-dependent kinases. *Mol Cell* **2**(1)**:** 43-53

Hennig L, Christner C, Kipping M, Schelbert B, Rucknagel KP, Grabley S, Kullertz G, Fischer G (1998) Selective inactivation of parvulin-like peptidyl-prolyl cis/trans isomerases by juglone. *Biochemistry* **37**(17)**:** 5953-5960

Hirose Y, Manley JL (2000) RNA polymerase II and the integration of nuclear events. *Genes Dev* **14**(12)**:** 1415-1429

Ho CK, Shuman S (1999) Distinct roles for CTD Ser-2 and Ser-5 phosphorylation in the recruitment and allosteric activation of mammalian mRNA capping enzyme. *Mol Cell* **3**(3)**:** 405-411

Hombauer H, Weismann D, Mudrak I, Stanzel C, Fellner T, Lackner DH, Ogris E (2007) Generation of active protein phosphatase 2A is coupled to holoenzyme assembly. *PLoS Biol* **5**(6)**:** e155

Horowitz DS, Kobayashi R, Krainer AR (1997) A new cyclophilin and the human homologues of yeast Prp3 and Prp4 form a complex associated with U4/U6 snRNPs. *RNA* **3**(12)**:** 1374-1387

Huang HK, Forsburg SL, John UP, O'Connell MJ, Hunter T (2001) Isolation and characterization of the Pin1/Ess1p homologue in Schizosaccharomyces pombe. *J Cell Sci* **114**(Pt 20)**:** 3779-3788

Hutten S, Walde S, Spillner C, Hauber J, Kehlenbach RH (2009) The nuclear pore component Nup358 promotes transportin-dependent nuclear import. *J Cell Sci* **122**(Pt 8)**:** 1100-1110

Itoh S, Navia MA (1995) Structure comparison of native and mutant human recombinant FKBP12 complexes with the immunosuppressant drug FK506 (tacrolimus). *Protein Sci* **4**(11)**:** 2261-2268

Jang MK, Mochizuki K, Zhou M, Jeong HS, Brady JN, Ozato K (2005) The bromodomain protein Brd4 is a positive regulatory component of P-TEFb and stimulates RNA polymerase II-dependent transcription. *Mol Cell* **19**(4)**:** 523-534

Janssens V, Goris J (2001) Protein phosphatase 2A: a highly regulated family of serine/threonine phosphatases implicated in cell growth and signalling. *Biochem J* **353**(Pt 3)**:** 417-439

Jenuwein T, Allis CD (2001) Translating the histone code. *Science* **293**(5532)**:** 1074-1080

Jones JC, Phatnani HP, Haystead TA, MacDonald JA, Alam SM, Greenleaf AL (2004) C-terminal repeat domain kinase I phosphorylates Ser2 and Ser5 of RNA polymerase II C-terminal domain repeats. *J Biol Chem* **279**(24)**:** 24957-24964

Jordens J, Janssens V, Longin S, Stevens I, Martens E, Bultynck G, Engelborghs Y, Lescrinier E, Waelkens E, Goris J, Van Hoof C (2006) The protein phosphatase 2A phosphatase activator is a novel peptidyl-prolyl cis/trans-isomerase. *J Biol Chem* **281**(10)**:** 6349-6357

Kallen J, Spitzfaden C, Zurini MG, Wider G, Widmer H, Wuthrich K, Walkinshaw MD (1991) Structure of human cyclophilin and its binding site for cyclosporin A determined by X-ray crystallography and NMR spectroscopy. *Nature* **353**(6341)**:** 276-279

Kang CB, Feng L, Chia J, Yoon HS (2005) Molecular characterization of FK-506 binding protein 38 and its potential regulatory role on the anti-apoptotic protein Bcl-2. *Biochem Biophys Res Commun* **337**(1)**:** 30-38

Kang CB, Hong Y, Dhe-Paganon S, Yoon HS (2008) FKBP family proteins: immunophilins with versatile biological functions. *Neurosignals* **16**(4)**:** 318-325

Kao CF, Hillyer C, Tsukuda T, Henry K, Berger S, Osley MA (2004) Rad6 plays a role in transcriptional activation through ubiquitylation of histone H2B. *Genes Dev* **18**(2)**:** 184-195

Karagiannis J, Balasubramanian MK (2007) A cyclin-dependent kinase that promotes cytokinesis through modulating phosphorylation of the carboxy terminal domain of the RNA Pol II Rpb1p sub-unit. *PLoS One* **2**(5)**:** e433

Karagiannis J, Bimbo A, Rajagopalan S, Liu J, Balasubramanian MK (2005) The nuclear kinase Lsk1p positively regulates the septation initiation network and promotes the successful completion of cytokinesis in response to perturbation of the actomyosin ring in Schizosaccharomyces pombe. *Mol Biol Cell* **16**(1)**:** 358-371

Ke HM, Zydowsky LD, Liu J, Walsh CT (1991) Crystal structure of recombinant human T-cell cyclophilin A at 2.5 A resolution. *Proc Natl Acad Sci U S A* **88**(21)**:** 9483-9487

Kiernan RE, Emiliani S, Nakayama K, Castro A, Labbe JC, Lorca T, Nakayama Ki K, Benkirane M (2001) Interaction between cyclin T1 and SCF(SKP2) targets CDK9 for ubiquitination and degradation by the proteasome. *Mol Cell Biol* **21**(23)**:** 7956-7970

Kim JB, Sharp PA (2001) Positive transcription elongation factor B phosphorylates hSPT5 and RNA polymerase II carboxyl-terminal domain independently of cyclin-dependent kinase-activating kinase. *J Biol Chem* **276**(15)**:** 12317-12323

Kim M, Suh H, Cho EJ, Buratowski S (2009) Phosphorylation of the yeast RPB1 C-terminal domain at serines 2, 5, and 7. *J Biol Chem*

Kim SH, Lessner SM, Sakurai Y, Galis ZS (2004) Cyclophilin A as a novel biphasic mediator of endothelial activation and dysfunction. *Am J Pathol* **164**(5)**:** 1567-1574

Kohoutek J (2009) P-TEFb- the final frontier. *Cell Div* **4**(1)**:** 19

Komarnitsky P, Cho EJ, Buratowski S (2000) Different phosphorylated forms of RNA polymerase II and associated mRNA processing factors during transcription. *Genes Dev* **14**(19)**:** 2452-2460

Kops O, Zhou XZ, Lu KP (2002) Pin1 modulates the dephosphorylation of the RNA polymerase II C-terminal domain by yeast Fcp1. *FEBS Lett* **513**(2-3)**:** 305-311

Kouzarides T (2007) Chromatin modifications and their function. *Cell* **128**(4)**:** 693-705

Krishnamurthy S, Ghazy MA, Moore C, Hampsey M (2009) Functional interaction of the Ess1 prolyl isomerase with components of the RNA polymerase II initiation and termination machineries. *Mol Cell Biol* **29**(11)**:** 2925-2934

Krishnamurthy S, He X, Reyes-Reyes M, Moore C, Hampsey M (2004) Ssu72 Is an RNA polymerase II CTD phosphatase. *Mol Cell* **14**(3)**:** 387-394

Krogan NJ, Kim M, Tong A, Golshani A, Cagney G, Canadien V, Richards DP, Beattie BK, Emili A, Boone C, Shilatifard A, Buratowski S, Greenblatt J (2003) Methylation of histone H3 by Set2 in Saccharomyces cerevisiae is linked to transcriptional elongation by RNA polymerase II. *Mol Cell Biol* **23**(12)**:** 4207-4218

Krzywicka A, Beisson J, Keller AM, Cohen J, Jerka-Dziadosz M, Klotz C (2001) KIN241: a gene involved in cell morphogenesis in Paramecium tetraurelia reveals a novel protein family of cyclophilin-RNA interacting proteins (CRIPs) conserved from fission yeast to man. *Mol Microbiol* **42**(1)**:** 257-267

Kurdistani SK, Grunstein M (2003) Histone acetylation and deacetylation in yeast. *Nat Rev Mol Cell Biol* **4**(4)**:** 276-284

Kwak YT, Guo J, Prajapati S, Park KJ, Surabhi RM, Miller B, Gehrig P, Gaynor RB (2003) Methylation of SPT5 regulates its interaction with RNA polymerase II and transcriptional elongation properties. *Mol Cell* **11**(4)**:** 1055-1066

Laribee RN, Krogan NJ, Xiao T, Shibata Y, Hughes TR, Greenblatt JF, Strahl BD (2005) BUR kinase selectively regulates H3 K4 trimethylation and H2B ubiquitylation through recruitment of the PAF elongation complex. *Curr Biol* **15**(16)**:** 1487-1493

Lau J, Lew QJ, Diribarne G, Michels AA, Dey A, Bensaude O, Lane DP, Chao SH (2009) Ubiquitination of HEXIM1 by HDM2. *Cell Cycle* **8**(14)**:** 2247-2254

Lavoie SB, Albert AL, Handa H, Vincent M, Bensaude O (2001) The peptidyl-prolyl isomerase Pin1 interacts with hSpt5 phosphorylated by Cdk9. *J Mol Biol* **312**(4)**:** 675-685

Lee KM, Miklos I, Du H, Watt S, Szilagyi Z, Saiz JE, Madabhushi R, Penkett CJ, Sipiczki M, Bahler J, Fisher RP (2005) Impairment of the TFIIH-associated CDK-activating kinase selectively affects cell cycle-regulated gene expression in fission yeast. *Mol Biol Cell* **16**(6)**:** 2734-2745

Leverson JD, Ness SA (1998) Point mutations in v-Myb disrupt a cyclophilin-catalyzed negative regulatory mechanism. *Mol Cell* **1**(2)**:** 203-211

Li Q, Price JP, Byers SA, Cheng D, Peng J, Price DH (2005) Analysis of the large inactive P-TEFb complex indicates that it contains one 7SK molecule, a dimer of HEXIM1 or HEXIM2, and two P-TEFb molecules containing Cdk9 phosphorylated at threonine 186. *J Biol Chem* **280**(31)**:** 28819-28826

Lin PS, Dubois MF, Dahmus ME (2002) TFIIF-associating carboxyl-terminal domain phosphatase dephosphorylates phosphoserines 2 and 5 of RNA polymerase II. *J Biol Chem* **277**(48)**:** 45949-45956

Liou YC, Sun A, Ryo A, Zhou XZ, Yu ZX, Huang HK, Uchida T, Bronson R, Bing G, Li X, Hunter T, Lu KP (2003) Role of the prolyl isomerase Pin1 in protecting against age-dependent neurodegeneration. *Nature* **424**(6948)**:** 556-561

Lippens G, Landrieu I, Smet C (2007) Molecular mechanisms of the phospho-dependent prolyl cis/trans isomerase Pin1. *FEBS J* **274**(20)**:** 5211-5222

Lis J (1998) Promoter-associated pausing in promoter architecture and postinitiation transcriptional regulation. *Cold Spring Harb Symp Quant Biol* **63:** 347-356

Liu CL, Kaplan T, Kim M, Buratowski S, Schreiber SL, Friedman N, Rando OJ (2005) Single-nucleosome mapping of histone modifications in S. cerevisiae. *PLoS Biol* **3**(10)**:** e328

Liu Y, Warfield L, Zhang C, Luo J, Allen J, Lang WH, Ranish J, Shokat KM, Hahn S (2009) Phosphorylation of the transcription elongation factor Spt5 by yeast Bur1 kinase stimulates recruitment of the PAF complex. *Mol Cell Biol* **29**(17)**:** 4852-4863

Lolli G (2009) Binding to DNA of the RNA-polymerase II C-terminal domain allows discrimination between Cdk7 and Cdk9 phosphorylation. *Nucleic Acids Res* **37**(4)**:** 1260-1268

Lorkovic ZJ, Lopato S, Pexa M, Lehner R, Barta A (2004) Interactions of Arabidopsis RS domain containing cyclophilins with SR proteins and U1 and U11 small nuclear ribonucleoprotein-specific proteins suggest their involvement in pre-mRNA Splicing. *J Biol Chem* **279**(32)**:** 33890-33898

Lorkovic ZJ, Skrahina T, Kautmanova H, Tschuden B, Gullerova M (2009) Deletion analysis of the nuclear multidomain cyclophilin Rct1 reveals its involvement in mitotic cell cycle regulation and genome stability. *Manuscript in preparation*

Lu KP (2004) Pinning down cell signaling, cancer and Alzheimer's disease. *Trends Biochem Sci* **29**(4)**:** 200-209

Lu KP, Finn G, Lee TH, Nicholson LK (2007) Prolyl cis-trans isomerization as a molecular timer. *Nat Chem Biol* **3**(10)**:** 619-629

Lu KP, Hanes SD, Hunter T (1996) A human peptidyl-prolyl isomerase essential for regulation of mitosis. *Nature* **380**(6574)**:** 544-547

Lu KP, Zhou XZ (2007) The prolyl isomerase PIN1: a pivotal new twist in phosphorylation signalling and disease. *Nat Rev Mol Cell Biol* **8**(11)**:** 904-916

Maestre-Martinez M, Edlich F, Jarczowski F, Weiwad M, Fischer G, Lucke C (2006) Solution structure of the FK506-binding domain of human FKBP38. *J Biomol NMR* **34**(3)**:** 197-202

Maleszka R, Hanes SD, Hackett RL, de Couet HG, Miklos GL (1996) The Drosophila melanogaster dodo (dod) gene, conserved in humans, is functionally interchangeable with the ESS1 cell division gene of Saccharomyces cerevisiae. *Proc Natl Acad Sci U S A* **93**(1)**:** 447-451

Mandal SS, Cho H, Kim S, Cabane K, Reinberg D (2002) FCP1, a phosphatase specific for the heptapeptide repeat of the largest subunit of RNA polymerase II, stimulates transcription elongation. *Mol Cell Biol* **22**(21)**:** 7543-7552

Mandal SS, Chu C, Wada T, Handa H, Shatkin AJ, Reinberg D (2004) Functional interactions of RNA-capping enzyme with factors that positively and negatively regulate promoter escape by RNA polymerase II. *Proc Natl Acad Sci U S A* **101**(20)**:** 7572-7577

Maniatis T, Reed R (2002) An extensive network of coupling among gene expression machines. *Nature* **416**(6880)**:** 499-506

Marks AR (1996) Cellular functions of immunophilins. *Physiol Rev* **76**(3)**:** 631-649

Marshall NF, Peng J, Xie Z, Price DH (1996) Control of RNA polymerase II elongation potential by a novel carboxyl-terminal domain kinase. *J Biol Chem* **271**(43)**:** 27176-27183

Marz M, Donath A, Verstraete N, Nguyen VT, Stadler PF, Bensaude O (2009) Evolution of 7SK RNA and its Protein Partners in Metazoa. *Mol Biol Evol*

Maudsley S, Mattson MP (2006) Protein twists and turns in Alzheimer disease. *Nat Med* **12**(4)**:** 392-393

McKee AE, Minet E, Stern C, Riahi S, Stiles CD, Silver PA (2005) A genome-wide in situ hybridization map of RNA-binding proteins reveals anatomically restricted expression in the developing mouse brain. *BMC Dev Biol* **5:** 14

Meinhart A, Kamenski T, Hoeppner S, Baumli S, Cramer P (2005) A structural perspective of CTD function. *Genes Dev* **19**(12)**:** 1401-1415

Mesa A, Somarelli JA, Herrera RJ (2008) Spliceosomal immunophilins. *FEBS Lett* **582**(16)**:** 2345-2351

Missiakas D, Raina S (1997) Protein folding in the bacterial periplasm. *J Bacteriol* **179**(8)**:** 2465-2471

Moreno S, Klar A, Nurse P (1991) Molecular genetic analysis of fission yeast Schizosaccharomyces pombe. *Methods Enzymol* **194:** 795-823

Morris DP, Phatnani HP, Greenleaf AL (1999) Phospho-carboxyl-terminal domain binding and the role of a prolyl isomerase in pre-mRNA 3'-End formation. *J Biol Chem* **274**(44)**:** 31583-31587

Mosley AL, Pattenden SG, Carey M, Venkatesh S, Gilmore JM, Florens L, Workman JL, Washburn MP (2009) Rtr1 is a CTD phosphatase that regulates RNA polymerase II during the transition from serine 5 to serine 2 phosphorylation. *Mol Cell* **34**(2)**:** 168-178

Moteki S, Price D (2002) Functional coupling of capping and transcription of mRNA. *Mol Cell* **10**(3)**:** 599-609

Mount SM, Salz HK (2000) Pre-messenger RNA processing factors in the Drosophila genome. *J Cell Biol* **150**(2)**:** F37-44

Munshi A, Shafi G, Aliya N, Jyothy A (2009) Histone modifications dictate specific biological readouts. *J Genet Genomics* **36**(2)**:** 75-88

Murawala P, Tripathi MM, Vyas P, Salunke A, Joseph J (2009) Nup358 interacts with APC and plays a role in cell polarization. *J Cell Sci* **122**(Pt 17)**:** 3113-3122

Narita T, Yamaguchi Y, Yano K, Sugimoto S, Chanarat S, Wada T, Kim DK, Hasegawa J, Omori M, Inukai N, Endoh M, Yamada T, Handa H (2003) Human transcription elongation factor NELF: identification of novel subunits and reconstitution of the functionally active complex. *Mol Cell Biol* **23**(6)**:** 1863-1873

Ni Z, Saunders A, Fuda NJ, Yao J, Suarez JR, Webb WW, Lis JT (2008) P-TEFb is critical for the maturation of RNA polymerase II into productive elongation in vivo. *Mol Cell Biol* **28**(3)**:** 1161-1170

Nonet M, Sweetser D, Young RA (1987) Functional redundancy and structural polymorphism in the large subunit of RNA polymerase II. *Cell* **50**(6)**:** 909-915

Orphanides G, Reinberg D (2002) A unified theory of gene expression. *Cell* **108**(4)**:** 439-451

Ostapenko D, Solomon MJ (2005) Phosphorylation by Cak1 regulates the C-terminal domain kinase Ctk1 in Saccharomyces cerevisiae. *Mol Cell Biol* **25**(10)**:** 3906-3913

Pal D, Chakrabarti P (1999) Cis peptide bonds in proteins: residues involved, their conformations, interactions and locations. *J Mol Biol* **294**(1)**:** 271-288

Palancade B, Bensaude O (2003) Investigating RNA polymerase II carboxyl-terminal domain (CTD) phosphorylation. *Eur J Biochem* **270**(19)**:** 3859-3870

Pap T (2005) Cyclophilins in rheumatoid arthritis--stepping into an undiscovered country? *Clin Immunol* **116**(3)**:** 199-201

Pei Y, Du H, Singer J, Stamour C, Granitto S, Shuman S, Fisher RP (2006) Cyclin-dependent kinase 9 (Cdk9) of fission yeast is activated by the CDK-activating kinase Csk1, overlaps functionally with the TFIIH-associated kinase Mcs6, and associates with the mRNA cap methyltransferase Pcm1 in vivo. *Mol Cell Biol* **26**(3)**:** 777-788

Pei Y, Schwer B, Shuman S (2003) Interactions between fission yeast Cdk9, its cyclin partner Pch1, and mRNA capping enzyme Pct1 suggest an elongation checkpoint for mRNA quality control. *J Biol Chem* **278**(9)**:** 7180-7188

Pei Y, Shuman S (2002) Interactions between fission yeast mRNA capping enzymes and elongation factor Spt5. *J Biol Chem* **277**(22)**:** 19639-19648

Pei Y, Shuman S (2003) Characterization of the Schizosaccharomyces pombe Cdk9/Pch1 protein kinase: Spt5 phosphorylation, autophosphorylation, and mutational analysis. *J Biol Chem* **278**(44)**:** 43346-43356

Pemberton TJ, Kay JE (2005) The cyclophilin repertoire of the fission yeast Schizosaccharomyces pombe. *Yeast* **22**(12)**:** 927-945

Peterlin BM, Price DH (2006) Controlling the elongation phase of transcription with P-TEFb. *Mol Cell* **23**(3)**:** 297-305

Phatnani HP, Greenleaf AL (2006) Phosphorylation and functions of the RNA polymerase II CTD. *Genes Dev* **20**(21)**:** 2922-2936

Pirngruber J, Shchebet A, Johnsen SA (2009a) Insights into the function of the human P-TEFb component CDK9 in the regulation of chromatin modifications and co-transcriptional mRNA processing. *Cell Cycle* **8**(22)

Pirngruber J, Shchebet A, Schreiber L, Shema E, Minsky N, Chapman RD, Eick D, Aylon Y, Oren M, Johnsen SA (2009b) CDK9 directs H2B monoubiquitination and controls replication-dependent histone mRNA 3'-end processing. *EMBO Rep* **10**(8)**:** 894-900

Pokholok DK, Harbison CT, Levine S, Cole M, Hannett NM, Lee TI, Bell GW, Walker K, Rolfe PA, Herbolsheimer E, Zeitlinger J, Lewitter F, Gifford DK, Young RA (2005) Genome-wide map of nucleosome acetylation and methylation in yeast. *Cell* **122**(4)**:** 517-527

Poulter MO, Payne KB, Steiner JP (2004) Neuroimmunophilins: a novel drug therapy for the reversal of neurodegenerative disease? *Neuroscience* **128**(1)**:** 1-6

Price DH (2000) P-TEFb, a cyclin-dependent kinase controlling elongation by RNA polymerase II. *Mol Cell Biol* **20**(8)**:** 2629-2634

Proudfoot NJ, Furger A, Dye MJ (2002) Integrating mRNA processing with transcription. *Cell* **108**(4)**:** 501-512

Qiu H, Hu C, Hinnebusch AG (2009) Phosphorylation of the Pol II CTD by KIN28 enhances BUR1/BUR2 recruitment and Ser2 CTD phosphorylation near promoters. *Mol Cell* **33**(6)**:** 752-762

Rahfeld JU, Schierhorn A, Mann K, Fischer G (1994) A novel peptidyl-prolyl cis/trans isomerase from Escherichia coli. *FEBS Lett* **343**(1)**:** 65-69

Ramachandran GN, Sasisekharan V (1968) Conformation of polypeptides and proteins. *Adv Protein Chem* **23:** 283-438

Ranganathan R, Lu KP, Hunter T, Noel JP (1997) Structural and functional analysis of the mitotic rotamase Pin1 suggests substrate recognition is phosphorylation dependent. *Cell* **89**(6)**:** 875-886

Rao B, Shibata Y, Strahl BD, Lieb JD (2005) Dimethylation of histone H3 at lysine 36 demarcates regulatory and nonregulatory chromatin genome-wide. *Mol Cell Biol* **25**(21)**:** 9447-9459

Rasmussen EB, Lis JT (1993) In vivo transcriptional pausing and cap formation on three Drosophila heat shock genes. *Proc Natl Acad Sci U S A* **90**(17)**:** 7923-7927

Rempola B, Kaniak A, Migdalski A, Rytka J, Slonimski PP, di Rago JP (2000) Functional analysis of RRD1 (YIL153w) and RRD2 (YPL152w), which encode two putative activators of the phosphotyrosyl phosphatase activity of PP2A in Saccharomyces cerevisiae. *Mol Gen Genet* **262**(6)**:** 1081-1092

Rickert P, Corden JL, Lees E (1999) Cyclin C/CDK8 and cyclin H/CDK7/p36 are biochemically distinct CTD kinases. *Oncogene* **18**(4)**:** 1093-1102

Rodriguez CR, Cho EJ, Keogh MC, Moore CL, Greenleaf AL, Buratowski S (2000) Kin28, the TFIIH-associated carboxy-terminal domain kinase, facilitates the recruitment of mRNA processing machinery to RNA polymerase II. *Mol Cell Biol* **20**(1)**:** 104-112

Sabo A, Lusic M, Cereseto A, Giacca M (2008) Acetylation of conserved lysines in the catalytic core of cyclin-dependent kinase 9 inhibits kinase activity and regulates transcription. *Mol Cell Biol* **28**(7)**:** 2201-2212

Saunders A, Core LJ, Lis JT (2006) Breaking barriers to transcription elongation. *Nat Rev Mol Cell Biol* **7**(8)**:** 557-567

Schiene C, Fischer G (2000) Enzymes that catalyse the restructuring of proteins. *Curr Opin Struct Biol* **10**(1)**:** 40-45

Schneider R, Bannister AJ, Myers FA, Thorne AW, Crane-Robinson C, Kouzarides T (2004) Histone H3 lysine 4 methylation patterns in higher eukaryotic genes. *Nat Cell Biol* **6**(1)**:** 73-77

Schreiber SL (1991) Chemistry and biology of the immunophilins and their immunosuppressive ligands. *Science* **251**(4991)**:** 283-287

Schroeder SC, Schwer B, Shuman S, Bentley D (2000) Dynamic association of capping enzymes with transcribing RNA polymerase II. *Genes Dev* **14**(19)**:** 2435-2440

Schwer B, Schneider S, Pei Y, Aronova A, Shuman S (2009) Characterization of the Schizosaccharomyces pombe Spt5-Spt4 complex. *RNA* **15**(7)**:** 1241-1250

Sharma VK, Li B, Khanna A, Sehajpal PK, Suthanthiran M (1994) Which way for drug-mediated immunosuppression? *Curr Opin Immunol* **6**(5)**:** 784-790

Shaw PE (2007) Peptidyl-prolyl cis/trans isomerases and transcription: is there a twist in the tail? *EMBO Rep* **8**(1)**:** 40-45

Shirane M, Nakayama KI (2003) Inherent calcineurin inhibitor FKBP38 targets Bcl-2 to mitochondria and inhibits apoptosis. *Nat Cell Biol* **5**(1)**:** 28-37

Siekierka JJ, Hung SH, Poe M, Lin CS, Sigal NH (1989) A cytosolic binding protein for the immunosuppressant FK506 has peptidyl-prolyl isomerase activity but is distinct from cyclophilin. *Nature* **341**(6244)**:** 755-757

Sims RJ, 3rd, Belotserkovskaya R, Reinberg D (2004) Elongation by RNA polymerase II: the short and long of it. *Genes Dev* **18**(20)**:** 2437-2468

Sinars CR, Cheung-Flynn J, Rimerman RA, Scammell JG, Smith DF, Clardy J (2003) Structure of the large FK506-binding protein FKBP51, an Hsp90-binding protein and a component of steroid receptor complexes. *Proc Natl Acad Sci U S A* **100**(3)**:** 868-873

Singh N, Ma Z, Gemmill TR, Wu X, Defiglio H, Rossettini A, Rabeler C, Beane O, Morse RH, Palumbo MJ, Hanes SD (2009) The Ess1 prolyl isomerase is required for transcription termination of small noncoding RNAs via the Nrd1 pathway. *Mol Cell* **36**(2)**:** 255-266

St-Pierre B, Liu X, Kha LC, Zhu X, Ryan O, Jiang Z, Zacksenhaus E (2005) Conserved and specific functions of mammalian ssu72. *Nucleic Acids Res* **33**(2)**:** 464-477

Steinmetz EJ, Brow DA (2003) Ssu72 protein mediates both poly(A)-coupled and poly(A)-independent termination of RNA polymerase II transcription. *Mol Cell Biol* **23**(18)**:** 6339-6349

Stewart DE, Sarkar A, Wampler JE (1990) Occurrence and role of cis peptide bonds in protein structures. *J Mol Biol* **214**(1)**:** 253-260

Stiller JW, Cook MS (2004) Functional unit of the RNA polymerase II C-terminal domain lies within heptapeptide pairs. *Eukaryot Cell* **3**(3)**:** 735-740

Suganuma T, Workman JL (2008) Crosstalk among Histone Modifications. *Cell* **135**(4)**:** 604-607

Sun X, Zhang Y, Cho H, Rickert P, Lees E, Lane W, Reinberg D (1998) NAT, a human complex containing Srb polypeptides that functions as a negative regulator of activated transcription. *Mol Cell* **2**(2)**:** 213-222

Takahashi K, Saitoh S, Yanagida M (2000) Application of the chromatin immunoprecipitation method to identify in vivo protein-DNA associations in fission yeast. *Sci STKE* **2000**(56)**:** PL1

Takahashi K, Uchida C, Shin RW, Shimazaki K, Uchida T (2008) Prolyl isomerase, Pin1: new findings of post-translational modifications and physiological substrates in cancer, asthma and Alzheimer's disease. *Cell Mol Life Sci* **65**(3)**:** 359-375

Ursic D, Finkel JS, Culbertson MR (2008) Detecting phosphorylation-dependent interactions with the C-terminal domain of RNA polymerase II subunit Rpb1p using a yeast two-hybrid assay. *RNA Biol* **5**(1)**:** 1-4

Van Hoof C, Cayla X, Bosch M, Merlevede W, Goris J (1994) The phosphotyrosyl phosphatase activator of protein phosphatase 2A. A novel purification method, immunological and enzymic characterization. *Eur J Biochem* **226**(3)**:** 899-907

Van Hoof C, Martens E, Longin S, Jordens J, Stevens I, Janssens V, Goris J (2005) Specific interactions of PP2A and PP2A-like phosphatases with the yeast PTPA homologues, Ypa1 and Ypa2. *Biochem J* **386**(Pt 1)**:** 93-102

Verdecia MA, Bowman ME, Lu KP, Hunter T, Noel JP (2000) Structural basis for phosphoserine-proline recognition by group IV WW domains. *Nat Struct Biol* **7**(8)**:** 639-643

Viladevall L, St Amour CV, Rosebrock A, Schneider S, Zhang C, Allen JJ, Shokat KM, Schwer B, Leatherwood JK, Fisher RP (2009) TFIIH and P-TEFb coordinate transcription

with capping enzyme recruitment at specific genes in fission yeast. *Mol Cell* **33**(6)**:** 738-751

Wada T, Takagi T, Yamaguchi Y, Ferdous A, Imai T, Hirose S, Sugimoto S, Yano K, Hartzog GA, Winston F, Buratowski S, Handa H (1998) DSIF, a novel transcription elongation factor that regulates RNA polymerase II processivity, is composed of human Spt4 and Spt5 homologs. *Genes Dev* **12**(3)**:** 343-356

Wang P, Heitman J (2005) The cyclophilins. *Genome Biol* **6**(7)**:** 226

Wang S, Simon BP, Bennett DA, Schneider JA, Malter JS, Wang DS (2007) The significance of Pin1 in the development of Alzheimer's disease. *J Alzheimers Dis* **11**(1)**:** 13-23

Wang T, Donahoe PK, Zervos AS (1994) Specific interaction of type I receptors of the TGF-beta family with the immunophilin FKBP-12. *Science* **265**(5172)**:** 674-676

Wang Y, Dow EC, Liang YY, Ramakrishnan R, Liu H, Sung TL, Lin X, Rice AP (2008) Phosphatase PPM1A regulates phosphorylation of Thr-186 in the Cdk9 T-loop. *J Biol Chem* **283**(48)**:** 33578-33584

Weake VM, Workman JL (2008) Histone ubiquitination: triggering gene activity. *Mol Cell* **29**(6)**:** 653-663

Weiwad M, Kullertz G, Schutkowski M, Fischer G (2000) Evidence that the substrate backbone conformation is critical to phosphorylation by p42 MAP kinase. *FEBS Lett* **478**(1-2)**:** 39-42

West ML, Corden JL (1995) Construction and analysis of yeast RNA polymerase II CTD deletion and substitution mutations. *Genetics* **140**(4)**:** 1223-1233

Wilcox CB, Rossettini A, Hanes SD (2004) Genetic interactions with C-terminal domain (CTD) kinases and the CTD of RNA Pol II suggest a role for ESS1 in transcription initiation and elongation in Saccharomyces cerevisiae. *Genetics* **167**(1)**:** 93-105

Wood A, Schneider J, Dover J, Johnston M, Shilatifard A (2005) The Bur1/Bur2 complex is required for histone H2B monoubiquitination by Rad6/Bre1 and histone methylation by COMPASS. *Mol Cell* **20**(4)**:** 589-599

Wood A, Shilatifard A (2006) Bur1/Bur2 and the Ctk complex in yeast: the split personality of mammalian P-TEFb. *Cell Cycle* **5**(10)**:** 1066-1068

Wu B, Li P, Liu Y, Lou Z, Ding Y, Shu C, Ye S, Bartlam M, Shen B, Rao Z (2004) 3D structure of human FK506-binding protein 52: implications for the assembly of the glucocorticoid receptor/Hsp90/immunophilin heterocomplex. *Proc Natl Acad Sci U S A* **101**(22)**:** 8348-8353

Wu J, Matunis MJ, Kraemer D, Blobel G, Coutavas E (1995) Nup358, a cytoplasmically exposed nucleoporin with peptide repeats, Ran-GTP binding sites, zinc fingers, a cyclophilin A homologous domain, and a leucine-rich region. *J Biol Chem* **270**(23)**:** 14209-14213

Wu JQ, Snyder M (2008) RNA polymerase II stalling: loading at the start prepares genes for a sprint. *Genome Biol* **9**(5)**:** 220

Wu X, Rossettini A, Hanes SD (2003) The ESS1 prolyl isomerase and its suppressor BYE1 interact with RNA pol II to inhibit transcription elongation in Saccharomyces cerevisiae. *Genetics* **165**(4)**:** 1687-1702

Wu X, Wilcox CB, Devasahayam G, Hackett RL, Arevalo-Rodriguez M, Cardenas ME, Heitman J, Hanes SD (2000) The Ess1 prolyl isomerase is linked to chromatin remodeling complexes and the general transcription machinery. *EMBO J* **19**(14)**:** 3727-3738

Wulf G, Finn G, Suizu F, Lu KP (2005) Phosphorylation-specific prolyl isomerization: is there an underlying theme? *Nat Cell Biol* **7**(5)**:** 435-441

Xiao T, Hall H, Kizer KO, Shibata Y, Hall MC, Borchers CH, Strahl BD (2003) Phosphorylation of RNA polymerase II CTD regulates H3 methylation in yeast. *Genes Dev* **17**(5)**:** 654-663

Xiao T, Shibata Y, Rao B, Laribee RN, O'Rourke R, Buck MJ, Greenblatt JF, Krogan NJ, Lieb JD, Strahl BD (2007) The RNA polymerase II kinase Ctk1 regulates positioning of a 5' histone methylation boundary along genes. *Mol Cell Biol* **27**(2)**:** 721-731

Xu YX, Hirose Y, Zhou XZ, Lu KP, Manley JL (2003) Pin1 modulates the structure and function of human RNA polymerase II. *Genes Dev* **17**(22)**:** 2765-2776

Xu YX, Manley JL (2004) Pinning down transcription: regulation of RNA polymerase II activity during the cell cycle. *Cell Cycle* **3**(4)**:** 432-435

Xu YX, Manley JL (2007a) New insights into mitotic chromosome condensation: a role for the prolyl isomerase Pin1. *Cell Cycle* **6**(23)**:** 2896-2901

Xu YX, Manley JL (2007b) Pin1 modulates RNA polymerase II activity during the transcription cycle. *Genes Dev* **21**(22)**:** 2950-2962

Xu YX, Manley JL (2007c) The prolyl isomerase Pin1 functions in mitotic chromosome condensation. *Mol Cell* **26**(2)**:** 287-300

Yaffe MB, Schutkowski M, Shen M, Zhou XZ, Stukenberg PT, Rahfeld JU, Xu J, Kuang J, Kirschner MW, Fischer G, Cantley LC, Lu KP (1997) Sequence-specific and phosphorylation-dependent proline isomerization: a potential mitotic regulatory mechanism. *Science* **278**(5345)**:** 1957-1960

Yamada T, Yamaguchi Y, Inukai N, Okamoto S, Mura T, Handa H (2006) P-TEFb-mediated phosphorylation of hSpt5 C-terminal repeats is critical for processive transcription elongation. *Mol Cell* **21**(2)**:** 227-237

Yamaguchi Y, Inukai N, Narita T, Wada T, Handa H (2002) Evidence that negative elongation factor represses transcription elongation through binding to a DRB sensitivity-inducing factor/RNA polymerase II complex and RNA. *Mol Cell Biol* **22**(9)**:** 2918-2927

Yamaguchi Y, Takagi T, Wada T, Yano K, Furuya A, Sugimoto S, Hasegawa J, Handa H (1999) NELF, a multisubunit complex containing RD, cooperates with DSIF to repress RNA polymerase II elongation. *Cell* **97**(1)**:** 41-51

Yao S, Prelich G (2002) Activation of the Bur1-Bur2 cyclin-dependent kinase complex by Cak1. *Mol Cell Biol* **22**(19)**:** 6750-6758

Yeh ES, Means AR (2007) PIN1, the cell cycle and cancer. *Nat Rev Cancer* **7**(5)**:** 381-388

Yeo M, Lin PS, Dahmus ME, Gill GN (2003) A novel RNA polymerase II C-terminal domain phosphatase that preferentially dephosphorylates serine 5. *J Biol Chem* **278**(28)**:** 26078-26085

Yoh SM, Cho H, Pickle L, Evans RM, Jones KA (2007) The Spt6 SH2 domain binds Ser2-P RNAPII to direct Iws1-dependent mRNA splicing and export. *Genes Dev* **21**(2)**:** 160-174

Zeng L, Zhou Z, Xu J, Zhao W, Wang W, Huang Y, Cheng C, Xu M, Xie Y, Mao Y (2001) Molecular cloning, structure and expression of a novel nuclear RNA-binding cyclophilin-like gene (PPIL4) from human fetal brain. *Cytogenet Cell Genet* **95**(1-2)**:** 43-47

Zhang Y, Kim Y, Genoud N, Gao J, Kelly JW, Pfaff SL, Gill GN, Dixon JE, Noel JP (2006) Determinants for dephosphorylation of the RNA polymerase II C-terminal domain by Scp1. *Mol Cell* **24**(5)**:** 759-770

Zheng H, You H, Zhou XZ, Murray SA, Uchida T, Wulf G, Gu L, Tang X, Lu KP, Xiao ZX (2002) The prolyl isomerase Pin1 is a regulator of p53 in genotoxic response. *Nature* **419**(6909)**:** 849-853

Zhou K, Kuo WH, Fillingham J, Greenblatt JF (2009) Control of transcriptional elongation and cotranscriptional histone modification by the yeast BUR kinase substrate Spt5. *Proc Natl Acad Sci U S A* **106**(17)**:** 6956-6961

Zhou M, Halanski MA, Radonovich MF, Kashanchi F, Peng J, Price DH, Brady JN (2000a) Tat modifies the activity of CDK9 to phosphorylate serine 5 of the RNA polymerase II carboxyl-terminal domain during human immunodeficiency virus type 1 transcription. *Mol Cell Biol* **20**(14)**:** 5077-5086

Zhou XZ, Kops O, Werner A, Lu PJ, Shen M, Stoller G, Kullertz G, Stark M, Fischer G, Lu KP (2000b) Pin1-dependent prolyl isomerization regulates dephosphorylation of Cdc25C and tau proteins. *Mol Cell* **6**(4)**:** 873-883

Zhou XZ, Lu PJ, Wulf G, Lu KP (1999) Phosphorylation-dependent prolyl isomerization: a novel signaling regulatory mechanism. *Cell Mol Life Sci* **56**(9-10)**:** 788-806

6. Curriculum Vitae

Name Tatsiana Skrahina

Date and place of birth 27.08.1984, Minsk, Republic of Belarus

Nationality Belarus

EDUCATION

2006-present **Max F. Perutz Laboratories (MFPL), University of Vienna**
The Vienna BioCenter (VBC) International PhD program
Doctoral studies

2001-2006 **ISEU, Minsk, Belarus**
Diploma in Environmental Medicine and Radiobiology

- Graduated with excellent marks (GPA 5.0/5.0)
- Qualified as a high-school teacher for biology, chemistry and ecology

1994-2001 **First National Gymnasium, Minsk, Belarus**

- High-school class with bias on business, mathematics and foreign languages
- Graduated with excellent marks (GPA 5.0/5.0)

EXPERIENCE

2006-present **Doctoral Student Researcher**, Laboratory of Dr. Zdravko Lorkovic
MFPL, University of Vienna
The VBC International PhD program
Supervisors: Prof. Dr. Barta, Dr. Peters, Prof. Dr. Warren
Topic: The role of *Schizosaccharomyces pombe* cyclophilin Rct1 in RNA polymerase II transcription

- Presented findings at five internationally recognized scientific conferences
- Obtained relevant work experience in biochemistry, molecular biology and genetics

2005-2006 **EMBL (European Molecular Biology Laboratory), Heidelberg, Germany**

2006 **Diploma student,** Laboratory of Dr. Carsten Schultz

- Performed research on membrane-mediated assembly of annexins using complex imaging techniques

2005 **Summer student,** Laboratory of Dr. Carsten Schultz

- Developed genetically encoded reporters for protein kinase C activity based on fluorescence resonance energy transfer

2003-2005 **Undergraduate student**
International Laboratory of Resonance Methods in Biology and Medicine, International Sakharov Environmental University (ISEU), Minsk, Belarus

- Awarded first prize in a University competition for research on fatty acids metabolism in patients with type 2 diabetes mellitus and myocardial ischemia
- Received student grant for the project "Optimization of recombinant adrenodoxin expression and purification"
- Presented results at 2 scientific conferences in Belarus and Russia

PUBLICATIONS

- Skrahina T., Piljic A., Schultz C. (2008) Heterogeneity and timing of translocation and membrane-mediated assembly of different annexins. Exp Cell Res 314(5):1039-47.
- Skrahina T., Gullerova M. and Lorkovic Z. The role of *Schizosaccharomyces pombe* cyclophilin Rct1 in RNA polymerase II transcription. *Manuscript in preparation.*
- Lorkovic Z.L., Skrahina T., Kautmanova H., Tschuden B. and Gullerova M. Deletion analysis of the nuclear multidomain cyclophilin Rct1 reveals its involvement in mitotic cell cycle regulation and genome stability. *Submitted manuscript.*

SCHOLARSHIPS

- Member of the VBC International PhD program, 2006-2009
- Scholarship of the President of Belarus for particular academic and research progress, 2005
- Research student grant of Ministry of Education of Belarus, 2003

EDUCATIONAL ACTIVITIES

- Gave a practical course on molecular biology to undergraduate students, VBC, 2007
- A year of teaching practice in biology, chemistry and ecology, Minsk, 2005

LANGUAGES

- Belarus, Russian - native
- English - fluent; working language, gymnasium with English language bias
- German - fluent; Goethe-Institute ZOP (central advanced grade exam)

7. Appendix

7.1. Deletion analysis of the nuclear multidomain cyclophilin Rct1 reveals its involvement in mitotic cell cycle regulation and genome stability. *Submitted manuscript.*

Deletion analysis of the nuclear multidomain cyclophilin Rct1 reveals its involvement in mitotic cell cycle regulation and genome stability

Zdravko J. Lorković[1*] Tatsiana Skrahina[1], Hana Kautmanova[1], Brigitte Tschuden[1], and Monika Gullerova[1,2]

Max F. Perutz Laboratories, Medical University of Vienna, Department of Medical Biochemistry, Dr. Bohrgasse 9/3, A-1030 Vienna, Austria[1] Sir William Dunn School of Pathology, Department of Biochemistry, University of Oxford, UK[2]

Running title: Cyclophilin and cell cycle regulation

[*]Corresponding author:

Zdravko J. Lorković

Tel. +43 1 4277 61642

Fax. +43 1 4277 9616

E-mail: zdravko.lorkovic@meduniwien.ac.at

Summary

Rct1 is an essential and evolutionary conserved nuclear peptidyl-prolyl isomerase (PPIase) consisting of three distinct domains, the PPIase domain, an RNA recognition motif (RRM) and the C-terminal domain rich in arginine/serine and arginine/aspartate dipeptides (RS/RD). We performed mutational and deletion analysis and found that none of the domains alone is sufficient for the observed lethality upon *rct1* deletion. However, strong phenotypes were observed upon deletion of either PPIase or RRM domain. Cells expressing Rct1 without the PPIase domain exhibit problems in mitotic cell cycle regulation, as revealed by the appearance of lagging chromosomes, entrance into second mitotic division without prior cell separation and septum formation, and sensitivity to mitotic spindle poison thiabendazole and DNA damage agents. We also demonstrate genetic interaction of Rct1 with the Dis2 phosphatase which is involved in mitotic chromosome segregation and which regulates activity of the G2 DNA damage checkpoint kinase Chk1. Altogether our data strongly suggest that Rct1, in addition to regulation of RNAP II transcription, is required for correct cell cycle progression by regulating one or more checkpoints.

Introduction

Cyclophilins belong to a family of immunosuppressant receptor proteins called immunophilins, which in addition to cyclophilins include the FK506 binding proteins and the parvulins. Immunophilins possess peptidyl-prolyl *cis-trans* isomerase (PPIase) activity; e.g. they catalyze *cis* to *trans* isomerisation of peptide bonds preceding proline (Barik, 2006; Schiene and Fischer, 2000). As this could be a rate limiting step in protein folding the importance of this enzyme family is best highlighted by the fact that over 90% of prolyl imide bonds are in *trans* conformation (Barik, 2006; Schiene and Fischer, 2000). It is now clear that immunophilins are important cellular regulators of transcription (Gullerova *et al.,* 2007; Shaw, 2007; Xu *et al.,* 2003; Xu and Manley, 2007a), pre-mRNA processing (Mesa *et al.,* 2008), signalling and pathological changes (Bell *et al.,* 2006; Esnault *et al.,* 2008; Finn and Lu, 2008; Lu, 2003; Lu, 2004; Lu and Zhou, 2007), chromatin modification and gene silencing (Arevalo-Rodriguez *et al.,* 2000; Arevalo-Rodriguez and Heitman, 2005; Nelson *et al.,* 2006), chromosome structure (Xu and Manley, 2007b), and genome stability (Wulf *et al.,* 2002; Zacchi et al. 2002; Zheng *et al.,* 2002; Hochwagen et al. 2005). Importantly, as best exemplified by the human parvulin Pin1, it seems that each immunophilin have multiple cellular targets and is therefore involved in regulation of multiple cellular processes (Esnault *et al.,* 2008; Finn and Lu, 2008; Lu, 2003; Lu, 2004; Lu and Zhou, 2007; Lu et al, 2007; Wulf *et al.,* 2005). However, in the yeast *Saccharomyces cerevisiae* none of the genes encoding immunophilins was found to be essential (Dolinski *et al.,* 1997) which might indicate that they are not required under normal growth conditions or their functions are partially redundant.

Most cyclophilins are small proteins, although complex proteins with several distinct domains have also been described (Pemberton and Kay, 2005; Romano *et al.,* 2004). Multidomain cyclophilins from *Arabidopsis* AtCyp59 (Gullerova *et al.,* 2006), *Paramecium tetraurelia* Kin241p (Krzywicka *et al.,* 2001), and *Schizosaccharomyces pombe* Rct1 (Gullerova *et al.,* 2007) have a unique domain organization, consisting of a PPIase domain at the N-terminus, followed by an RNA recognition motif (RRM) and a C-terminal domain enriched in charged amino acids and

serines or Arg/Ser (RS) and Arg/Asp (RD) dipeptides. *P. tetraurelia* Kin241p was identified as a protein involved in cell morphogenesis (Krzywicka *et al.,* 2001). AtCyp59 is a nuclear protein and it was identified in a yeast two-hybrid screen as an interacting partner of *Arabidopsis* SR proteins (Gullerova *et al.,* 2006), an important family of splicing regulators. As it also interacted with the C-terminal domain (CTD) of RNA polymerase II (RNAP II), a function for this protein at the interface between transcription and pre-mRNA splicing was proposed (Gullerova *et al.,* 2006).

Rct1 is the only immunophilin which is encoded by an essential gene. Interestingly, reduced levels of Rct1 in *rct1* heterozygous cells resulted in considerably slower growth when compared to *WT* cells. Cell polarity and, as revealed by an enhanced entrance into meiosis under restrictive conditions, mitotic cell cycle were also affected in $rct1^{+/-}$ cells. As Rct1 protein levels were found to be decreased in $rct1^{+/-}$ cells deletion of one *rct1* allele obviously led to haploinsufficiency, leading to a highly complex phenotype. Most strikingly, an increase in CTD phosphorylation at both Ser2 and Ser5 and an associated reduction of ongoing transcription have also been found in $rct1^{+/-}$ cells. Chromatin immunoprecipitation (ChIP) assays revealed that Rct1 is closely associated with the transcriptionally active chromatin. Ectopic expression of Rct1 in $rct^{+/-}$ cells resulted in complementation of all growth, morphological and CTD phosphorylation defects. Together, these data suggested that Rct1 is likely regulating several different processes in the cell (Gullerova *et al.,* 2007).

Given that Rct1 is a multidomain cyclophilin, we set out to dissect function of individual Rct1 domains. Therefore, we performed mutational and deletion analysis of Rct1. Surprisingly, we found that none of the domains alone is essential for cell viability. However, strong phenotypes were observed upon deletion of either PPIase or RRM domain. Here, we present data which indicate that, in addition to previously described effect of Rct1 depletion on RNAP II transcription (Gullerova *et al.,* 2007) Rct1 likely regulates activities of several other proteins which are involved in cell cycle regulation.

Results

Rct1 is a complex cyclophilin consisting of three structuraly distinct domains, the N-terminal PPIase domain, the RNA recognition motif (RRM) and the C-terminal domain rich is Arg/Ser (RS) and Arg/Asp (RD) dipeptides (Gullerova *et al.,* 2007). Rct1 is the only cyclophilin which is encoded by an essential gene, raising the question whether the whole protein or only a specific Rct1 domain is required for cell viability. Therefore, we performed mutational and deletion analyses of Rct1. All constructs were made in a plasmid (Gullerova *et al.,* 2007), where the expression of Rct1 is controlled by the thiamine repressible *nmt1* promoter. Plasmids were transformed into *rct1* heterozygous strain (Gullerova *et al.,* 2007) and analyzed for complementation of the *rct1* disruption by either tetrad dissection or random spore analysis.

Mutational and deletion analyses of the PPIase domain

As evident from the alignment in Fig. S1, most amino acids which are thought to be important for catalytic activity of cyclophilins, are not conserved in Rct1 (see also Pemberton and Kay, 2005). This raises an interesting question whether PPIase domain and its assumed PPIase activity are required for Rct1 function or the PPIase domain serves solely to interact with other proteins (thus acting as a chaperone; Barik, 2006), whereby the main function of Rct1 would be executed by the RRM and/or the RS/RD domain. Single and combined point mutations in the PPIase domain and possible consequences thereof are listed in Fig. S2A and mutated amino acids are highlighted in boxes in Fig. S1. Tetrad analysis of *rct1* heterozygous cells expressing Rct1 with single or combined point mutations revealed that none of the mutations results in loss of viability or significant reduction of growth rates (Fig. S2D). Growth analysis at different temperatures (data not shown) and microscopic examination of cells stained with aniline blue (to visualise cell wall and septum) and Hoechst (Fig. S2C) did not reveal any difference between individual mutants and *WT* cells. From these analyses it seems that the PPIase domain of Rct1 is not essential and that the loss of viability upon *rct1* deletion is mediated by other Rct1 domain(s). However, it is not

excluded that our mutagenesis approach did not hit the most important residues in the PPIase domain. Therefore, to get further insight into the function of the PPIase domain we constructed three Rct1 deletion mutants fused to HA tag (Fig. 1A) and transformed them into *rct1* heterozygous cells. All deletion mutants (including those lacking RRM domain; see Fig. S3A) were found to be expressed at similar levels in diploid cells, without evidence for protein instability (supplementary material Fig. S3B) and surprisingly produced viable haploids (Fig. 1B and Fig. S3A). Growth analysis revealed that haploid strains expressing Rct1 deletion without the PPIase domain (pMG4), and without PPIase and RS/RD domains (pMG6) are viable at 32^{o}C. However, their growth was slightly inhibited at 20^{o}C and *rct1Δ[pMG6]* cells were strongly affected at 36^{o}C (Fig. 1B). In addition, liquid growth assay revealed that their generation times were approximately two times longer as compared to *WT* cells (Fig. 1C). Deletion of the RS/RD domain only (pMG2) did not show any effect on cell viability and growth which was similar to that of *WT* cells (Fig. 1B,C).

Rct1 is a nuclear protein (Gullerova *et al.,* 2007) and it remains in the nucleus throughout the cell cycle (Fig. 1D). Therefore, to find out whether growth defects observed with Rct1 deletion mutants are due to miss-localization of proteins, we performed localization analysis by using indirect immunofluorescence. Cells were grown overnight in EMM, fixed, and immunostained by using anti-HA antibodies. Clearly, deletion of RS/RD domain (pMG2) resulted in nuclear and cytoplasmic localization (Fig. 1D), indicating that this domain, like in its *Arabidopsis* homolog AtCyp59 (Gullerova *et al.,* 2006), is important for efficient nuclear import. Expression of the RRM domain only (pMG6) resulted in predominant cytoplasmic localization of the protein, although low levels of nuclear staining were also observed (Fig. 1D). Finally, deletion of the PPIase domain (pMG4) did not affect nuclear localization of the protein (Fig. 1D) indicating that the observed growth defects are due to deletion of the PPIase domain.

Cell cycle and mitotic cell division are affected upon deletion of the PPIase domain

Since *rct1Δ[pMG4]* and *rct1Δ[pMG6]* cells displayed strong growth defects we next analyzed their morphology. Cells were grown overnight in EMM medium, diluted to fresh EMM and YE5S medium and further grown to mid-exponential phase. Cells were fixed with ethanol and analyzed by microscopy after DNA and cell wall staining. As shown in Fig. 2A, *rct1Δ[pMG2]* cells expressing Rct1 without the RS/RD domain are of the same size as haploid *WT* or *rct1Δ[pMG1]* cell which express full length Rct1 protein. Deletion of the PPIase domain (*rct1Δ[pMG4]* strain), in contrast to PPIase domain point mutants caused severe phenotype characterised by high proportion of extremely elongated cells with the average length being up to five times that of *WT* cells. Many bi or tetranucleated-like cells without indication of septum formation or cells with irregular chromosome segregation, nuclear fragmentation or hyper-condensation were predominantly observed (Fig. 2A). Thus, the cell growth and mitosis and/or cell cycle seem to be uncoupled in cells lacking the PPIase domain of Rct1. Similar phenotype was observed with *rct1Δ[pMG6]* strain (Fig. 2A) or previously with *rct1Δ* cells expressing full length Rct1 after prolonged growth in the presence of thiamine (Gullerova *et al.,* 2007). *WT* strains *rct1[pMG1]* and *rct1[pMG4]* overexpressing Rct1 or Rct1 without the PPIase domain, respectively did not show any aberrant morphology or DNA staining indicating that the observed phenotypes are due to the PPIase deletion and not due to the dominant negative effect caused by overexpression of truncated protein. In *S. pombe* major cell cycle regulator is Cdc2 kinase which is regulated by reversible phosphorylation on tyrosine 15 (Calonge and O'Connell, 2008; Hochegger *et al.,* 2008; Karlson-Rosenthal and Millar, 2005; Kelogg, 2003; O'Connell and Cimprich, 2005). Analyses of Cdc2 levels and Tyr15 phosphorylation and Cdc2 activity towards the histone H1 in *rct1Δ[pMG4]* and *rct1Δ[pMG6]* cells did not reveal significant changes as compared to *WT* or *rct1Δ[pMG1]* and *rct1Δ[pMG2]* cells (Fig. 2B and data not shown). This data indicated that Cdc2 and its regulators Wee1 and Cdc25 are not likely candidates being affected by deletion of the PPIase domain of Rct1.

DNA staining of *rct1Δ[pMG4]* and *rct1Δ[pMG6]* cells revealed that many cells exhibit unusual DNA staining patterns (Fig. 4A). This phenotype is reminiscent of some DNA damage checkpoint mutants indicating that these cells might have defect in DNA repair and checkpoint responses to DNA damage. Therefore, we analyzed sensitivity of these strains to genotoxic drugs camptothecin (Cpt), hydroxyurea (HU), and 4-nitroquinoline 1-oxide (4-NQO). Serial dilutions of overnight cultures grown in EMM were spotted on YE5S plates containing indicated concentration of the above drugs. Plates were incubated for three days at 32^{o}C. Figure 2C demonstrates that *rct1Δ[pMG4]* and *rct1Δ[pMG6]* strains are hypersensitive to Cpt and 4-NQO and less so to HU. As controls we used *rad3Δ* and *chk1Δ* strains which are known to be sensitive to HU and 4-NQO and which did not show any growth under conditions investigated here (Fig. 2C). Together, the data presented in Figure 2 indicate that Rct1, in particular its PPIase domain, is required for responses to DNA damage and correct cell cycle progression.

Deletion of PPIase domain results in abnormal chromosome segregation

From the DNA staining shown in Figure 2A it was not entirely clear whether deletion of the PPIase domain causes defects in mitotic chromosome segregation or the observed scattered DNA is a result of nuclear fragmentation or both. Therefore, mid-log phase cells were fixed and the chromosomal DNA and microtubules were stained with Hoechst and anti-tubulin antibodies, respectively. In *WT* cells several microtubules can be observed at the interphase, which upon mitotic entry reorganize and form mitotic spindle which separates sister chromatids to the opposite poles of the cell (Sawin and Tran, 2006; see Fig. 3A). Microtubules in *rct1Δ[pMG4]* cells did not show any aberrant morphology. However, staining of the DNA revealed lagging chromosomes/chromatides on mitotic spindle (Fig. 3B, i), scattered chromosomes along the spindle (Fig. 3B, ii) or disattached chromosomes from the kinetochore before the end of mitosis (Fig. 3B, iii). In addition,

many cells contained two (and in rare cases three) mitotic spindles, indicating that cells entered second and third mitotic division without prior cell separation (Fig. 3B, iv). In order to find out if this effect is due to incorrect localization or duplication of spindle pole body (SPB) we crossed *rct1Δ[pMG1]*, *rct1Δ[pMG2]*, and *rct1Δ[pMG4]* strains with cells expressing SPB marker Sid4 fused to GFP (Tomlin *et al.,* 2002). As shown in Figure 4B, SPB in *rct1Δ[pMG4]* cells were, like in *WT* or *rct1Δ[pMG1]* and *rct1Δ[pMG2]* cells (Fig. 4A), correctly duplicated and localized on the poles of the mitotic spindle (see also Fig. S3) although DNA staining revealed hyper-condensed chromatin (Fig. 4B, i), lagging chromosomes (Fig. 4B, ii), and all three chromosomes on one pole of the cell (Fig. 4Biii). Also, tetranucleated-like cells clearly contained four SPBs indicating that *rct1Δ[pMG4]* cells either entered (Fig. S3, iii) or finished (Fig. S3, iv) second mitotic division without septum formation and cell separation.

Fission yeast mutants that are defective in kinetochore-microtubule attachment are usually hypersensitive to microtubule destabilizing drugs. Therefore, we examined sensitivity of *rct1Δ[pMG4]* and *rct1Δ[pMG6]* cells to thiabendazole (TBZ). Overnight cultures grown in EMM were serially diluted and spotted on YE5S plates with (10 µg/ml) or without TBZ. Clearly, both strains were hypersensitive to TBZ at 32^{o}C (Fig. 4C). In contrast, *rct1Δ[pMG1]* and *rct1Δ[pMG2]* cells, which did not show any indication for defects in mitotic chromosome segregation as well as *WT* and *WT* cells overexpressing Rct1 (*rct1[pMG1]*) were not sensitive (Fig. 4C). Altogether, the data presented in Figs. 3 and 4 and in supplementary material Fig. S4 suggest that normal kinetochore-microtubule attachment is partially impaired in cells expressing Rct1 without the PPIase domain.

Genetic interaction of Rct1 with the Dis2 phosphatase

Phenotype of the *rct1Δ[pMG4]* cells described above indicated that Rct1 is required for correct mitotic chromosome segregation and for responses of cells to DNA damage. Similarity of this phenotype with the previously described cold-sensitive (c.s.) mutants in *dis1*, *dis2*, and *dis3* genes (Ohkura *et al.,* 1988) raised a possibility that Rct1 interacts with some of them. To this end *dis1Δ*, *dis2Δ*, and *dis3-54* strains were transformed with the plasmid expressing Rct1 fused to FLAG tag and analysed for complementation of the c.s. phenotype. Cells were grown in EMM media and serial dilutions were spotted on EMM plates and incubated at 32^{o}C and 20^{o}C. Figure 5 demonstrates that overexpression of Rct1 does not rescue cold-sensitivity of *dis1Δ* (Fig. 5A) and *dis3-54* (Fig. 5B) mutants but it does that of *dis2Δ* strain (Fig. 5C). In addition, sensitivity of *dis2Δ* strain, but not that of *dis1Δ* and *dis3-54* strains, to TBZ was also rescued by Rct1 overexpression (Fig. 5).

Dis2, in addition to its role in mitotic chromosome segregation, was also reported to regulate activity of the G2 DNA damage checkpoint kinase Chk1. Overexpression of Dis2 results in hypersensitivity to DNA damaging drugs MMS and 4-NQO. Consistent with this finding *dis2Δ* cells were also found to be hypersensitive to DNA damaging drugs MMS and 4-NQO, but not to HU which induces S-phase checkpoint (den Elzen and O'Connell, 2004). By contrast to previously published insensitivity of *dis2Δ* cells to HU we found that *dis2Δ* and *chk1Δ* cells are, like *rad3Δ* cells, hypersensitive to 7.5 mM HU. In addition, we also found that *dis2Δ* cells are hypersensitive to Cpt (Fig. 6). Therefore, we analysed sensitivity of Rct1 overexpressing *dis2Δ* strain to HU and Cpt. As shown in Figure 6, *dis2Δ* cells overexpressing Rct1 were no longer sensitive to either HU or Cpt further supporting involvement of Rct1 in regulation of DNA damage checkpoint responses.

Cytokinesis is affected upon deletion of the RRM domain or by introduction of three point mutations in the RNP1 motif of the RRM

Sequence analysis of Rct1 revealed that the RRM domain is much more conserved between *S. pombe* and higher eukaryotes than the PPIase domain (Gullerova *et al.,* 2006; see also Fig. S5A). Each RRM contains two highly conserved motifs, RNP1 and RNP2, and mutational analyses showed that aromatic amino acids in RNP1 at the positions 3, 5, and 8 are important for RNA binding (Mayeda, *et al.,* 1994). Therefore, three point mutations in the RNP1 motif of Rct1 were introduced (Fig. S5A). All three mutant Rct1 proteins expressed in *rct1* heterozygous cells produced viable *rct1Δ* spores. Haploid *rct1Δ[pMGR1]* and *rct1Δ[pMGR2]* cells expressing Rct1R1 and Rct1R2 proteins, respectively were comparable to *WT* cells in all growth assays (Fig. 7A and B; cells expressing Rct1R2 did show slight decrease in growth rates in liquid medium at 32^{o}C) and their morphology, as revealed by aniline blue and DNA staining, was also comparable to that of *WT* cells (Fig. 7C). By contrast, *rct1Δ[pMGR3]* strain expressing Rct1R3 protein mutated in all three aromatic residues in RNP1, although being able to complement *rct1* deletion, resulted in strongly reduced growth (Fig. 7A and B) an effect which was further elevated by cold (Fig. 7A). Interestingly, microscopic examination of cells grown at 32^{o}C revealed the inability of daughter cells to separate following mitosis resulting in branched chains of cells. Similarly, *rct1Δ[pMG3]* and *rct1Δ[pMG5]* strains expressing Rct1 without the RRM domain showed comparable cytokinesis defect. Like for *rct1Δ[pMGR3]* cells, their growth was inhibited at low temperature (Fig. 7A) and it was almost fully abolished in liquid medium growth assay (Fig. 7B). Because these cells strongly flocculated in liquid culture, this precluded further analysis. DNA staining on ethanol fixed cells revealed that in all three strains the morphology of nuclei was like in *WT* cells, indicating that the mitotic chromosome segregation was not affected (Fig. 7C). However, *rct1Δ[pMGR3]* cells were hypersensitive to the actin depolymerising drug Latrunculin A (Fig. 7D). In addition, *rct1Δ[pMGR3]* strain was also slightly sensitive to S-phase inhibitors Cpt and HU as well as to genotoxic drug 4-NQO (Fig. S5D). As all three mutated proteins as well as RMM deletion mutant (pMG5) localized to the nucleus (data not shown and Fig. 7E), and were

expressed at the comparable levels (Fig. S5C and Fig. S3B), the observed phenotypes of *rct1Δ[pMGR3], rct1Δ[pMG3]* and *rct1Δ[pMG5]* cells must be due to three mutations in Rct1 RNP1 motif and deletion of the RRM domain. Finally, *WT* haploid or *rct1+/-* diploid cells expressing Rct1 with three point mutations or without the RRM domain were also analyzed but we could not find comparable phenotype (Fig. S5B and data not shown) which indicated that they do not confer dominant negative effect.

Discussion

By using mutational and deletion approaches we analysed the role of PPIase and RS/RD domains of the essential *S. pombe* nuclear multidomain cyclophilin Rct1. Cells lacking RS/RD domain did not show any difference compared to *WT* cells in all physiological assays performed, although Rct1 without RS/RD domain is localised in both the nucleus and the cytoplasm. This is consistent with the results obtained with the *Arabidopsis* Rct1 homolog, AtCyp59, of which the C-terminal RS/RD domain is likewise required for efficient nuclear localisation of the protein (Gullerova *et al.,* 2006). Mutational and deletion analysis revealed that both, PPIase and RRM domains are likewise not essential for cell viability. From the deletion and mutational analyses of Rct1 we can conclude that depletion of the whole Rct1 protein is necessary for the observed lethality (Gullerova et al., 2007). However, deletion of the whole PPIase domain does confer strong phenotype which is characterised by strongly elongated cells with multiple nuclei, incorrect chromosome segregation, and sensitivity to genotoxic and microtubule destabilising drugs. Many *rct1Δ[pMG4]* cells proceeded with the second nuclear division without cytokinesis, resulting in three- or tetra-nuclear cells. As revealed by actin staining these cells do assemble contractile actomyosine ring but septation and/or septum degradation seem to be affected. This, together with their sensitivity to genotoxic drugs, indicates that Rct1 likely regulates component(s) of the various cell cycle checkpoints.

Presented data indicate that cells lacking PPIase domain fail to regulate correct progression through the cell cycle. Control of the cell cycle progression is achieved by the Cdc2 kinase which, if active, can promote mitosis from any point in the cell cycle. The activity of Cdc2 depends on the phosphorylation status of Tyr15. Wee1 kinase phosphorylates Tyr15 during the G2 phase and this prevents entry into mitosis until cells reach appropriate mass and size. This inhibitory phosphorylation is removed by the Cdc25 phosphatase which itself is inactivated by the phosphorylation by the checkpoint effector kinases Chk1 (in case of DNA damage) and Cds1 (in case of replication block) (Calonge and O'Connell, 2008; Hochegger *et al.,* 2008; Karlson-

Rosenthal and Millar, 2005; Kelogg, 2003). Cell cycle checkpoints are activated if cells encounter problems in DNA replication, chromosome segregation or if the DNA damage occur (Calonge and O'Connell, 2008; Clarke and Allan, 2009; Hochegger *et al.,* 2008; Karlson-Rosenthal and Millar, 2005; Kelogg, 2003). From our current analyses it is difficult to predict which of the cell cycle regulators would be target for Rct1. Analysis of Cdc2 levels and phosphorylation status of Tyr15 in *rct1Δ[pMG4]* and *rct1Δ[pMG6]* cells did not reveal significant changes as compared to *WT*, *rct1Δ[pMG1]*, and *rct1Δ[pMG2]* cells. Therefore, it is unlikely that Rct1 directly regulates activities of Cdc2, Cdc25, and Wee1. However, we could show that Rct1 interacts genetically with Dis2, one of the two PP1-type phosphatases in fission yeast. Dis2 was identified in a genetic screen for factors required for normal chromosome segregation during mitosis (Ohkura *et al.,* 1988, 1989) and its activity is regulated by Cdc2-mediated phosphorylation (Yamano *et al.,* 1994). More recently, it has been shown that Dis2 is also required for G2 checkpoint release (den Elzen and O'Connell, 2004). Dis2 dephosphorylates Chk1 kinase, which leads to Chk1 inactivation and re-entry into mitosis following repair of DNA damage in the G2 phase. The mechanism how Rct1 contributes to chromosome segregation and genome stability remains elusive. As overexpression of Rct1 in *dis2Δ* cells rescued their cold-sensitivity, sensitivity to TBZ, HU, and Cpt it is unlikely that Rct1 regulates Dis2 itself. One possibility is that it could in some way change the activity of second PP1 phosphatase Sds21, which like Dis2 is not essential (Ohkura *et al.,* 1989). Overexpression of Sds21 causes cell cycle delay indicating its involvement in cell cycle regulation and possible functional overlap with the Dis2.

Involvement of PPIases in cell cycle regulation has already been reported. It has been shown that overexpression of parvulin-type PPIase Pin1 in *S. pombe* causes a severe growth defect and a significant G1 delay during cell cycle progression. However, *pin1Δ* cells were not sensitive to either UV-C or bleomycin suggesting that *S. pombe* Pin1 does not play a major role in DNA damage checkpoint control (Huang *et al.,* 2001). Human Pin1 seems to be required for p53 regulation in response to DNA damage (Wulf *et al.,* 2002; Zacchi *et al.,* 2002; Zhang *et al.,* 2002). In addition, human Pin1 interacts and regulates the activities of several mitotic phosphoproteins

and inhibits G2/M progression in *Xenopus* extracts. Depletion and overexpression of Pin1 in HeLa cells results in mitotic arrest (Lu *et al.,* 1996). An additional immunophilin, the *S. cerevisae* FK506 binding protein Fpr3, was found to prevent premature adaptation to DNA damage by maintaining recombination checkpoint activity during meiosis. Interestingly, Fpr3 functions in the checkpoint by regulating PP1 localization and counteracting its activity in vivo (Hochwagen *et al.,* 2005). Thus, these and our study clearly show that immunophilins are important regulators of diverse cell cycle components. The fact that neither Pin1 nor Fpr3 are essential for viability suggests that their functions might not be required under normal growth conditions. In addition, as in most cases effects of PPIases on cell cycle are rather mild it is also plausible that they have partially overlapping function.

We could show previously that partial depletion of Rct1 causes deregulation in RNP II CTD phosphorylation which is accompanied by the reduction in the RNAP II transcriptional activity (Gullerova *et al.,* 2007). Our unpublished data indicate that this effect is likely mediated by Rct1 regulating activities of two CTD kinases Cdk9 and Lsk1 (T. Skrahina and Z. J. Lorkovic, unpublished). Both, Cdk9 and Lsk1 have conserved functions in the transcription cycle of RNAP II by regulating phosphorylation of CTD Ser2. However, it is unlikely that diverse phenotypic changes observed upon deletion of specific Rct1 domains are due to the reduced transcriptional activity of the RNAP II or changes in CTD phosphorylation. Rct1 probably has functions in several processes, as shown here by its involvement in cell cycle regulation and genome stability, in addition to transcription regulation. Our efforts to identify Rct1 interacting proteins by the TAP-tagging approach failed, indicating that Rct1 regulates its targets by transient or weak interactions without assembly into stable protein complexes. Indeed, we found that Rct1 interacts either physically or genetically with several proteins involved in transcription, pre-mRNA splicing, cell cycle regulation and chromosome segregation (H. Kautmanova, T. Skrahina and Z. J. Lorkovic, unpublished and this work). One common characteristic of all Rct1 interacting proteins is that they are kinases, phosphatases or proteins which are regulated by phosphorylation, suggesting that Rct1 has important role in regulating protein phosphorylation/dephosphorylation in diverse cellular

processes. What are the physiological consequences of these interactions and how Rct1 contributes to the described process mechanistically remains to be established. Yet, presented data clearly implicate Rct1 in regulation of several cellular processes, in particular in regulation of mitotic cell cycle and its connection with the RNAP II transcription.

Experimental procedures

S. pombe strains and handling of cells

Genotypes of strains used are listed in Table 1. Media as well as standard genetic methods used throughout were described previously (Moreno *et al.,* 1991; Forsburg and Rhind, 2006). *Rct1Δ* haploid cells expressing mutated versions of the protein or its deletion mutants were generated by tetrad dissection (point mutants) or random spore analysis (deletion mutants). If not stated otherwise, cells for all experiments were grown at 32^{o}C. Geneticin (G418, Gibco) and ClonNat (BioAgents) were used at the final concentration of 100 µg/ml.

Plasmids

All plasmids were prepared by inserting *rct1* mutations or deletions tagged with hemagglutinine (HA) into pMG (Gullerova *et al.,* 2007).

Plasmid encoding Rct1 without RS/RD domain was created by amplifying respective *rct1* part from pMG1 by using following primers: forward, 5'gtcagtctcgagatgtctgtactaattgaa-3', which introduces XhoI site in front of ATG codon and reverse, 5'-gtcagtgtcgactcatgcgtaaggcacatcatacggatacacgctttgggaaaaatctacgtg-3' which encodes HA tag, stop codon, and SalI site, in the described order. The PCR product was cut with XhoI and SalI and ligated into Xho/SalI cut pMG, resulting in pMG2. To construct the plasmid expressing HA tagged PPIase domain of Rct1, corresponding domain was PCR amplified with forward oligonucleotide 5'-gactagctcgagatgtctgtactaattgaaactacagttgg-3', which introduces XhoI site in front of ATG codon, and reverse oligonucleotide 5'gactagcccgggtcatgcgtagtcaggcacatcatacggataactagtttccttctctctttgcaatttatcttccg-3', which encodes HA tag, stop codon, and XmaI site, in the described order. The PCR product was cut with XhoI and XmaI and ligated into Xho/XmaI cut pMG, resulting in pMG3. Plasmid encoding Rct1 without PPIase domain (pMG4) was created by amplifying respective *rct1* part from pMG1 by

using following primers: forward 5'-gacgacctcgagatggaggcagaagca-3', which introduces XhoI site in front of ATG codon, and reverse, 5'-ctcatctaaaccactttctaa-3' which primes downstream of the HA tag in the pMG1. PCR product was cut with XhoI and XmaI and ligated into XhoI/XmaI linearized pMG, resulting in pMG4. Plasmid encoding Rct1 lacking RRM domain was created by fusing same PCR product used for pMG3 construction, which also has SpeI site in front of HA tag. The PCR product was cut with XmaI and SpeI. RS domain of Rct1 was amplified using pMG1 as a template. Olidonucleotides used for RS domain amplification were: forward 5'-gactagactagtgctcgttacagacaatattacaactcc-3', that introduces SpeI site, and reverse 5'-ctcatctaaaccactttctaa-3'. Amplified RS domain was cut with SpeI and XmaI, ligated with PCR mentioned before (PPIase domain) through SpeI site. The product of ligation was cloned into XhoI/XmaI opened pMG resulting in pMG5 plasmid. To generate plasmid expressing RRM domain only, RRM encoding region was amplified with the same forward primer as described for pMG4 and with 5'-gactagcccgggtcatgcgtagtcaggcacatcatacggatacacgctttgggaaaaatctacg-3' reverse primer, which introduces XmaI site after HA tag and the stop codon. The PCR product was cloned into XmaI/XhoI digested pMG resulting in pMG6. To construct plasmid expressing Rct1 fused to FLAG tag Rct1 coding region was amplified with following primers: forward 5'-gactagctcgagatgtctgtactaattgaaactacagtt-3' and reverse 5'-gactagcccgggctatttatcatcgtcatctttataatctcgatatctatcatctctataacg-3' which encodes FLAG tag, stop codon, and XmaI site, in the described order. PCR product was cut with XhoI/XmaI and ligated into pMG resulting in pMG1F.

In vitro mutagenesis

Point mutations in PPIse domain of *rct1* were introduced by using QuickChange II XL Site-Directed Mutagenesis Kit from Stratagene. Rct1 coding region together with the HA tag was sub-cloned from pMG1 into pGEX-4T-1 as an XhoI/XmaI fragment and resulting plasmid was used for PCR amplification using mutagenic oligonucleotides. PCR conditions used were: 1 min at

92°C; 20 sec 92°C, 30 sec 20°C, 30 min 68°C, 15 times; 45 min 68°C. After sequencing same fragment was cloned back into pMG plasmid, resulting in pMGM1-M9. Sequences of mutagenic oligonucleotides are available on request and the amino acids mutated are indicated in supplementary material Fig. S1 and S2A.

Immunofluorescence and microscopy

Cell wall and septum staining on living or ethanol fixed cells was done with aniline blue. If not stated otherwise cells were grown until mid-exponential phase in YE5S or EMM media and analyzed by microscopy (Zeiss, Axioplan epifluorescence microscope) by using differential interference contrast (DIC) optics and 100 × oil objective. Immunofluorescence for detection of HA tagged Rct1 point and deletion mutants was performed on formaldehyde fixed cells grown in EMM medium as described (Rabitsch *et al.,* 2004). Rat anti-HA monoclonal antibody (3F10, Roche) was used at 1:100 dilution. Secondary antibody was goat anti-rat Alexa Flour 568 (Molecular Probes) at 1:100 dilution. Immunodetection of tubulin with TAT1 antibody (1:10 dilution; Woods *et al.,* 1989) was carried out as described (Mata and Nurse, 1997). Secondary antibody was goat anti-mouse Alexa Flour 568 (Molecular Probes) at 1:100 dilution. DNA was visualised by Hoechst 33342 (Molecular Probes) staining. Images were acquired by a Zeiss Axioplan epifluorescence microscope equipped with CCD camera by using 100 × oil objective and they were further processed by using Adobe Photoshop.

SDS-PAGE and Western blotting

Protein extracts were prepared as described (Gullerova *et al.,* 2007). Proteins were separated by SDS-PAGE (10% gels), transferred to the PVDF membrane (Millipore), followed by Western blotting according to standard procedures. Rat anti-HA mAb (3F10) (Roche), mouse anti-cdc2 mAb (PSTAIR; SigmaAldrich), rabbit polyclonal anti-cdc2Y15 (Cell Signalling), mouse anti-tubulin mAb (SigmaAldrich), and rabbit anti-Fcp1 (kind gift of M. Kimura) were used at 1:1,000

dilutions. Secondary antibodies, goat anti-rat (SigmaAldrich), goat anti-mouse (Bio-Rad), and goat anti-rabbit (Bio-Rad) IgGs conjugated with horseradish peroxidase, were used at 1:10,000 dilutions. Chemiluminescence kit (AmershamPharmacia Biotech) was used for developing the blots.

Acknowledgements

We would like to thank to Dr. Andrea Barta for the financial support during initial stages of this work, Drs. Anthony Carr, Matthew O'Connell, Kathy Gould and Yeast Genetic Resource Centre for providing strains, and Drs. Keith Gull and Makoto Kimura for TAT-1 and Fcp1 antibodies, respectively. This work was supported by the grant (P-19929-B26) from the Austrian Science Foundation (FWF) to ZJL.

References

Arévalo-Rodríguez, M., Cardenas, M. E., Wu, X., Hanes, S.D. and Heitman, J. (2000) Cyclophilin A and Ess1 interact with and regulate silencing by the Sin3-Rpd3 histone deacetylase. *EMBO J* **19:** 3739-3749.

Arévalo-Rodríguez, M. and Heitman, J. (2005) Cyclophilin A is localized to the nucleus and controls meiosis in *Saccharomyces cerevisiae*. *Eukaryot Cell* **4:** 17-29.

Bähler, J. (2005) A transcriptional pathway for cell separation in fission yeast. *Cell Cycle* **4:** 39-41.

Barik, S. (2006) Immunophilins: for the love of proteins. *Cell Mol Life Sci* **63:** 2889-2900.

Bell, A., Monaghan, P. and Page, A.P. (2006) Peptidyl-prolyl cis-trans isomerases (immunophilins) and their roles in parasite biochemistry, host-parasite interaction and antiparasitic drug action. *Int J.Parasitol* **36:** 261-276.

Calonge, T.M., and O'Connell, M.J. (2008) Turning off the G2 DNA damage checkpoint. *DNA Repair (Amst)* **7:** 136-140.

Clarke, P.R., and Allan, L.A. (2009) Cell-cycle control in the face of damage – matter of life and death. *Trends Cell Biol* **19:** 89-98.

Dolinski, K., Muir, S., Cardenas, M., and Heitman, J. (1997) All cyclophilins and FK506 binding proteins are, individually and collectively, dispensable for viability in Saccharomyces cerevisiae. *Proc Natl Acad Sci USA* **94:** 13093-13098.

den Elzen, N., and O'Connell, M.J. (2004) Recovery from DNA damage checkpoint arrest by PP1-mediated inhibition of Chk1. *EMBO J* **23:** 908-918.

Esnault, S., Shen, Z.J., and Malter, J.S. (2008) Pinning down signalling in the immune system: the role of the peptidyl-prolyl isomerase Pin1 in immune cell function. *Crit Rev Immunol* **28:** 45-60.

Finn, G., and Lu, K.P. (2008) Phosphorylation-specific prolyl isomerase Pin1 as a new diagnostic and therapeutic target for cancer. *Curr Cancer Drug Targets* **8:** 223-229.

Forsburg, S.L., and Rhind, N. (2006) Basic methods for fission yeast. *Yeast* **23:** 173-183.

Gullerova, M., Barta, A., and Lorković, Z.J. (2006) AtCyp59 is a multidomain cyclophilin from *Arabidopsis thaliana* that interacts with SR proteins and the C-terminal domain of the RNA polymerase II. *RNA* **12:** 631-643.

Gullerova, M., Barta, A., and Lorković, Z.J. (2007) Rct1, a nuclear RRM-containing cyclophilin, regulates phosphorylation of RNA polymerase II C-terminal domain. *Mol Cell Biol* **27:** 3601-3611.

Hochegger, H., Takeda, S., and Hunt, T. (2008) Cyclin-dependent kinases and cell-cycle transitions: does one fit all? *Nat Rev Mol Cell Biol* **9:** 910-916.

Hochwagen, A., Tham, W.H., Brar, G.A., and Amon, A. (2005) The FK506 binding protein Fpr3 counteracts protein phosphatase 1 to maintain meiotic recombination checkpoint activity. *Cell* **122:** 861-873.

Huang, H.-K., Forsburg, S.L., John, U.P., O'Connell, M.J., and Hunter, T. (2001) Isolation and characterisation of the Pin1/Ess1p homologue in *Schizosaccharomyces pombe*. *J Cell Sci* **114:** 3779-3788.

Karagiannis ,J., and Balasubramanian, M.K. (2007) A cyclin-dependent kinase that promotes cytokinesis through modulating phosphorylation of the carboxy terminal domain of the RNA Pol II Rpb1p sub-unit. *PLoS ONE* **2:** e433.

Karagiannis, J., Bimbó, A., Rajagopalan, S., Liu, J., and Balasubramanian, M.K. (2005) The nuclear kinase Lsk1p positively regulates the septation initiation network and promotes the successful completion of cytokinesis in response to perturbation of the actomyosin ring in *Schizosaccharomyces pombe. Mol Biol Cell* **16:** 358-371.

Karagiannis, J., Oulton, R., and Young, P.G. (2002) The Scw1 RNA-binding domain protein regulates septation and cell-wall structure in fission yeast. *Genetics* **162:** 45-58.

Karlsson-Rosenthal, C., and Millar, J.B.A. (2006) Cdc25: mechanisms of checkpoint inhibition and recovery. *Trends Cell Biol* **16:** 285-292.

Kellogg, D.R. (2003) Wee1-dependent mechanisms required for coordination of cell growth and cell division. *J Cell Sci* 116: 4883-4890.

Krzywicka, A., Beisson, J., Keller, A.-M., Cohen, J., Jerka-Dziadosz, M., and Klotz, C. (2001) KIN241: a gene involved in cell morphogenesis in *Paramecium tetraurelia* reveals a novel protein family of cyclophilin-RNA interacting proteins (CIRPs) conserved from fission yeast to man. *Mol Microbiol* **42:** 257-267.

Lee , K.M., Miklos, I., Du, H., Watt, S., Szilagyi, Z., Saiz, J.E., Madabhushi, R., Penkett, C.J., Sipiczki, M., Bähler, J., and Fisher, R.P. (2005) Impairment of the TFIIH-associated CDK-activating kinase selectively affects cell cycle-regulated gene expression in fission yeast. *Mol Biol Cell* **16:** 2734-2745.

Lu, K.P. (2003) Prolyl isomerase Pin1 as a molecular target for cancer diagnostics and therapeutics. *Cancer Cell* **4:** 175-180.

Lu, K.P. (2004) Pinning down cell signalling, cancer and Alzheimer's disease. *Trends Biochem Sci* **29:** 200-209.

Lu, K. P., Hanes, S. D., and Hunter, T. (1996). A Human peptidyl-prolyl isomerase essential for regulation of mitosis. Nature *380,* 544-547.

Lu, K.P., and Zhou, X.Z. (2007) The prolyl isomerase PIN1: a pivotal new twist in phosphorylation signalling and disease. *Nat Rev Mol Cell Biol* **8:** 904-916.

Lu, K.P., Finn, G., Lee, T.H., and Nicholson, L.K. (2007) Prolyl cis-trans isomerization as a molecular timer. *Nat Chem Biol* **3:** 619-629.

Mata, J., and Nurse, P. (1997) Tea1 and the microtubular cytoskeleton are important for generating global spatial order within the fission yeast cell. *Cell* **89:** 939-949.

Mayeda, A., Munroe, S.H., Caseres, J.F., and Krainer, A.R. (1994) Function of conserved domains of hnRNP A1 and other hnRNP A/B proteins. *EMBO J* **13:** 5483-5495.

Mesa, A., Somarelli, J.A. and Herrera, R.J. (2008) Spliceosomal immunophilins. *FEBS Lett* **582:** 2345-2351.

Moreno, S., Klar, A., and Nurse, P. (1991) Molecular genetic analysis of fission yeast *Schizosaccharomyces pombe*. *Methods Enzymol* **194:** 795-823.

Nelson, C.J., Santos-Rosa, H., and Kouzarides, T. (2006) Proline isomerization of histone H3 regulates lysine methylation and gene expression. *Cell* **126:** 905-916.

Ohkura, H., Adachi, Y., Kinoshita, N., Niwa, O., Toda, T., et al. (1988) Cold-sensitive and caffeine-supersensitive mutants of the *Schizosaccharomyces pombe* dis genes implicated in sister chromatid separation during mitosis. *EMBO J* **7:** 1465–1473.

Ohkura, H., Kinoshita, N., Miyatani, S., Toda, T., and Yanagida, M. (1989) The fission yeast dis2^{+} gene required for chromosome disjoining encodes one of two putative type 1 protein phosphatases. *Cell* **57:** 997–1007.

Pemberton, T.J., and Kay, J.E. (2005) The cyclophilin repertoire of the fission yeast *Schizosaccharomyces pombe*. *Yeast* **22:** 927-945.

Rabitsch, K.P., Gregan, J., Schleiffer, A., Javarzat, J.-P., Eisenhaber, F., and Nasmyth, K. (2005) Two fission yeast homologs of *Drosophila* Mei-S332 are required for chromosome segregation during meiosis I and II. *Curr Biol* **14:** 287-301.

Romano, P.G., Horton, P., and Gray, P.E. (2004) The *Arabidopsis* cyclophilin gene family. *Plant Physiol* **134:** 1-15.

Sawin, K.E., and Tran, P.T. (2006) Cytoplasmic microtubule organization in fission yeast. *Yeast* **23:** 1001-1014.

Schiene, C., and Fischer, G. (2000) Enzymes that catalyse the restructuring of proteins. *Curr Opin Struct Biol* **10:** 40-45.

Shaw, P.E. (2007) Peptidyl-prolyl cis/trans isomerases and transcription: is there a twist in the tail? *EMBO Rep* **8:** 40-45.

Sipiczki, M. (2007) Splitting of the fission yeast septum. *FEMS Yeast Res* **7:** 761-770.

Tomlin, G.C., Morrell, J.L., and Gould, K.L. (2002) The spindle pole body protein Cdc11p links Sid4p to the fission yeast septation initiation network. *Mol Biol Cell* **13:** 1203-1214.

Viladevall, L., St Amour, C.V., Rosebrock, A., Schneider, S., Zhang, C., Allen, J.J., Shokat, K.M., Schwer, B., Leatherwood, J.K. and Fisher, R.P. (2009) TFIIH and P-TEFb coordinate transcription with capping enzyme recruitment at specific genes in fission yeast. *Mol Cell* **33:** 738-751.

Woods, A., Sherwin, T., Sasse, R., MacRae, T.H., Baines, A.J., and Gull, K. (1989) Definition of individual components within the cytoskeleton of *Trypanosoma brucei* by a library of monoclonal antibodies. *J Cell Sci* 93: 491-500.

Wulf, G., Finn, G., Suizu, F., and Lu, K.P. (2005) Phosphorylation-specific prolyl isomerisation: is there an underlying theme? *Nature Cell Biol* **7:** 345-441.

Wulf, G.M., Liou, Y.C., Ryo, A., Lee, S.W., and Lu, K.P. (2002) Role of Pin1 in the regulation of p53 stability and p21 transactivation, and cell cycle checkpoints in response to DNA damage. *J Biol Chem* **277:** 47976-47979.

Xu, Y.-X., Hirose, Y., Zhou, X.Z., Lu, K.P., and Manley, J.L. (2003) Pin1 modulates the structure and function of human RNA polymerase II. *Genes Dev* **17:** 2765-2776.

Xu, Y.-X., and Manley, J.L. (2007a) Pin1 modulates RNA polymerase II activity during the transcription cycle. *Genes Dev* **21:** 2950-2962.

Xu, Y.-X., and Manley, J.L. (2007b) The prolyl isomerase Pin1 functions in mitotic chromosome condensation. *Mol Cell* **26:** 287-300.

Yamano, H., Ishii, K., and Yanagida, M. (1994) Phosphorylation of dis2 protein phosphatase at the C-terminal cdc2 consensus and its potential role in cell cycle regulation. *EMBO J* **13:** 5310–5318.

Zacchi, P., Gostissa, M., Uchida, T., Salvagno, C., Avolio, F., Volinia, S., Ronai, Z., Blandino, G., Schneider, C., and Del Sal, G. (2002) The prolyl isomerase Pin1 reveals a mechanism to control p53 functions after genotoxic insults. *Nature* **419:** 853-857.

Zheng, H., You, H., Zhou, X.Z., Murray, S. A., Uchida, T., Wulf ,G., Gu, L., Tang, X., Lu, K.P. and Xiao, Z.X. (2002) The prolyl isomerase Pin1 is a regulator of p53 in genotoxic response. *Nature* **419:** 849-853.

Figure legends

Fig. 1. Growth analyses of Rct1 deletion mutants lacking PPIase and RS/RD domains.

A. Schematic presentation of all Rct1 deletion mutants fused to HA tag used in this study.

B. Plate growth assay of PPIase and RS/RD domain deletion strains at different temperatures. Cells were grown overnight in EMM medium and serial dilutions were spotted on YE5S plates. Plates were incubated at indicated temperatures for three (32^{o}C, and 36^{o}C) or five days (20^{o}C).

C. Growth analysis in liquid medium. Overnight cultures grown in EMM were diluted to an OD_{600} of 0.1 and further incubated in EMM at 32^{o}C. ODs were measured every 2.5 hours.

D. Cellular localization of Rct1 deletion mutants lacking PPIase and RS/RD domains. Cells were grown overnight in EMM medium, fixed, and processed for indirect immunoflourescence with anti-HA antibody. Images were acquired with the cooled CCD camera with the 100 × oil objective. *WT* cells were used as a negative control. Localization of full length Rct1 through the cell cycle is shown. Because of the strong growth defect of *rct1Δ[pMG6]* haploid strain in liquid medium we used *rct1* heterozygous diploid cells transformed with pMG6.

Fig. 2. Morphology and sensitivity to genotoxic drugs of strains expressing Rct1 deletions without PPIase and RS/RD domains.

A. Indicated haploid strains were grown in EMM to mid-exponential phase (OD_{600} 0.5), fixed with ethanol, and stained with aniline blue (cell wall and septa) and Hoechst (DNA). Images were acquired with the cooled CCD camera with the 100 × oil objective. Bar, 15 µm.

B. Deletion of the PPIase domain does not affect Cdc2 levels and phosphorylation. Western blots of protein extracts prepared from indicated strains grown in EMM were probed with antibodies

against Cdc2 and phosphor-Tyr15 of Cdc2. Blots were also probed with anti-tubulin and anti-Fcp1 antibodies as loading controls.

C. Sensitivity of *rct1Δ* cells expressing Rct1 deletion mutants to Cpt, HU, and 4-NQO. Cells were grown overnight in EMM medium and serial dilutions were spotted on YE5S plates containing indicated amounts of drugs. Plates were incubated for four days at 32^{o}C.

Fig. 3. *rct1Δ[pMG4]* cells exhibit defects in cell cycle and mitotic chromosome segregation.

A. WT, *rct1Δ[pMG1],* and *rct1Δ[pMG2]* cells exhibit normal DNA and microtubule staining.

B. *rct1Δ[pMG4]* cells stained with TAT-1 antibody and Hoechst to visualise microtubules and DNA, respectively. Note lagging chromosomes (i), dispersed DNA staining (ii), detached chromosomes from the mitotic spindle (iii), and cells with two mitotic nuclei (iv).

Fig. 4. Spindle pole bodies (SPBs) are correctly duplicated in *rct1Δ[pMG4]* cells.

A. Spindle pole body and DNA staining in *rct1Δ[pMG1]* and *rct1Δ[pMG2]* cells.

B. Spindle pole body and DNA staining in *rct1Δ[pMG4]* cells. A and B Cells were grown overnight in EMM, diluted to a fresh medium and grown further until mid-exponential phase. Cells were fixed with ethanol and analysed by microscopy to visualise DNA and SPBs.

C. Sensitivity of Rct1 deletion mutants to TBZ. Cells were grown overnight in EMM and serial dilutions were spotted on YE5S plates containing indicated amount of TBZ. Plates were incubated for three days at 32^{o}C.

Fig. 5. Synthetic interaction of Rct1 with *dis2*. Overexpression of Rct1 rescues cold and TBZ sensitivity of *dis2Δ* (C.) but not of *dis1Δ* (A.) and *dis3-54* (B.) strains. *Dis1Δ*, *dis2Δ*, and *dis3-54* strains were transformed with a plasmid expressing FLAG-tagged Rct1. Overnight cultures were serially diluted and spotted on EMM plates or EMM plates containing 10μg/ml TBZ. Plates were incubated for three days at 32°C (to assay for normal growth of all strains and TBZ sensitivity of *dis3-54* strain) or five days at 26°C (to assay for sensitivity of *dis1Δ* and *dis2Δ* cells to TBZ) and 20°C (to assay for cold sensitivity of strains).

Fig. 6. Overexpression of Rct1 in *dis2Δ* strain confers resistance to DNA damaging agents. Indicated strains were grown overnight in EMM and serial dilutions were spotted on EMM plates without or with indicated amounts of HU and Cpt. Plates were incubated for four days at 32°C. Two independent *dis2Δ* strains expressing Rct1-FLAG were analysed.

Fig. 7. Analysis of *rct1Δ* strains expressing either Rct1 containing point mutation in the RNP1 motif of RRM or deletion mutants lacking the whole RRM domain.

A. Plate growth assay at different temperatures. Cells were grown overnight in EMM medium and serial dilutions were spotted on YE5S plates. Plates were incubated at indicated temperatures for three (26°C, 32°C, and 36°C) or five days (20°C).

B. Growth analysis in liquid medium. Overnight cultures grown in EMM were diluted to an OD_{600} of 0.06 and further incubated in EMM at 32°C. ODs were measured every 2.5 hours.

C. Cell phenotype. Cells were grown in EMM to mid-exponential phase (OD_{600} of 0.5), fixed with ethanol, and stained with aniline blue (cell wall) and Hoechst (DNA). Images were acquired with the cooled CCD camera with the 100 × oil objective. Bar, 15 μm.

D. Sensitivity to latrunculin A. Cells were streaked on YE5S plates containing 0.2 µM latrunculin A and incubated at 32°C for three days.

E. Localisation analyses of Rct1 deletion mutants lacking the RRM domain. As both strains do not grow well in liquid medium, we used *rct1* heterozygous diploid strains grown in EMM.

Fig. S1. Sequence alignment of Rct1 PPIase domain with the human cyclophilin A. Amino acids important for the PPIase activity and for cyclosporine A binding are indicated in bold. Amino acids mutated in Rct1 are in boxes.

Fig. S2. Analysis of *rct1Δ* strains expressing Rct1 containing point mutations in the PPIase domain. (A) List of point mutations introduced into PPIase domain and expected consequences thereof. (B) Expression analysis of Rct1 point mutants. Western blotting analysis was performed with anti-HA and anti-tubulin antibodies of overnight cultures grown in EMM. (C) Morphology of strains expressing Rct1 point mutants. Cells were grown in EMM to mid-exponential phase (OD_{600} 0.5), fixed with ethanol, and stained with aniline blue (cell wall) and Hoechst (DNA). Images were acquired with the cooled CCD camera with the 100 × oil objective. Bar, 15 µm. (D) Growth analyses in liquid medium. Overnight cultures grown in EMM were diluted to an OD_{600} of 0.06 and further incubated in EMM at 32°C. ODs were measured every 2.5 hours.

Fig. S3. (A) Schematic presentation of all Rct1 deletion mutants and their effect on cell survival. (B) Expression analysis of Rct1 deletion mutants in *rct1* heterozygous diploid strains. Cells were grown overnight in EMM and protein extracts were subjected to Western blotting with anti-HA antibody.

Fig. S4. (A) Expression analysis of Rct1 deletion mutants in *rct1Δ* haploid strains expressing Sid4-GFP. Spindle pole body, tubulin, and DNA staining in *rct1Δ[pMG1] sid4-GFP* (B) and *rct1Δ[pMG4] sid4-GFP* (C) cells.

Fig. S5. Analysis of rct1Δ strains expressing Rct1 containing point mutations in the RRM domain. (A) Multiple sequence alignment of RRM domains from Rct1 and homologous proteins different organisms. RNP1 and RNP2 motifs are in red boxes and three point mutations introduced into *S. pombe* Rct1 are indicated below. (B) Morphology of WT cells expressing Rct1 with three point mutations or WT cells expressing two deletion mutants without the RRM domain. (C) Expression analysis of Rct1 point mutants in RRM. Western blotting analysis of overnight cultures grown in EMM was performed with anti-HA and anti-tubulin antibodies. (D) Sensitivity to genotoxic drugs. Serially diluted overnight cultures grown in EMM are spotted onto YE5S plates containing indicated concentration of Cpt, 4-NQO, and HU. Plates were incubated for four days at 32^{o}C.

Figure 1

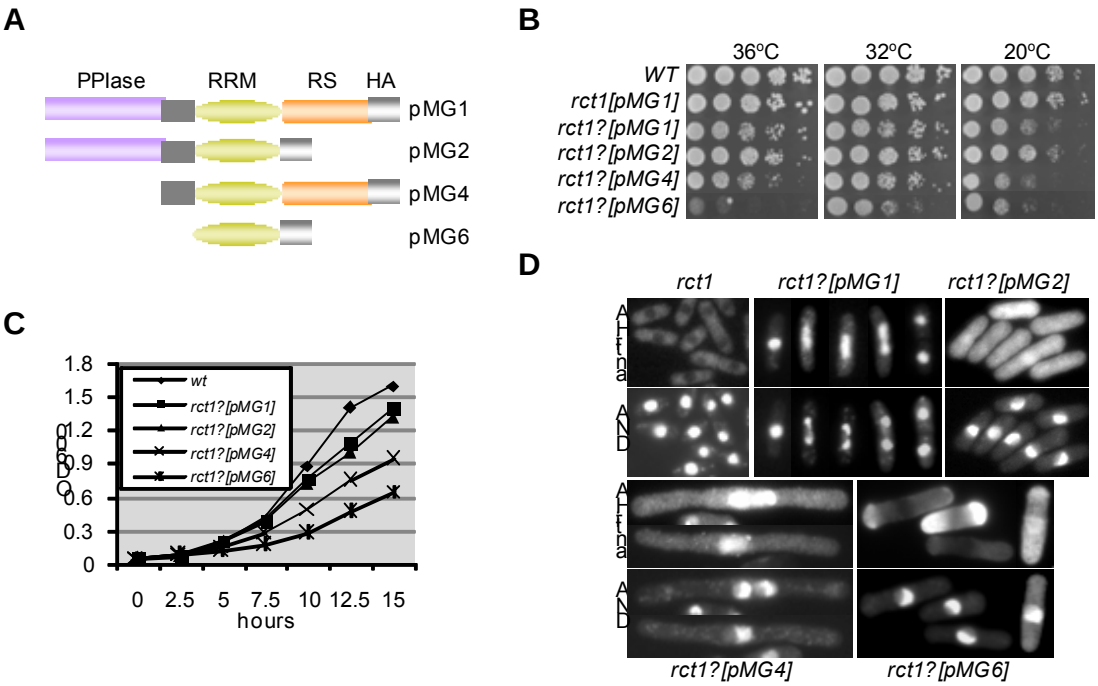
A
PPIase
RRM
RS
HA
pMG1
pMG2
pMG4
pMG6
B
36°C
32°C
20°C
WT
rct1[pMG1]
rct1?[pMG1]
rct1?[pMG2]
rct1?[pMG4]
rct1?[pMG6]
C
OD600
1.8
1.5
1.2
0.9
0.6
0.3
0
wt
rct1?[pMG1]
rct1?[pMG2]
rct1?[pMG4]
rct1?[pMG6]
0
2.5
5
7.5
10
12.5
15
hours
D
rct1
rct1?[pMG1]
rct1?[pMG2]
rct1?[pMG4]
rct1?[pMG6]

Figure 2

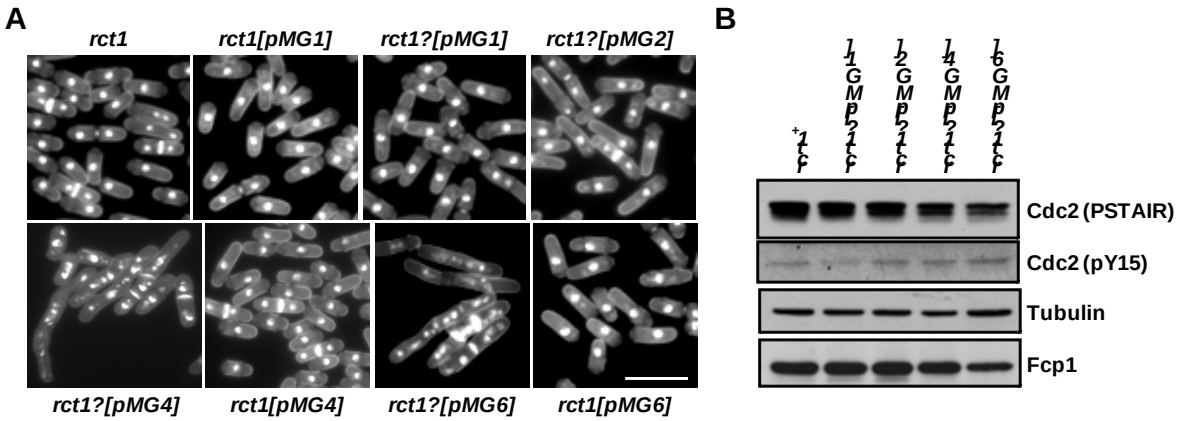
A
rct1
rct1[pMG1]
rct1?[pMG1]
rct1?[pMG2]
rct1?[pMG4]
rct1[pMG4]
rct1?[pMG6]
rct1[pMG6]
B
Cdc2 (PSTAIR)
Cdc2 (pY15)
Tubulin
Fcp1

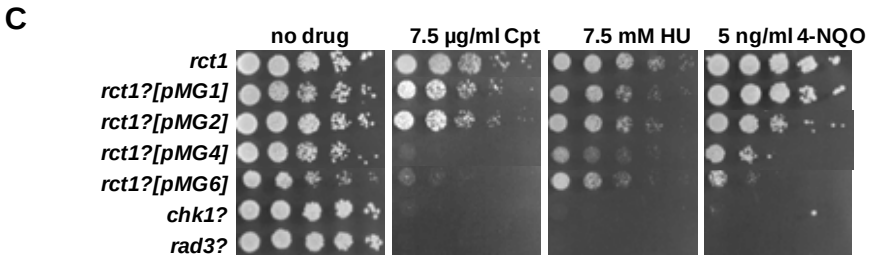
C
no drug
7.5 µg/ml Cpt
7.5 mM HU
5 ng/ml 4-NQO
rct1
rct1?[pMG1]
rct1?[pMG2]
rct1?[pMG4]
rct1?[pMG6]
chk1?
rad3?

Figure 3

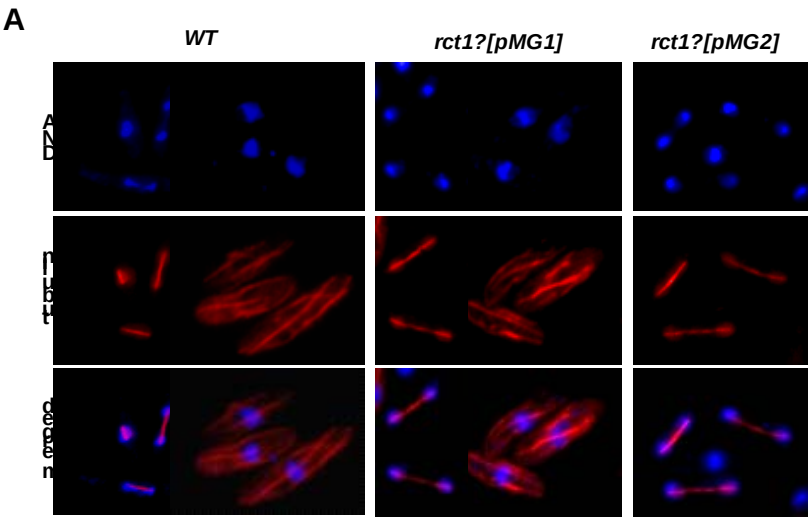
A
WT
rct1?[pMG1]
rct1?[pMG2]

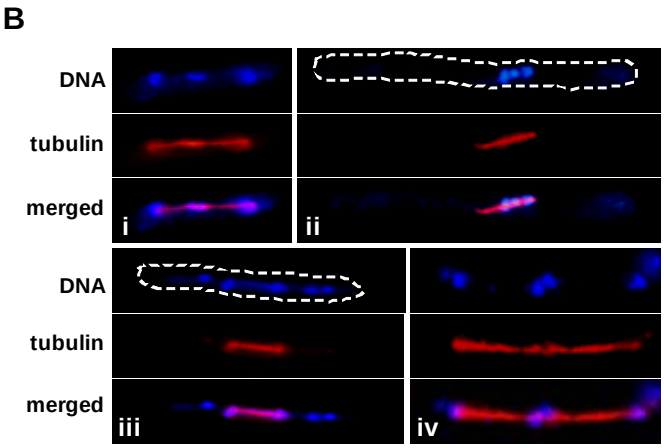
B
DNA
tubulin
merged
i
ii
DNA
tubulin
merged
iii
iv

Figure 4

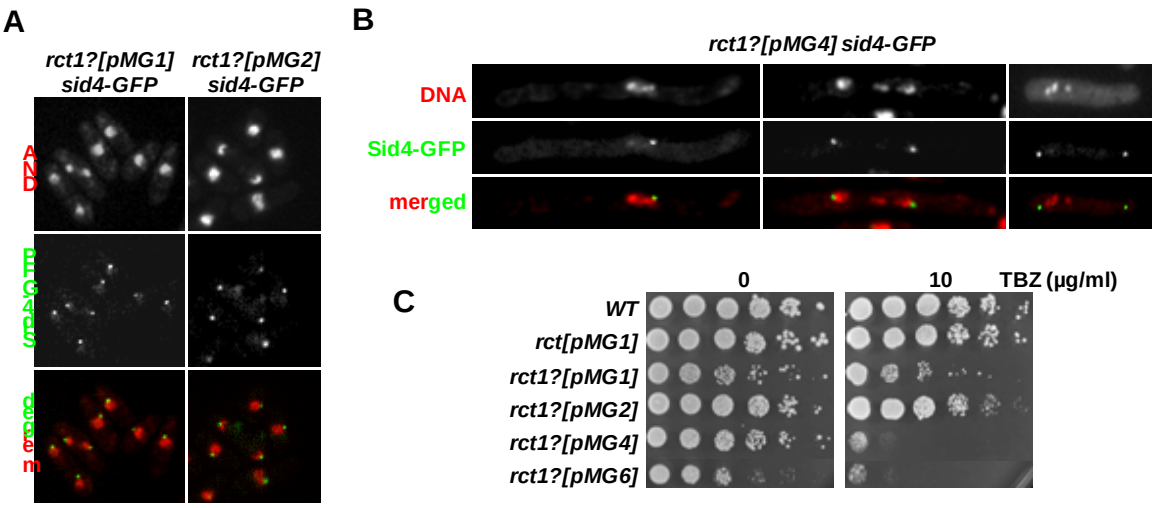
A
rct1?[pMG1] sid4-GFP
rct1?[pMG2] sid4-GFP
DAPI
Sid4-GFP
merged
B
rct1?[pMG4] sid4-GFP
DNA
Sid4-GFP
merged
C
0
10
TBZ (µg/ml)
WT
rct[pMG1]
rct1?[pMG1]
rct1?[pMG2]
rct1?[pMG4]
rct1?[pMG6]

Figure 5

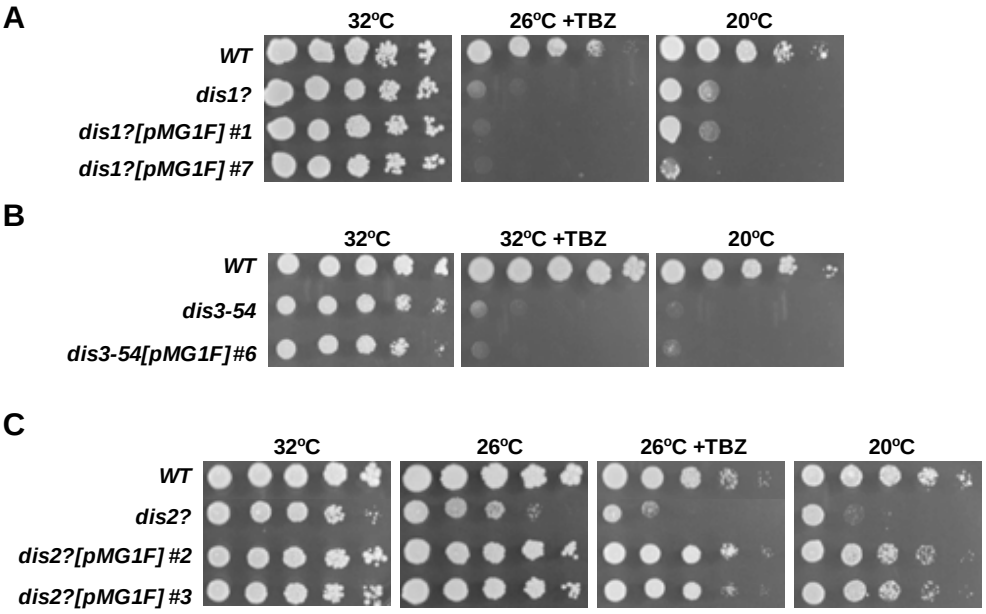
A
32ºC
26ºC +TBZ
20ºC
WT
dis1?
dis1?[pMG1F] #1
dis1?[pMG1F] #7
B
32ºC
32ºC +TBZ
20ºC
WT
dis3-54
dis3-54[pMG1F]#6
C
32ºC
26ºC
26ºC +TBZ
20ºC
WT
dis2?
dis2?[pMG1F] #2
dis2?[pMG1F] #3

Figure 6

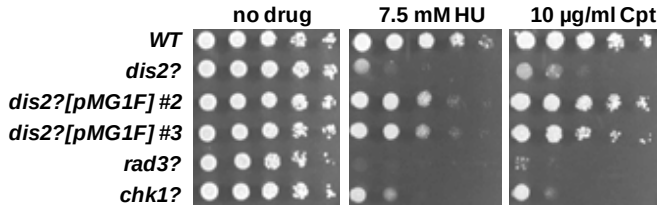
no drug
7.5 mM HU
10 µg/ml Cpt
WT
dis2?
dis2?[pMG1F] #2
dis2?[pMG1F] #3
rad3?
chk1?

Figure 7

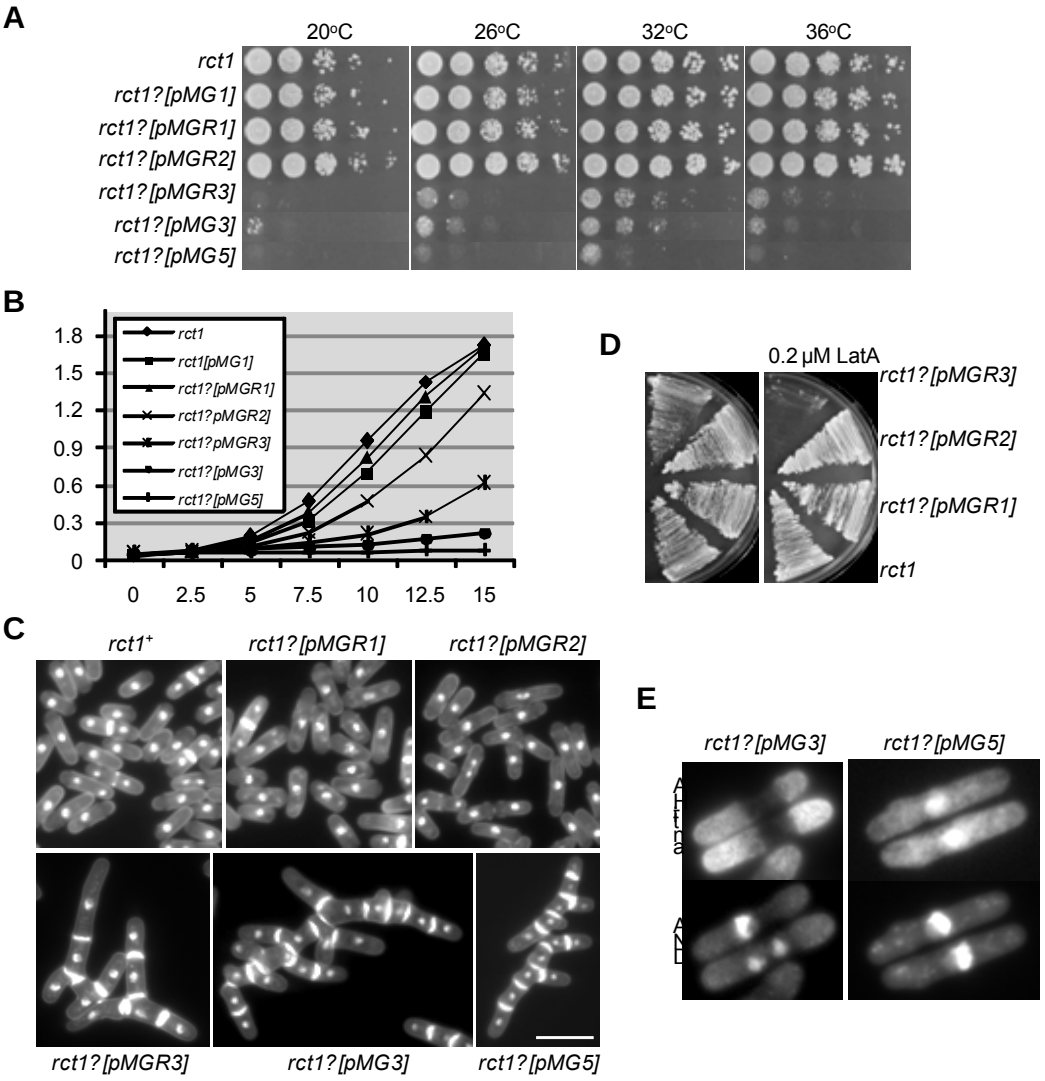
A
20°C
26°C
32°C
36°C
rct1
rct1?[pMG1]
rct1?[pMGR1]
rct1?[pMGR2]
rct1?[pMGR3]
rct1?[pMG3]
rct1?[pMG5]
B
rct1
rct1[pMG1]
rct1?[pMGR1]
rct1?pMGR2]
rct1?pMGR3]
rct1?[pMG3]
rct1?[pMG5]
1.8
1.5
1.2
0.9
0.6
0.3
0
0
2.5
5
7.5
10
12.5
15
C
rct1+
rct1?[pMGR1]
rct1?[pMGR2]
rct1?[pMGR3]
rct1?[pMG3]
rct1?[pMG5]
D
0.2 µM LatA
rct1?[pMGR3]
rct1?[pMGR2]
rct1?[pMGR1]
rct1
E
rct1?[pMG3]
rct1?[pMG5]

Figure S1

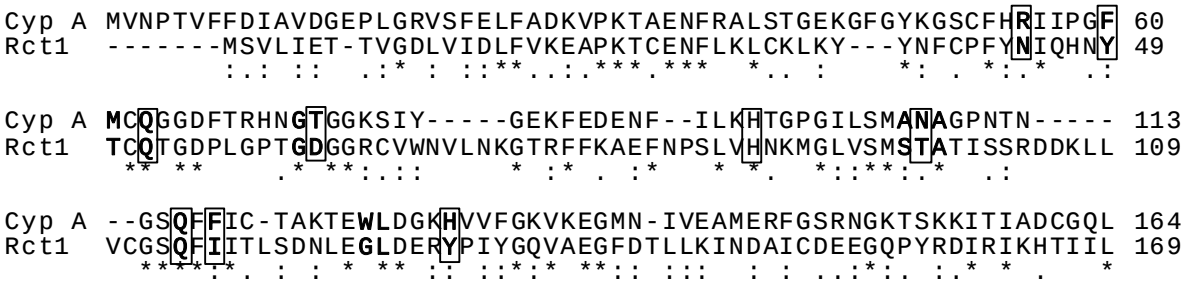
Cyp A MVNPTVFFDIAVDGEPLGRVSFELFADKVPKTAENFRALSTGEKGFGYKGSCFHRIIPGF 60
Rct1 -------MSVLIET-TVGDLVIDLFVKEAPKTCENFLKLCKLKY---YNFCPFYNIQHNY 49
Cyp A MCQGGDFTRHNGTGGKSIY-----GEKFEDENF--ILKHTGPGILSMANAGPNTN----- 113
Rct1 TCQTGDPLGPTGDGGRCVWNVLNKGTRFFKAEFNPSLVHNKMGLVSMSTATISSRDDKLL 109
Cyp A --GSQFFIC-TAKTEWLDGKHVVFGKVKEGMN-IVEAMERFGSRNGKTSKKITIADCGQL 164
Rct1 VCGSQFIITLSDNLEGLDERYPIYGQVAEGFDTLLKINDAICDEEGQPYRDIRIKHTIIL 169

Figure S2

A

Mutation	Effect
M1: N44A	PPIase activity
M2: Y49K	PPIase activity
M3: Q52L	PPIase activity
M4: H88Y	CsA binding
M5: Q114L	No effect
M6: Y130Q	PPIase activity
M7: M1+M3	PPIase activity
M8: M1+M4	PPIase activity
M9: M4+M5	CsA binding
M10: M4+M5+M6	PPIase activity

B

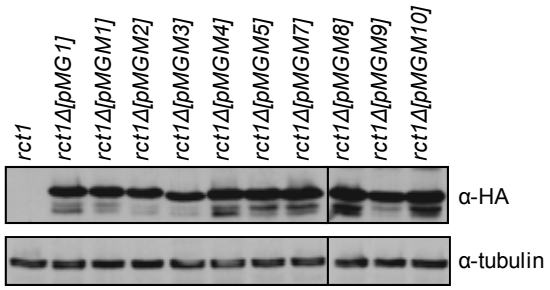

C

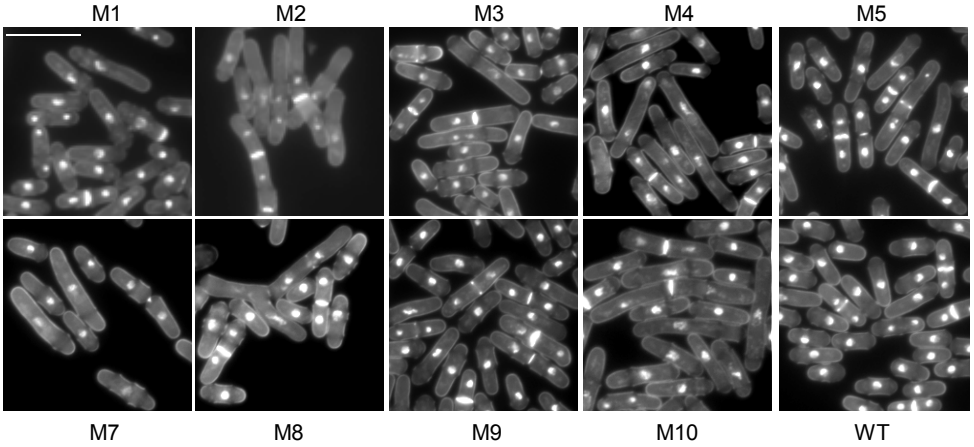

D

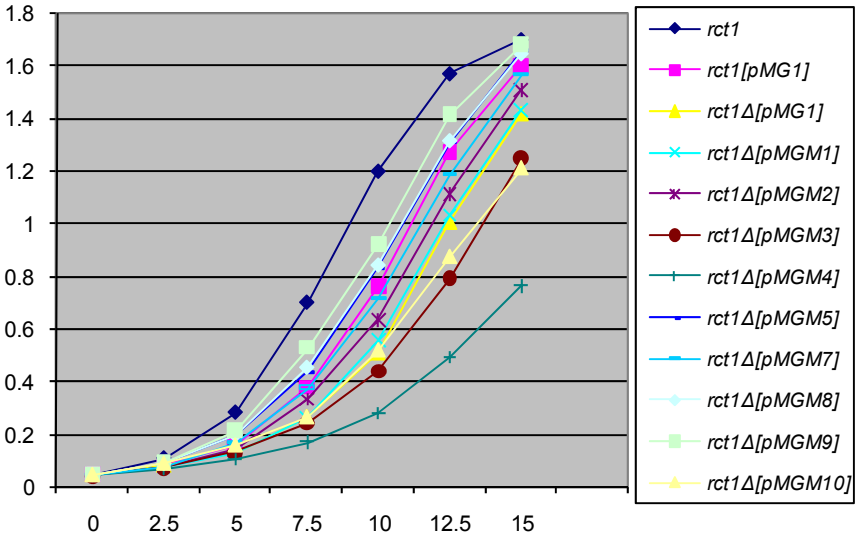

Figure S3

A

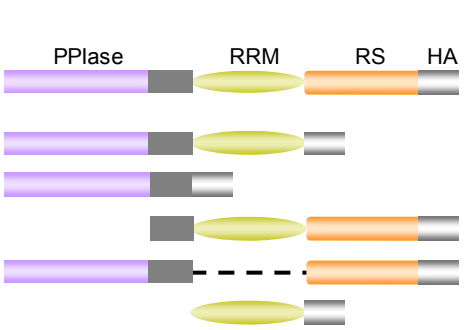

Construct	Viable haploids
pMG1 (Rct1-HA)	+
pMG2 (Rct1ΔRS-HA)	+
pMG3 (Rct1ΔRSΔRRM-HA)	-/+
pMG4 (Rct1ΔPPIase-HA)	+
pMG5 (Rct1ΔRRM-HA)	-/+
pMG6 (Rct1ΔPPIaseΔRS-HA)	+

B

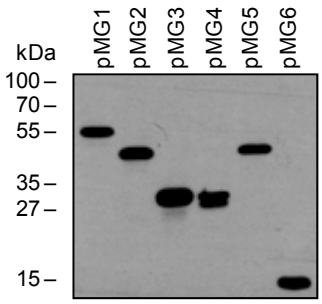

Figure S4

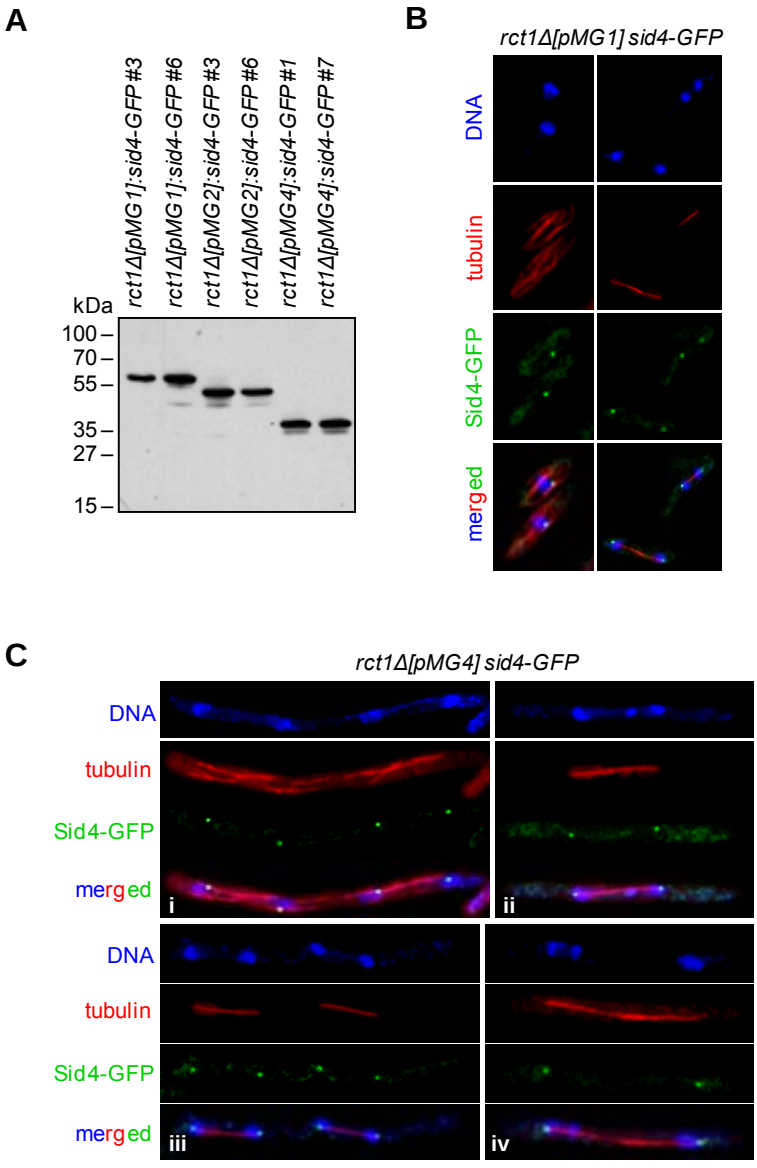
A
rct1Δ[pMG1]:sid4-GFP #3
rct1Δ[pMG1]:sid4-GFP #6
rct1Δ[pMG2]:sid4-GFP #3
rct1Δ[pMG2]:sid4-GFP #6
rct1Δ[pMG4]:sid4-GFP #1
rct1Δ[pMG4]:sid4-GFP #7
kDa
100
70
55
35
27
15
B
rct1Δ[pMG1] sid4-GFP
DNA
tubulin
Sid4-GFP
merged
C
rct1Δ[pMG4] sid4-GFP
DNA
tubulin
Sid4-GFP
merged
i
ii
iii
iv

Figure S5

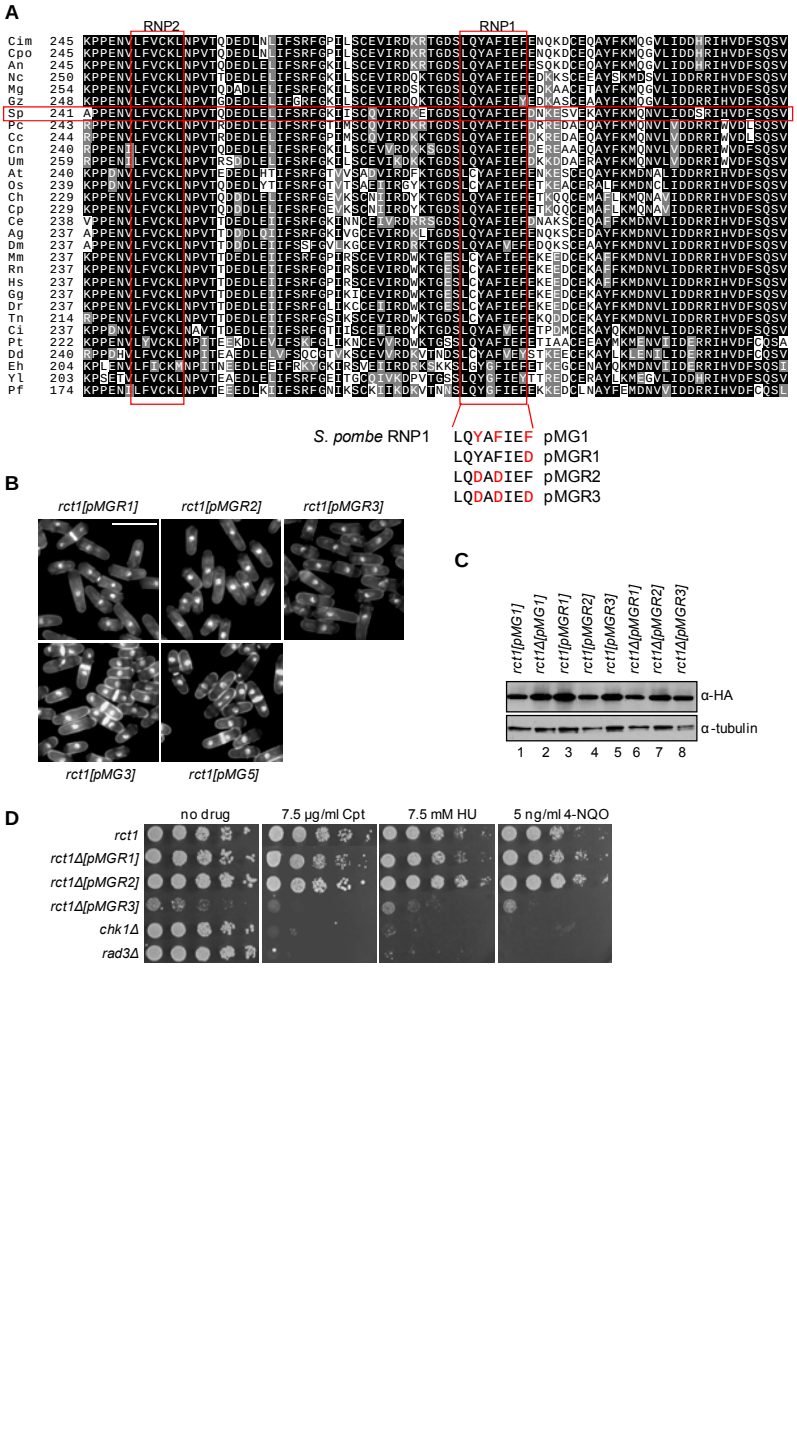
A
RNP2
RNP1
S. pombe RNP1 LQYAFIEF pMG1
LQYAFIED pMGR1
LQDADIEF pMGR2
LQDADIED pMGR3
B
rct1[pMGR1]
rct1[pMGR2]
rct1[pMGR3]
rct1[pMG3]
rct1[pMG5]
C
rct1[pMG1]
rct1Δ[pMG1]
rct1[pMGR1]
rct1[pMGR2]
rct1[pMGR3]
rct1Δ[pMGR1]
rct1Δ[pMGR2]
rct1Δ[pMGR3]
α-HA
α-tubulin
1 2 3 4 5 6 7 8
D
no drug
7.5 μg/ml Cpt
7.5 mM HU
5 ng/ml 4-NQO
rct1
rct1Δ[pMGR1]
rct1Δ[pMGR2]
rct1Δ[pMGR3]
chk1Δ
rad3Δ